Department of Precision and Microsystems Engineering

The design of a distributed sensing system for contactless substrate transport

Yvonne Voorrips

Report no : 2017.032
Professor : dr.ir R.A.J. van Ostayen
Specialisation : Mechatronic System design
Type of report : Master Thesis
Date : 8 August 2017

The design of a distributed sensing system for contactless substrate transport

by

Yvonne Voorrips

in partial fulfillment of the requirements for the degree of

Master of Science
in Mechanical Engineering

at the Delft University of Technology,
to be presented on Tuesday August 29, 2017 at 13:00.

Student number:	1510517	
Professor:	dr. ir. R. A. J. van Ostayen	
Thesis committee:	ir. J.W. Spronck	TU Delft
	Dr.ir. J.F.L. Goosen	TU Delft

An electronic version of this thesis is available at `http://repository.tudelft.nl/`.

TU Delft Delft University of Technology

Summary

In the PHD researches of Jasper Wesselingh [1] and Phuc Vuong [2], an active air film positioning system for thin substrates was developed. In order to apply this concept in an industrial environment, this research has to be extended. To compete with other contactless transport mechanisms already on the market, a system which can both transport and position a substrate with high speed and accuracy has to be developed. This leads to the following thesis objective: *"Design a distributed sensing system to measure the in-plane position and rotation of a substrate, which is transported by an air bearing"*.
All components of the (to be developed) sensing system will be located at the bottom side of the substrate, to leave the top side free for any process that is required during transportation and/or fabrication of the substrate. In this thesis a 100 mm wafer will be used as a basis for the sensor system design.

To reduce the costs of the upgraded system, the 'bearing cell' is introduced, where air is blown upwards through small tubes. The bearing cells only guide the substrate but cannot actively position it. The transportation and positioning system can now be divided into two sections as shown in figure 1. The substrate is positioned and accelerated by the active 'actuator' cells in routing station, and subsequently transported along a bearing lane (consisting of bearing cells) towards the next routing station.

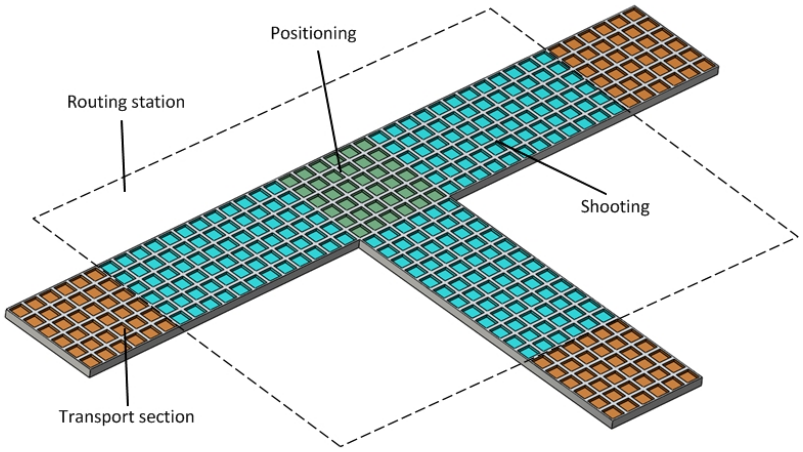

Figure 1: The system can be divided into a routing station and a transport section

In previous research it has been demonstrated that the wafer can be positioned very accurate with this type of actuation system [1]. By developing a sensor system that can measure the position of a substrate with a resolution of at least 15 μm it can be ensured that the wafer is accelerated with a high enough accuracy in the right direction to arrive safely at the next routing station.

There are many sensing principles that could be used to measure the substrate. Research has been done for capacitive sensing, optical displacement sensing and optical position sensing. The optical Linear Sensor Array, or LSA turned out to be the most suitable sensor. An LSA consists of an array of photosensitive diodes. The number of photo diodes defines the amount of 'pixels' that the sensor has. Each pixel generates an output voltage that is equivalent to the amount of incident light it is exposed to. The voltage output of the sensor is serial, it consists of a series of voltage values corresponding to the number of sensor pixels. The best suited sensor that meets the set requirements of resolution, size and price, is the TSL1402R (see figure 2), produced by the firm AMS/TAOS [5].

Illumination is placed on both sides of the linear sensor array. When a wafer is positioned above the sensor, a significant amount of reflected light is received by the sensor. Without the presence of a wafer, less light will be received which results in a lower output voltage.

Figure 2: A TSL1402R sensor [3]

The working principle of the sensor is tested by mounting the sensor onto a stage which is positioned next to a wafer with a diameter of 100 mm. The stage is moved underneath the wafer which makes the sensor move from a totally uncovered position, to a position where it is fully covered by the wafer. The stage can be moved electronically, which means that, once a reference measurement has been made, the exact position of the sensor in reference to the wafer is known. By moving the sensor in small steps a clear view of the achievable resolution is created. By varying the height and the light colour, additional information about the sensitivity of the sensor is acquired.

The sensor output data are processed with an analog to digital converter (ADC). When an analog integrator is used, the values of the serial voltage output from the sensor are added up to one value before it is read by an ADC. This reduces the amount of data that has to be processed. An analog integrator diminishes the accuracy of the sensor but saves time and money. If the lower resolution is still sufficient, this invention could make the sensor system a lot cheaper.

Due to some unforeseen circumstances, the experimental setup has been modified so that the illumination is now positioned on the opposite side of the moving wafer. The measurements confirm that the Linear Sensor Array is a suitable sensor for the distributed sensing system. The desired resolution has been achieved, and the speed at which the sensor can be driven ensures that this is also possible at higher substrate speeds. The variation in light colour and fly height did not clearly change the sensor output values, probably due to the changes that were made to the test setup.
The use of an analog integrator decreases the resolution, but also the costs of the system. The desired system resolution was not achieved with the analog integrator that was used in this test setup, but by using an ADC with a higher resolution this should be possible. As a recommendation for future research the fine tuning of the analog integrator could be very valuable, together with testing of this sensor system with a faster moving wafer.

Contents

Symbol list

Symbol	Description	Unit
η	Allowed offset from side of track	μm
γ	d_{wafer}/W_{track}	mm
μ	Friction coefficient	–
ρ	Density	kg/m^3
Δp	Pressure difference between actuator in-and outlet	Pa
b	Width of pocket of actuator	μm
d_{wafer}	Wafer diameter	mm
h	Film thickness in actuator pocket	μm
h_w	Height of wafer	μm
l	Length of pocket of actuator	μm
l	Half chord length	mm
m	Wafer mass	kg
p_2	Pressure at actuator inlet	Pa
p_3	Pressure at actuator outlet	Pa
$\dot{q}_a$	Air flow through one actuator cell	l/s
r	Radius	mm
s	Sagitta length	mm
t	Nominal fly height of substrate above dam	μm
w	Length of actuator dam	μm
x_0	Wafer position offset from centre in x-direction	μm
x_c	Centre of routing station in x-direction	μm
$\dot{x}_s$	Wafer velocity	m/s
x_T	x-position of w	μm
v	Velocity	m/s
y_0	Wafer position offset from centre in y-direction	μm
y_c	Centre of routing station in y-direction	μm
y_T	y-position of wafer at end of track	μm
A_w	Surface area of wafer	m^2
E_{kin}	Kinetic energy	J
F_a	Force exerted by one actuator cell	N
F_d	Force created at dam	N
F_p	Force created at pocket	N
F_s	Force created at sides	N
L_r	Routing station length	mm
L_t	Transport section length	mm
S	Ideal distance between sensors	mm
W	Weight	kg
W_{track}	Track width	mm

1 Introduction

This thesis looks into the possibility of designing a low cost sensor system to measure the position of a substrate which is transported by an air bearing. Products that benefit from this type of transport are usually very sensitive and can often be found in the field of micro electronic fabrication. Examples are chips, printed circuit boards and solar cells. Another area of application is for example the transportation of sheet materials like glass plates or paper sheets, that have a large surface area compared to their weight.

This thesis follows on the research done by Wesselingh and Vuong, who both designed a positioning system which uses an active air film to contactlessly position a substrate [1] [2]. In order to use this design in a manufacturing process, the positioning device will have to be up-scaled to a combined positioning and transportation system, this is explained in detail in chapter 2. There are several contactless positioning and transportation systems already on the market. An analysis of comparable products is given in paragraph 2.3. The to be designed system should be able to compete with products already available on the market and meet at least the same requirements in terms of resolution, speed, throughput and costs.

An important part of the new system will be the measurement of the location of the substrate. The information provided by the measurement system will be used to determine the location of the substrate with a high resolution. The air supply can be turned off at locations where no substrate is present, which results in a reduction of the operating costs of the system.

Objective With this future plan for the project in mind, the following thesis objective has been determined: "Design a distributed sensing system to measure the in-plane position and rotation of a substrate which is transported by an air bearing." With the additional requirement that the sensing has to be one sided (at the bottom side of the substrate), so the top side will be available to whatever process is required during transportation/fabrication of the substrate. Besides, the cost, resolution and speed of the system should be at least comparable to similar existing systems.

Overview of thesis The working principle of the air actuated positioning and transportation system is explained in chapter 2. The measurement system requirements and lay out can be found in chapter 3. After a comparison between a variety of sensors, the type of sensor used to measure the wafer location is chosen in chapter 4. In chapter 5 the other components of the measuring system are matched to the chosen sensor type. In chapter 6, a setup is designed which can verify the predicted sensor characteristics. The results of the experiments can be found in chapter **??**, the conclusion is presented in chapter 8.

2

System overview

This chapter starts with an intensive study of the actuation system designed by Wesselingh [1]. Afterwards an investigation is done how this can be expanded to a transportation system. Paragraph 2.1 explains the working principle used to lift and move the substrate, followed by calculations on the dimensions, accuracy and other system specifications.
There are some considerations to take into account when up scaling an actuation system to also include transportation. A combined transportation and positioning system has to fulfil more functional requirements than just a positioning system, more details can be found in paragraph 2.4. The requirements for accuracy and specific system components are described in paragraph 2.5 and 2.6.

2.1 Working principle

The positioning system used in this research has been developed by Wesselingh [1]. In his research, he developed a system which consists of small, square cells which can exert a force in one direction. By combining a number of those cells, the wafer can be sent in any direction by controlling each cell individually. Figures 2.1 and 2.2 show the top and side view of such a cell. It consists of a lower lying 'pocket', which is surrounded by a 'dam'. The length of the pocket l is equal to the width b. The dam width is represented by w and the height between the floating substrate and the dam by t. The height between the substrate and the pocket is named h. The system can be scaled to suit a systems specific requirements. The original design consists of 10 by 10 mm cells with a pocket width of 8 mm and a dam width of 2 mm. The fly height of the substrate is 10 μm above the dam (t) and 30 μm above the pockets (h). These are the values with which the calculations in this chapter will be made.

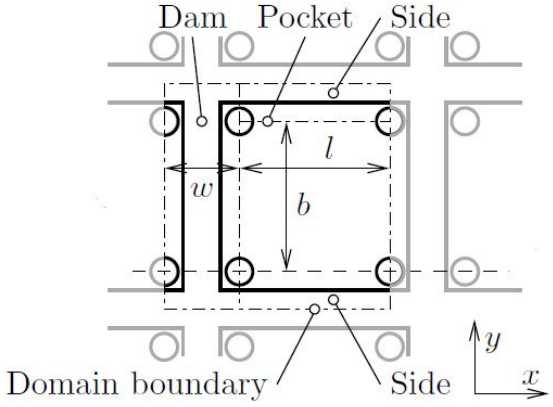

Figure 2.1: Top view of actuator cell [1]

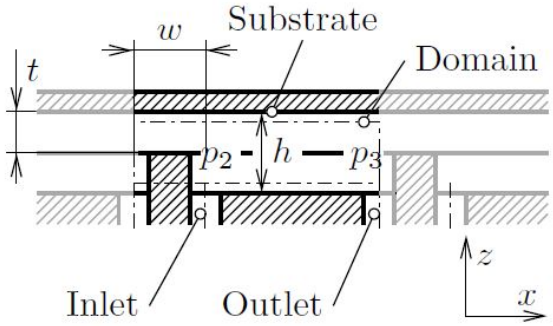

Figure 2.2: Side view of actuator cell [1]

Each cell has two separate air in- and outlet channels. The air flows from one side of the cell to the other, creating an air flow. This current then exerts a force on the substrate to move it in the desired direction. The air flow within the actuator cells is created by applying a pressure difference between the in- and outlet channels. The pressure at the inlet is higher than 1 bar absolute (p_2) and the pressure at the outlet (p_3) is lower. The total air flow through one actuator cell is $\dot{q}_a$. The flow is directly linked to the pressure difference, and reduced by the resistance created by obstacles in the air flow, like valves.
The force exerted by one cell is not enough to move the substrate with a high velocity, therefore multiple cells are placed in a grid to create the desired speed. Once the substrate is moving fast enough, it only has to be supported by an air film, also called an air bearing, to continue in the same direction. The bearing cells only have to blow air upwards (there are no currents in specific directions required), and are therefore less complex than the actuator cells. By combining bearing cells with actuator cells in a grid, both principles are combined to create a positioning and transportation system.

The actuators exert a force on the substrate which then accelerates in a certain direction (a_x,a_y). Disturbances from the environment will slightly move the substrate as well. Disturbances can be anything from vibrations that reach the system through the mounting on the floor, to a door that opens close to the track and causes a disturbance in the air flow. The position is measured by sensors and this information is used to move the substrate to the desired location with the actuators. Figure 2.3 gives an overview of a simple process scheme of the system. Due to the pure force actuation we can predict where the substrate will be in the next moment. By using feed forward control, the actuation system can anticipate to the desired movement of the substrate. This can increase the speed of the overall system. There are of course still sensors needed to prove if the assumption of where the substrate will be is correct (to detect the error).

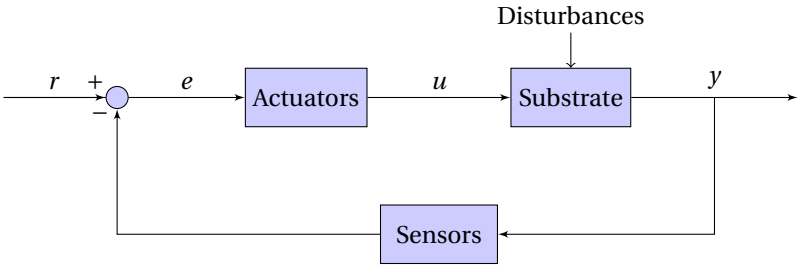

Figure 2.3: Simple process scheme of the actuator and sensor system

2.2 Substrate

Te positioning and transportation system can be used to handle products with a sheet-like shape (a large surface area compared to the height). Products made of sensitive materials would especially benefit from the non-contact transportation. Examples are wafers, printed circuit boards, solar cells, etc. Larger objects

like glass plates or sheets of paper/cardboard could be transported when the system is scaled to a larger size. The material properties and dimensions of several possible substrates are listed below. Regardless of the material, this type of system can handle any size of substrate. Handling consists of slowing down the item, possibly turning it a number of degrees, and sending it away in different direction.

Wafer Wafers are usually made of silicon ($\rho_{silicon} = 2328\ kg/m^3$) [12]. The most commonly used wafer has a diameter of 300 mm, which results in a cross section of $A_w = \pi r^2 = 7,07 * 10^{-2}\ m^2$. The thickness of a wafer is usually 775 μm [14]. This results in a wafer mass of 0.127 kg (see equation 2.2.1). A 100 mm wafer has a cross section of $7,85 * 10^{-3}\ m^2$, a thickness of 525 μm [11] [14] and a mass of 9.6 grams. This is the type of substrate for which the measurement system in this research will be initially designed. Figure 2.4 shows the shape of a typical wafer. The wafer has one flat edge, with which the in-plane rotation of the wafer can be detected.

$$m_{wafer} = A_w * h_w * \rho_{silicon} \tag{2.2.1}$$

Figure 2.4: A typical 100 mm wafer with a flat side

Solar cell There are many different types and sizes of solar cells on the market. A single solar cell usually has a square shape. The standard size of one square cell is 150 mm^2 [6]. The average weight of one cell is around 0.3 kg.

Flat panel displays Flat panel displays are large, flat pieces of glass. They are used for example as displays for televisions or touch screens. This type of substrate would benefit from contactless transport as the glass is easily scratched or damaged. The size of displays is still increasing. The newest 'generation' of glass substrate that has been mentioned is 'gen 10', with a size of 2850 mm x 3050 mm [15]. The size and weight are significantly higher than of the previously described substrate types. The handling force of the system is proportional with the surface area, as is the mass that can be lifted. By increasing the air pressure difference in the actuator cells, the maximum traction force is increased. Increasing the average pressure increases the load that can be lifted.

2.3 Similar existing systems

In the past decades, multiple investigations have been done in the same field of research as researched recently by Wesselingh [1] and Vuong [2]. This is the field of air bearing transportation and positioning systems. It is interesting to see that most of the resulting systems would work either for transportation or for positioning purposes. It is usually not possible to use one solution for both fields of application due to accuracy limitations (transportation systems) or high production costs (positioning systems).

One of the first systems that used air for levitation and transportation was developed by Luntz and Moon [18]. They used an air hockey table (a plate drilled with many small holes through which pressurized air flows) with several flow sinks (suction points). The sinks suck all the surrounding air in their direction, creating a flow pattern across the table. A substrate can be moved in a specific direction by turning the sinks on and off. This system works for transporting substrate in a certain direction, but cannot be used to position them.
A more complicated research where this is possible, is for example the Xerox Park paper handling system [20]. It consists of over 1100 directed air jets on an area of 300 x 300 millimetres. Each air jet is controlled separately by an independent valve. By controlling the amount of air jets turned on in each direction, the paper is lifted and moved with the desired direction and speed. This system can position a substrate very precisely, but every air jet has to be controlled separately. This makes it an expensive choice for upgrading to a transportation system.
Another system, the 'micro-conveyer' has been developed by Laurent [16]. It consists of a manipulation surface with holes that contain four nozzles each. This plate is mounted on top of two other plates with micro-channels. The micro-channels supply the nozzles with air. When the channels are connected to an air supply, air jets lift and move an object in a specific direction. By moving the manipulation plate, a different set of micro channels supplies air to a different set of nozzles, which results in a change in the orientation of the air jets. This system is much easier to control because the movement of one plate influences the air flow of many air outlets.

There are also systems that can both transport and position substrates easily that do not use air as a way of transportation. Park developed a contactless magnetically levitated transport system. This product uses magnetism instead of air [17]. The levitation and stabilization is done with a set of electromagnets. The propelling of the substrate is done with a separate set of electromagnets, and controlled with the amount of current sent through each propulsion coil. For a system like this, the type of substrate that can be transported is limited to metal objects. To be able to transport all substrate types, metal carriers could be used but then the substrate will be lying on a metal carrier and is no longer transported contactless.

From the above listed research the 'micro-conveyer' designed by Laurant comes closest to the design used in this system in terms of creating a system that can be up scaled easily without causing the amount of control required to regulate the air flow to get too complicated. However, the costs of the complicated plates can easily get very high. This means that the main challenge in designing a system that can both position and transport substrates, is to keep the costs at a low value by keeping the system as simple as possible. One way to do this is by dividing the system in different areas that have different requirements for measurement and positioning accuracy.

2.4 Routing station and transport section

The system can be divided into two different areas, as shown in figure 2.5, the so-called routing station and transport section. The routing station is responsible for actuating the substrate in all in-plane degrees of freedom (the motor function), while maintaining the out of plain stiffness to keep the substrate at a constant height (bearing function). This is the area where the substrate is decelerated, rotated, positioned and accelerated. The rotation and centring happens in the positioning area, the main acceleration and deceleration takes place at the shooting areas. The shooting area is followed by the transport section, which consists mainly of bearing cells. Its job is to transport the substrate to its next location without changing the direction in which it is going. With the help of sensors that measure the position of the wafer, actuator cells on the sides of the transport section can correct deviations along the track. Table 2.1 gives a summary of the functional requirements of both parts.

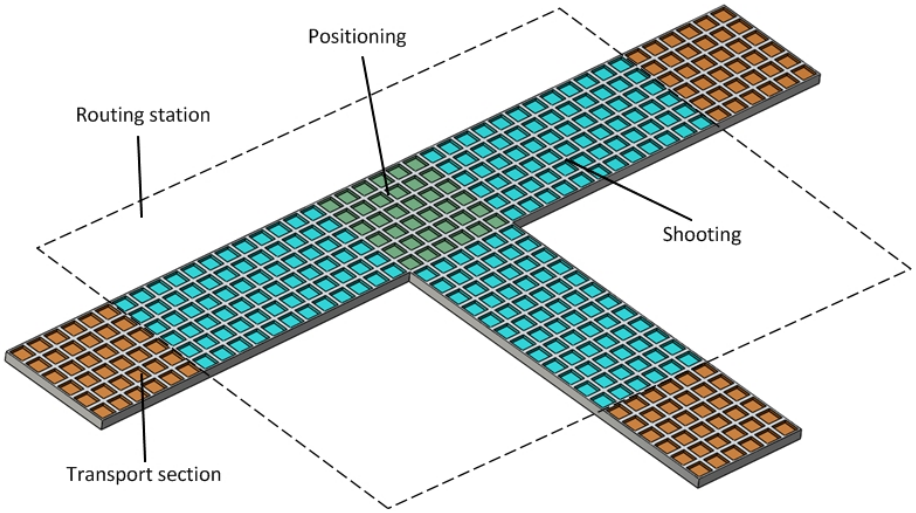

Figure 2.5: The system can be divided into a routing station and a transport section

Table 2.1: Functional description of routing station and transport section

	Requirements
Routing station	Decelerate incoming substrate
	Accelerate outgoing substrate to desired velocity and direction
	Position (centre) the substrate
	Rotate the substrate
	Keep the substrate at a constant fly height
Transport section	Keep the substrate at a constant fly height
	Correct small deviations perpendicular to travelling direction

Substrate and track width choice For this research, a 100 mm wafer will be used to dimension the size of the track and the placement of the sensors. The small wafer is chosen because of its small size and low weight. When eventually a test setup is made to test the working principle and sensors, a small test setup can be used with this type of substrate.

The proposed test system is a transport section with a linear transport line and a perpendicular branch line, as shown in figure 2.5. A possible solution for position sensing is placing the sensors along the sides of the transport and branch line. Using edge detection methods, this layout enables position measurement in both x- and y-direction. For edge detection, the track width should be smaller than the substrate diameter if we assume that the sensors are at the edge of the track. Placing the sensors at the side of the track means that the actuation and bearing cells can cover an uninterrupted area. Besides, the actuator cells in the centre of the track cover the largest part of the wafer and therefore deliver the mayor part of the actuation force. This is why a track is chosen that has a smaller width than the diameter of the substrate.

The measurement in both the x- and the y-direction is equally important. When the substrate circle is enclosed by a square, the positions in between which the measurement distance in both x- and y-direction is equal can be found, they are marked with green dots in figure 2.6. If sensors would be placed at these locations, you would be able to measure the change of position in either direction with an equal accuracy. The distance between two of these points can be calculated with the simple formula shown in equation 2.4.1. The red triangle shown in figure 2.6 has a 90 degrees angle in the centre of the substrate. Therefore the distance between the green dots can be calculated by computing the root of the squared sum of the sides x_1 and x_2. Both sides are equal to half of the substrate diameter (50 mm), which results in an ideal distance of 71 mm between two rows of sensors.

$$S = \sqrt{(x_1^2 + x_2^2)} = \sqrt{(2 * 50^2)} = 70,71mm \tag{2.4.1}$$

For the initial design of the system an actuator cell width of 10 mm will be used. The track should preferably have a width of a multiple of 2 cells, as each actuator cell can create a force in one direction, which means that they are grouped with 4 cells together in the centre of the routing station to ensure equal force in all directions.
When the ideal distance between two sensor rows is applied together with the track size requirement listed above, the result in an ideal track width of 60 mm, equal to six rows of actuator cells. With this composition, the actuator and bearing cells will cover almost 71 % of the wafer. The position sensor rows on each side of the track are ideally located 5.5 mm from the side of the track.
By implementing 2 rows of sensors, the edge of the substrate will be detected at four places simultaneously. This makes it possible to determine the in plane rotation of the wafer, by reconstructing the position of the flat wafer edge (see figure 2.4).

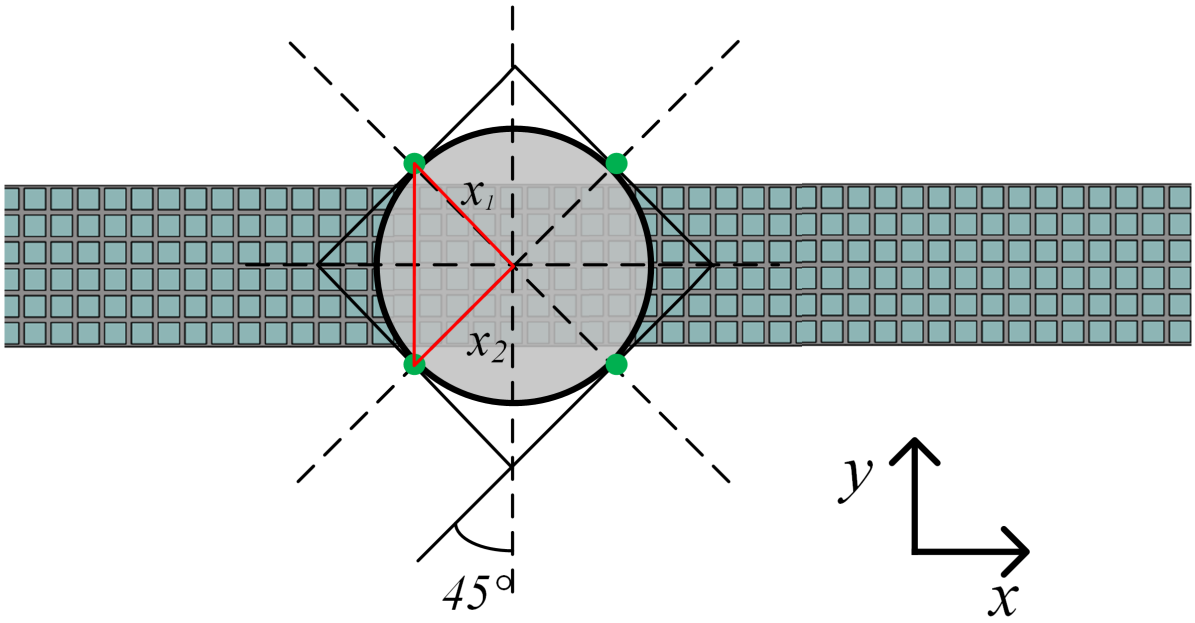

Figure 2.6: Overview of ideal position for sensing the substrate in both the x- and the y-direction

2.5 Dimensions and accuracy

The dimensions of the actuator cells for the system that will be developed in this thesis are taken the same as those in the research done by Wesselingh [1] (see paragraph 2.1). In the positioning part of the system the number of cells that exert a force in each direction has to be equal in order to be able to position, rotate and centre the substrate with the maximum speed in all directions. In the shooting section, where the wafer is accelerated or decelerated, there will be more cells in these two directions. As mentioned before, the track will have a width of 60 mm. There are many ways to travel from one routing station to the next. The required resolution for the (to be developed) system is determined by assuming that the substrate accelerates in a straight line. When the substrate arrives at the next routing station there are several possibilities, this is shown in figure 2.7. The substrate can be given an additional acceleration without stopping it first if it should travel on in a straight line (in the direction of number 4 in the figure). Another option is to decelerate the substrate and accelerate it in a different direction. Ideally the change in direction is done when the substrate is still moving to minimize the handling time. The substrate will then travel with a circular path similar to the dotted red line in figure 2.7.

There are two types of accuracy relevant to this system: The positioning accuracy is the position of the wafer (x,y) with respect to the centre of the track (x_{c1},y_{c1}). The shooting accuracy is defined as the position of the substrate at the end of the track (x_T,y_T) with respect to the position of the substrate if it was transported without any deviation in y-direction $(x_T\ ,y_0)$. Figure 2.8 gives an overview of all parameters required to calculate the accuracy. The diameter of the wafer is taken as ϕ, the ratio between the wafer diameter d and track width w as γ.

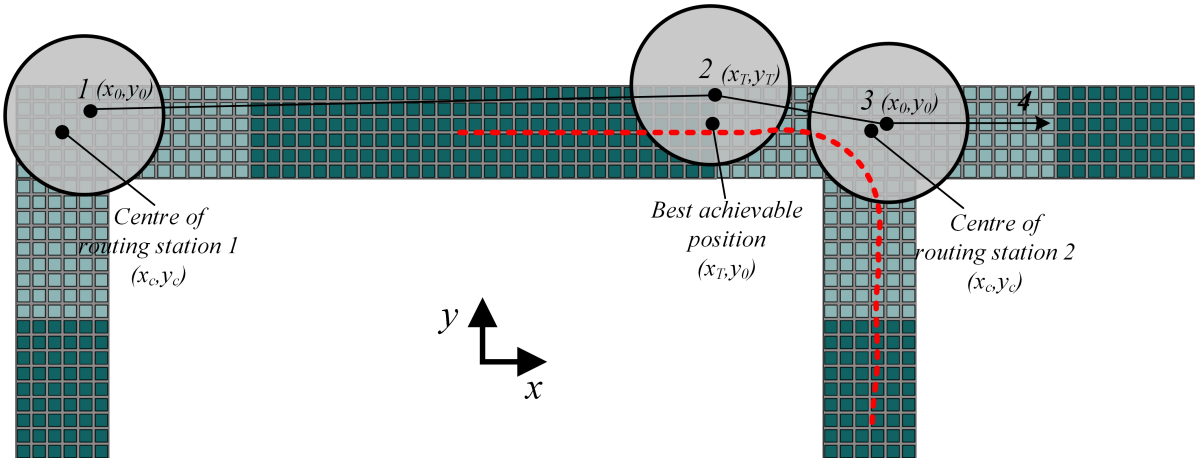

Figure 2.7: Overview of a positioning and shooting sequence along two routing stations and one transport section

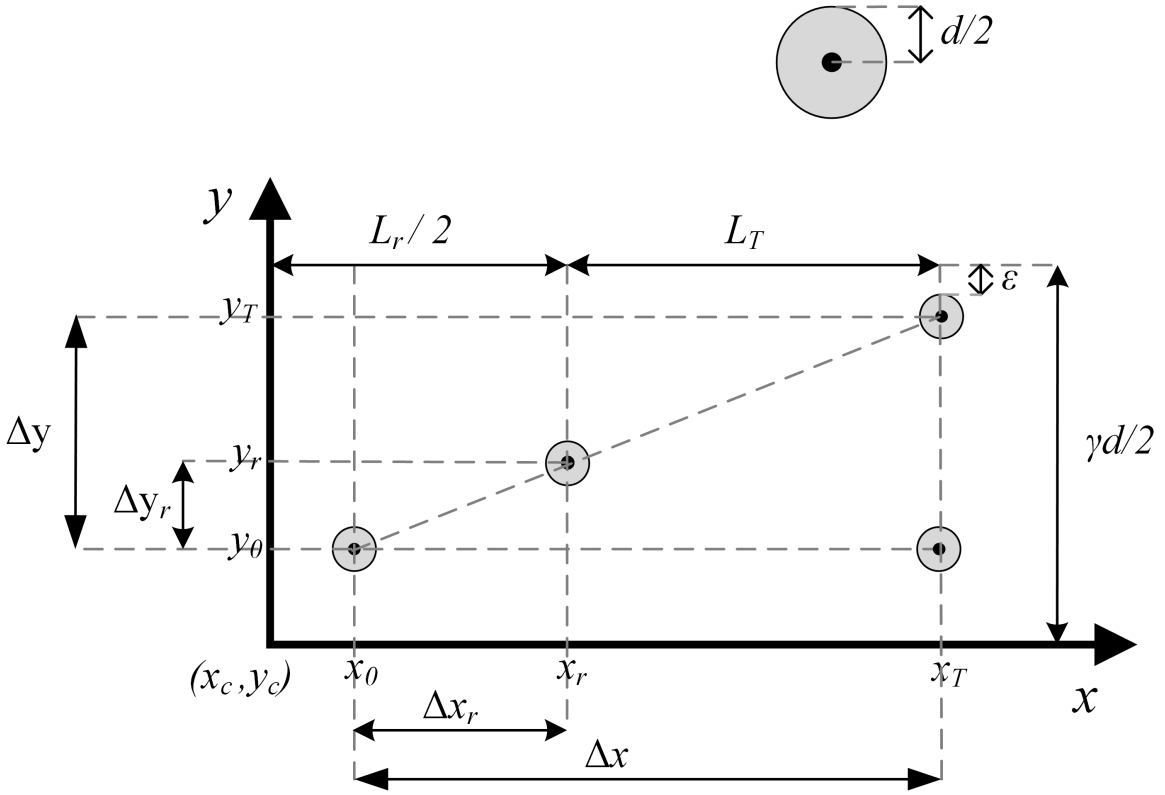

Figure 2.8: Overview of accuracy calculation parameters

When the substrate is decelerated by the routing station, it has to be centred before it can be accelerated again. This is done to minimize the initial offset from the centre (x_c,y_c). The substrate ends up at a position (x_0,y_0) close to the centre. The substrate is then accelerated along the track and ends up in its final position

(x_T, y_T). In between the starting and final position, the location of the wafer is given by (x_r, y_r). In the x-direction the centre of the wafer can be located at x_T, but in the y-direction we should take the position of the edge of the wafer into account, which is positioned at a distance of $\phi/2$ from the position y_T.
The distance travelled by the wafer in the x-direction is equal to half of the routing station length (L_r) plus the length of the transport section (L_T). The distance travelled in y-direction is equal to half of the track width, minus the wafer radius and a predefined safety distance ϵ. The safety distance is introduced as an extra measure to ensure the wafer stays on the track and within the region where the measurement system can determine its position. Due to similar triangles, the relation between Δx_r, Δx, Δy_r and Δy can be defined as in equation 2.5.4. When all previously defined values are substituted into this formula, this results in equation 2.5.5.

$$\Delta x = x_T - x_0 = L_r/2 + L_T - x_0 \tag{2.5.1}$$

$$\Delta y = y_T - y_0 = \gamma d/2 - \epsilon - d/2 - y_0 \tag{2.5.2}$$

$$\Delta x_r = x_r - x_0 \tag{2.5.3}$$

$$\frac{\Delta x_r}{\Delta x} = \frac{\Delta y_r}{\Delta y} \tag{2.5.4}$$

$$\Delta y_R = \frac{\Delta x_r * \Delta y}{\Delta x} = \frac{(L_r - 2x_0)(d(\gamma - 1) - 2\epsilon - 2y_0)}{L_r + 2L_T - 2x_0} \tag{2.5.5}$$

With equation 2.5.5 the shooting accuracy can be calculated when you insert the desired routing station length (see paragraph 2.7), transport section length, track width and safety distance. This results in the position and shooting accuracy mentioned in paragraph 2.6.
Figure 2.7 gives a schematic overview of a positioning and transport sequence between two routing stations. In the first routing station (the light blue part in figure 2.7) the wafer is positioned at position one. The positioning accuracy with which the wafer can be positioned is the maximum distance between the initial position of the wafer and the centre of the routing station (x_c, y_c). The wafer is then propelled across the remaining part of the routing station and the transport section (the dark blue part) to position 2. The place where the wafer enters the second routing station is taken as the final position (x_T, y_T). The difference between the final position and the best achievable position (x_T, y_0) is equal to the shooting accuracy. Afterwards the wafer is moved to the centre of the second routing station at point 3 and then it is ready to be shot away to point 4 along the second transport section.

2.6 System requirements

The specifications that we want to reach with the overall system have been determined by a combination of the wishes from the most important stakeholders and the information provided in the previous paragraphs. Requirements for the subsystems are listed below, except for the measurement system, for which details can be found in paragraph 3.1.

1. Dimensions, speed and accuracy of the overall system
    - Wafer speed of at least 1.7 m/s
    - Throughput of 1 wafer per second or 3600 per hour
    - Track width of 60 mm
    - Positioning accuracy of 150 μm
    - Shooting accuracy of 765 μm
    - Resolution of 15 μm
2. Actuators

- Capillary inlet restriction = $13 * 10^{-3} Pa/m^3 s$
- Air flow should be minimized
- The location of the pump should be close enough to the valves to prevent a delay

3. Valves
   - The volume flow through each valve will be 0 to 4000 mm^3/s
   - Proportional valves are preferred (variable resistance of valve to ensure possibility of partly opening the valve, which corresponds to the ability to exert only a part of the maximum force)
   - Quick response time of valve to input signal (high bandwidth)

2.7 Routing station size

The maximum speed with which the substrate has to be able to travel is chosen to a similar speed in comparable systems already on the market at 1.7 meters per second. The number of actuator cells which is needed to create enough force to give a 100 mm wafer this velocity can be found by calculating the time and distance it takes to stop a wafer which is moving with 1.7 m/s. The maximum speed that can be reached with the system depends on the number of actuation cells in the routing station and the pressure difference between the inlet and outlet of each actuator cell. The speed of a substrate increases with an increasing pressure difference and air flow when the number of actuator cells is kept constant.
For the calculation of the ideal routing station length equation 2.7.1, 2.7.2 and 2.7.3 are used. Equation 2.7.1 is directly derived from the research of Wesselink [1]. It explains how the force exerted by one actuator cell (F_a) is determined by the system dimensions, the pressure difference between the inlet and outlet channels ($p_2 - p_3$) and the velocity of the wafer ($\dot{x}_s$). The pressure difference is a set variable which will not change during acceleration or deceleration of the substrate. This means that the force exerted by an actuator cell is directly linked to the wafers velocity. The force exerted on the substrate will decrease with increasing velocity.

The minimum required routing station length can be found by calculating the distance that a wafer that is moving with 1.7 m/s has to travel before it is brought to a complete stop. A method that uses the kinetic energy of the wafer has been chosen to calculate how fast it is moving. The force exerted by the actuator cells slows the wafer down, which reduces the kinetic energy of the wafer. This back an forth calculation between the exerted force and the velocity is done by using an iterative process where the time is taken as the iteration variable. This method was chosen because it results in a simple formula (equation 2.7.3) due to the lack of friction and other forces acting on the wafer. The main goal of this calculation is to efficiently determine the breaking distance of the substrate. By using the kinetic energy you can use the direct relationship between F and v. We could use the acceleration and force relationship to determine the travelled distance, but this would require an extra integration step, which reduces the accuracy of the calculation. For the first part of the calculation, when the wafer enters the routing station with actuator cells, this calculation is quite accurate. There is room for improvement for the part where the velocity of the wafer gets lower than 0.5 m/s, because at this point the calculation of the distance travelled by the wafer gets influenced heavily by the chosen iteration step size and at this moment does not guarantee a converging solution yet.

The time starts when the wafer reaches the border between the shooting section and the routing station. The velocity with which the wafer is travelling is taken at 1.7 m/s. When the velocity of the wafer is known, the kinetic energy of the wafer can be calculated using equation 2.7.2. When the wafer enters the routing station, the force of the actuators starts to slow it down. Equation 2.7.1 shows how the force exerted by one actuator cell at a certain velocity can be found [1]. The force continues to increase because more actuators will be able to exert a force on the wafer as it continues its path above the routing station. When the time of one simulation step has passed, the travelled distance in this time can be calculated using the current velocity. The new velocity can then be calculated by subtracting the energy exerted by the actuators multiplied by the distance travelled by the wafer, from the current kinetic energy. This new number can then be used to calculate the new (reduced) speed (equation 2.7.3).

$$F_a = F_p + F_d + F_s = \frac{(h-t)b}{2}(p_2 - p_3) - \left(\frac{w^2 + wb + wl}{t} + \frac{bl}{h}\right)\mu\dot{x}_s \tag{2.7.1}$$

$$E_{kin} = \frac{1}{2} m v_0^2 \tag{2.7.2}$$

$$\frac{1}{2} m v_1^2 = Fs + \frac{1}{2} m v_2^2 \tag{2.7.3}$$

F_p, F_d and F_s represent the forces created at the pocket, dam and sides respectively. The shape of the actuators is square, which results in an equal value of b and l. This simplifies equation 2.7.1 to:

$$F_a = \frac{(h-t)b}{2}(p_2 - p_3) - \left(\frac{w^2 + 2wb}{t} + \frac{b^2}{h}\right)\mu \dot{x}_s \tag{2.7.4}$$

The process of calculating the new velocity is repeated every 0.0001 seconds. The required time and distance it takes to stop the wafer decreases when the pressure difference is increased. The results is shown in table 2.2. An overview of the speed during the decelleration, when the wafer has entered the actuator cell area, can be found in figure 2.9. In this calculation it is assumed that all actuator cells exert a force in a direction opposite to the direction in which the wafer is moving. The wafer moves with an initial speed of 1.7 m/s when it enters the routing station. In the beginning the wafer only covers a few actuator cells. When the wafer travels further along the routing station, more cells can exert a force on the wafer, which means that the decelleration rate increases.

Pressure difference (kPa)	Length required to stop wafer (m)	Time (s)
10	0.1998	0.2569
15	0.1656	0.2104
20	0.1464	0.1839
25	0.1337	0.1663
30	0.1245	0.1535
40	0.1119	0.1359
50	0.1034	0.1241
60	0.0973	0.1159
70	0.0925	0.1107
80	0.0886	0.1060

Table 2.2: Results for an iteration distance time of 0.0001 seconds

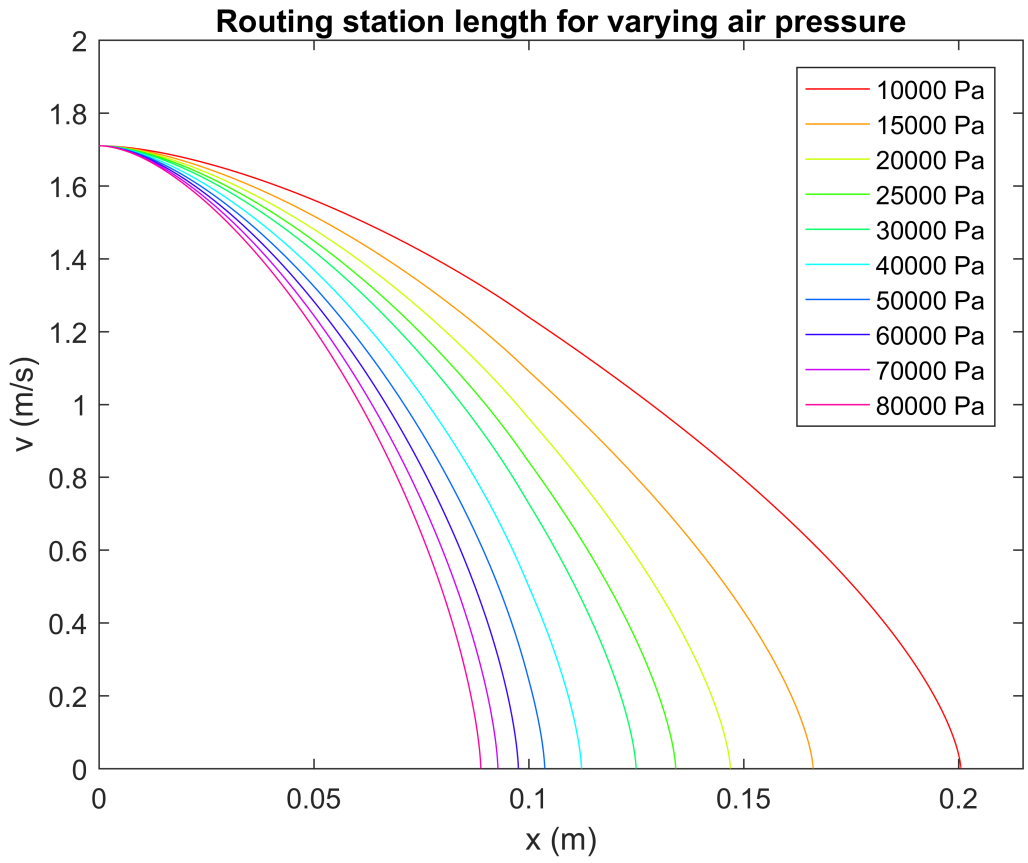

Figure 2.9: Routing station length for varying air pressure differences - wafer enters actuator cell area at 1.7 m/s

2.8 Actuator cell alignment

The calculations in paragraph 2.7 are valid for a system where all actuator cells exert a force in the longitudinal direction, the direction of the long bearing lane on which the wafer has been travelling. In the designed system, one actuator cell can only exert a force in one direction. Therefore it is not realistic to assume that all actuator cells will exert a force in the same direction. This would limit the performance of the system because then it would only be possible to accelerate or decellerate the substrate in the longitudinal direction. In reality the wafer can also deviate in lateral direction, perpendicular to the predicted path. If an equal amount of force has to be delivered in each direction, the routing station will be four times as long (we want to be able to move the wafer in the x-y-plane, so we need two orientations per axis to make this work).

For the positioning (central) part of the routing station, the force which can be exerted in each direction should be equal to guarantee a quick positioning of the substrate. For the shooting section, we mainly want to accelerate and decelerate the wafer in longitudinal direction, it does not have to be moved in the lateral direction with a high force. There only have to be some cells which can actuate the wafer in lateral direction. The layout in figure 2.10 shows a way to orient the shooting section actuator cells which decreases the acceleration time. With this layout five out of twelve actuator cells exert an acceleration force and five others in the opposite direction. The remaining two cells each exert a force to one of the remaining sides. Table 2.3 shows the values for the time and distance required to stop the wafer for this actuator cell layout.

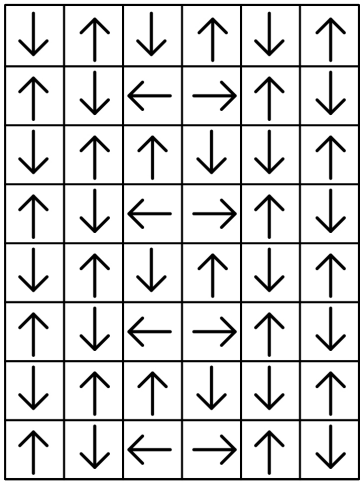

Figure 2.10: An efficient layout for the orientation of the actuator cells in the shooting section

Pressure difference (kPa)	Length required to stop wafer (mm)	Time (s)
10	0.4795	0.6166
15	0.3973	0.5050
20	0.3513	0.4414
25	0.3209	0.3991
30	0.2989	0.3684
40	0.2685	0.3262
50	0.2481	0.2978
60	0.2335	0.2782
70	0.2221	0.2657
80	0.2126	0.2544

Table 2.3: Required length of shooting area with actuator cell layout as shown in figure 2.10

With these overall system requirements we have determined the main factors for the layout of the system. We can now focus on improving the knowledge and performance of several components. Chapter 3 describes the requirements and specifications of the measurement system with greater detail.

3

Measurement system

The purpose of the measurement system is to provide data about the location of the wafer. This information is then used by the actuation system to accurately position and move the wafer. Besides, the air flow can be turned off in locations where the wafer is not present, which saves a lot of energy.

3.1 Requirements and specifications

The measurement system must meet several requirements which are determined by both the wishes of the stakeholders that are involved for this project and by the layout of the system. It has been decided in chapter 2 that the bearing lane will have a width of 6 actuator cells (and thus 60 mm). The sensors will be placed next to the track, in a 10 mm area on each side. With this setup, the ideal distance between the two rows of sensors is 70 mm. Figure 3.1 shows a cross-section of the system with dimensions. To guarantee that the actuation is not disturbed, the measurement has to be contactless. The upper side of the transportation system should remain free from any actuation or sensing components, to allow space for the process steps the wafer has to go through. For the measurement system this means all sensing must be done on the bottom side of the substrate. The sensors have to be able to measure the surface of the wafer, even if it has a very low roughness and a high reflectivity. Sensors with a diameter smaller than 10 mm are preferred, so that they can be placed at the calculated distance that was calculated with equation 2.4.1. If the sensing would be done at the far edge of the wafer, a deviated wafer would mean no measurement results. The number of sensors will mainly depend on the sensor type, but also on where they are placed along the system.

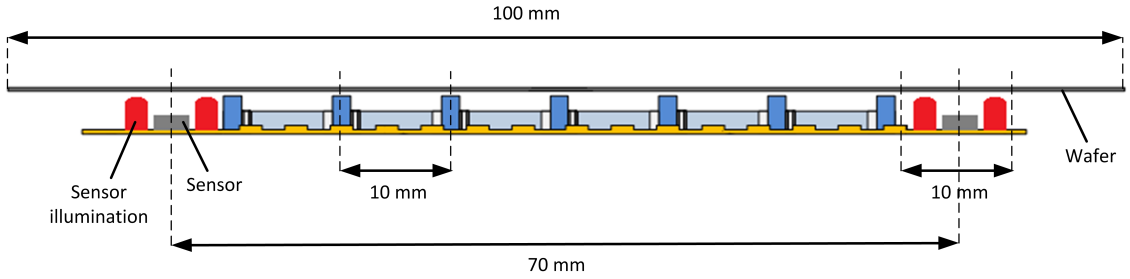

Figure 3.1: A cross section of the system with space for the sensors next to the actuator cells

The specifications for the measurements are higher than those of the overall system. This is because the overall system accuracy includes the error caused by the sensing system, as well as the error caused by the positioning system. The specifications for the measurement system are listed below:

- Accuracy of 15 μm
- Resolution of 3-5 μm

- Bandwidth of 1.5-2.0 kHz

Figure 3.2 shows a top-side view of a bearing lane. The measurement in longitudinal (x-) direction is needed to determine when the next group of cells has to be turned on/off. With the lateral (y-) direction measurement we can measure the deviation of the wafer from the centre. This means that ideally you would measure the position in lateral direction and the velocity in longitudinal direction. In reality you will measure either the position or the velocity in both directions, depending on the sensor type (assuming only one type of sensor is used). The position or velocity in the other direction will have to be calculated from the available sensor data.

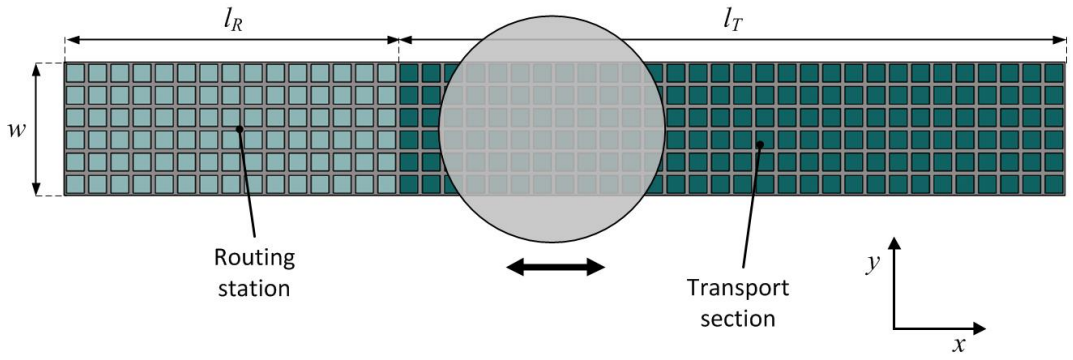

Figure 3.2: Top side view of a routing station and transport section

3.2 Location of sensors

As mentioned before, the location of the sensors will be on the sides of the track. In theory, there would be plenty of space for the sensors, we are not bound by a maximum system width. However, the wafer which will be used as the main substrate type has a diameter of only 100 mm. Therefore, the sensors have to measure close to the side of the actuation or bearing system, otherwise they might miss the wafer in their measurement. The wafer is allowed to deviate several millimetres from the centre of the track, therefore there is a space of about one centimetre on each side which can be utilised for sensing. If the centre of the measuring space a sensor is placed, the distance between the sensors on each side will be $70mm$. The sensors measure if there is a substrate present or not. If sensors would be placed along both sides of the track over the whole length as shown in figure 3.3, there are always 4 transition points measured. This would mean that besides the position of the wafer in both lateral and longitudinal direction, the in plane rotation of the wafer can also be measured. The 'edge' of the wafer will only be present at one measuring point. With one of the four distances shorter than the others, the in-plane rotation can be determined. There are a few exceptions: The length of the flat side is only 32.5 mm [26], this is shorter than the distance between two sensors ($71\ mm$, see paragraph 2.4) so when the edge is oriented close to the lateral or longitudinal plane of the bearing lane, it is not measured. In all other cases there are two orientation possibilities that fit the same measurement data since the wafer edge is symmetric. By comparing several succeeding measurements, this problem can be eliminated.

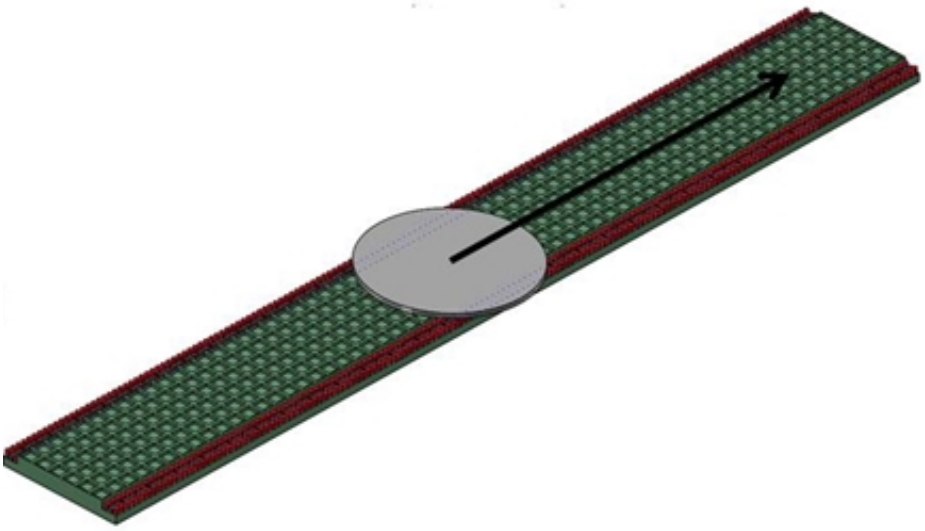

Figure 3.3: Transport section with sensors on both sides of the track

The flat side of the wafer can be used to determine the wafer orientation. The shape of the piece of material that is 'missing' between the circumference of the circle and the flat side of the wafer is called a sagitta. The length of the sagitta (s) can be calculated using formula 3.2.1. For this we need to know the radius of the wafer (r) which is equal to 50 mm and the half chord length (l). The half chord length is equal to half of the length of the horizontal chord that cuts of a portion of the circle (32.5 mm). Figure 3.4 gives a schematic overview of the variables used in equation 3.2.1. The length of the sagitta of a 100 mm wafer is 2,7 mm.

$$s = r - \sqrt{(r^2 - l^2)} \tag{3.2.1}$$

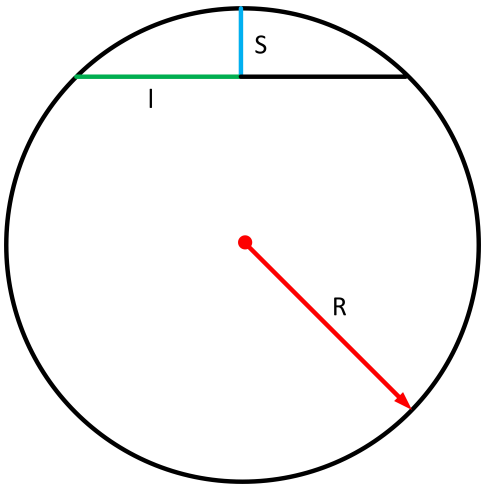

Figure 3.4: Schematic overview of half chord length (l), sagitta length (s) and radius (r)

With edge detection, four points along the wafer edge will be detected. With three points along the circumference of a circle, the location of the centre can be determined. The standard formula for a circle is shown in equation 3.2.2. The coordinates of the centre of the circle are (x_c, y_c). All measured points have an x- and y-coordinate which can be substituted in the formula. This results in three formula's with three unknown variables (x_c, y_c and r) which can be solved easily. The radius of the wafer is known. If the calculated radius is equal to 50 mm, the calculated coordinates for the centre of the wafer are correct. If the calculated radius has a different value, one of the three points measured the flat side of the wafer. Due to the four measuring points, it is always

possible to calculate the location of the centre of the wafer, since there are at least three points that lie on the circle. With the three other calculated values it is now possible to locate the two possibilities for the position of the flat(the shape is symmetrical).

$$(x - x_c)^2 + (y - y_c)^2 = r^2 \tag{3.2.2}$$

This type of sensor placement always gives you a reliable measurement, but it requires a high number of sensors. For the routing station this is a suitable solution as it requires a very high accuracy in order to shoot the substrate with a high enough precision towards its next location. For the transport section, we mainly want to know the wafers speed along the length of the track to predicts its location, and whether the wafer deviates too much from the centre of the track. This can be done with fewer sensors. One option would be to only measure on one side of the track. A downside would be that when the flat side of a deviated wafer is located parallel to the track, there will be moments when the wafer is not detectable. Another possibility is to measure for a certain length and predict the wafer speed and deviation with this measurement for the distance over which this is accurate enough. After this length the next measurement area should be implemented. When this is done it has to be assumed that the substrate will not move in an unexpected direction or have sudden changes in velocity. This can only be guaranteed if it is known for sure that there will be no irregularities in the air flow in the room. Due to the very low resistance of the air bearing transportation, the system is sensitive to outside disturbances.

4

Sensor selection

There are many types of position and displacement sensors. An overview of the most common contactless sensing methods is given by the list in appendix A. The different working principles are rated for a variety of characteristics that are important when selecting a sensor. The main criteria for sensors in this system can be found in paragraph 3.1. The physical principles with which the sensors work are very different. The main selection criteria are resolution, bandwidth, susceptibility to disturbances and cost effectiveness. The three sensing methods that look most promising will be explained and compared in paragraph 4.1. For the most suited category, several sensor types will be looked at into more detail in paragraph 4.3.

4.1 Sensing methods

4.1.1. Capacitive sensing

Capacitive sensors can find the proximity of a substrate by measuring the difference in capacitance between the substrate and plain air. The sensor output will have a constant value when there is no substrate present, the value will increase with an incoming wafer. Figure 4.1 shows how this sensor type can be integrated into the system. Two small metal plates will be placed close to each other (without touching), each with a different polarity. By measuring the output voltage you can determine if or how much of the substrate is flying above the sensor. When the sensor is completely covered by the substrate, the output value is once again constant. With this constant value you can measure the height at which the substrate is flying. The main advantage of this sensor is that it can measure both wafer location and height. The height measurement is done by initializing the sensor, by measuring the capacitance at different fly heights of the substrate. These data are then saved and can be used to determine the wafers fly height afterwards. Disadvantages of capacitive sensing are the relatively low resolution in the x-y-plane in comparison to other sensors. This means you would need a lot of sensors to reach an accurate enough resolution for the in plane location.

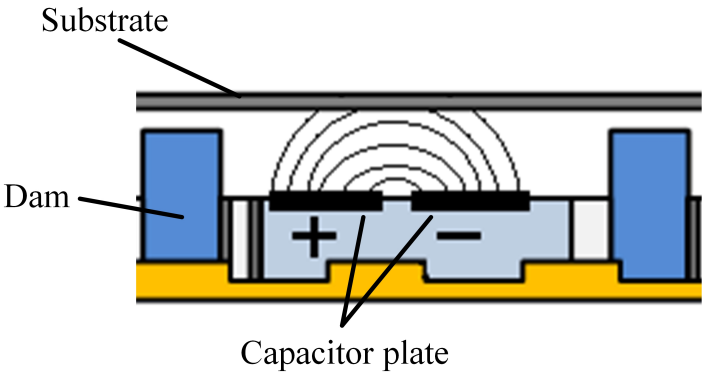

Figure 4.1: Working principle of capacitive sensing

4.1.2. Optical displacement sensing

Optical displacement sensing uses optical sensing to determine the displacement of an object. There are a lot of optical displacement sensors like the mouse sensor, which was used by Mok [24] to measure the sample of a microscope. This sensor compares a pixel field at the current moment to the field it received the moment before. By comparing the two images, the distance moved by an object can be determined. Figure 4.2 shows what this sensor looks like. The big advantage of this sensor is that it is used in a lot of applications, which means there are many inexpensive varieties available on the market. This sensor requires a certain roughness of the substrate surface to make it possible to track the object. To ensure that the surface of the wafer can be detected by a mouse sensor I have measured a moving wafer with a mouse sensor. The mouse sensor was attached rigidly to a surface and the wafer to a moving stage. By positioning the wafer very close to the sensor, to simulate the fly height, and then moving the stage, the detection of the wafer by the sensor can be tested. The stage was first moved with small steps, and afterwards with a continuous motion and it appeared that a wafer can be tracked. The mouse sensor gives output values of the movement it has detected in both the x- and y-direction. Depending on the surface roughness and reflectivity of the material, the output value range can be high or low. A high output range is preferred because with a larger difference in outputs a higher accuracy can be reached. The difference in output values for the wafer was small. The sensor could detect when the stage moved, but the number of output data it gave back was a different value for each step of the same size. This could be caused by the wafer, it had a lot of scratches on the surface which could have influenced the sensor output. A new wafer would probably give a more equal response, but the type of material that the wafer is made of will always give a small range in output values compared to other materials. The resolution of the mouse sensor does therefore not reach 15 micrometer, but it can be enhanced with a mirror system as designed by Mok [24]. This would increase the costs and complexity of the overall sensor system. Another disadvantage of this sensor enhancement is that it is not designed to measure objects that move large distances. There is an accumulating error which has to be reset frequently. Resetting the sensor takes time which decreases the bandwidth of the system.

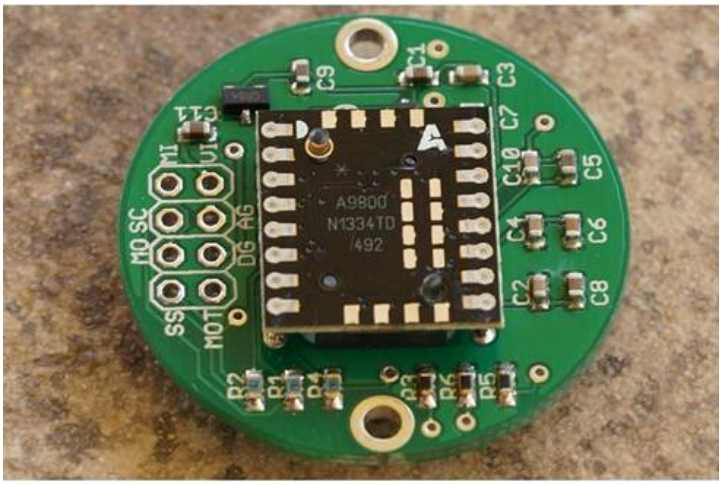

Figure 4.2: Mouse sensor

4.1.3. Optical position sensing

Optical position sensing uses optical sensing to determine the position of an object. A common type is an interferometer, which uses laser reflection to determine an object's location. The outgoing laser beam reflects from the objects surface and the sensor can calculate the distance to the object by comparing the time between sending and receiving the light. The substrates for which this system is designed are very thin, which makes the reflective surface very small. Lasers are too large to place underneath the system (this would measure the height and wafer presence), and this would require too many (expensive) sensors, therefore an interferometer is not an option. There are other optical position sensors that can measure the wafer presence and are small enough to integrate into the system. Examples are optical fibres, which send out a light and measure the light intensity of the reflection. When these fibres are placed close together in a row, a 'new' type of sensor is created called a linear sensing array. This is a compact form of many photo diodes and gives a high resolution data output of received light intensity. Another type is the position sensitive device, which gives a current output that lets you find the location of the highest received light intensity. This could be used to determine the location of the part of the sensor that is covered by the substrate and in this way define an accurate y-location of that particular wafer edge.

4.2 Sensing method comparison

Table 4.1 gives an overview of the most important criteria for each sensor type. The capacitive sensing method has the advantage of measuring both height and wafer presence (position). The height measurement can be very accurate, but the position measurement is much less accurate. This can be solved by placing multiple sensors close to each other (without letting the different metal plates influence each others capacitance). However, this would require a large area on the side of the track (this number of sensors could not be integrated into the air cell pockets anymore) and a lot of processing power to form an accurate pixel field of the sensor's location. Optical displacement sensing seems like the best option, but unfortunately due to the accumulating error the bandwidth is reduced by such a factor that the sensor cannot fulfil the requirements (mainly due to the required substrate speed of 1.7 meters per second). Then we are left with the optical position measurement. This sensing method can reach the right accuracy, although there are still many sensors necessary to be able to calculate the centre (and position) of the substrate. The sensors themselves are not very expensive, but there is a lot of post-processing needed before an accurate pixel field can be created. When the costs of the processing equipment can be kept within the financial limits this sensor type will be the best choice.

Table 4.1: Comparison between three different sensor types

Sensor type	Capacitive sensing	Optical displacement sensing	Optical position sensing
Working principle	Measure the varying capacitance (wafer is present or not) between two metal plates located on the surface of the actuation system.	Overlapping two pictures and calculating the difference between them	Edge detection by locating the transition between high and low light intensity
Sensor size	The metal plates can be very small and can be integrated into the actuator cells which saves space	Most mouse sensors have a diameter of a few centimetres	Small sensors exist, but most optical position sensors require extra illumination
Resolution	Height resolution is within micrometer range, but in-plane position measurement resolution is around 0.1 mm	Typically between 10 and 20 μm, can be enhanced with complicated mirror system	Minimum resolution is around 2 μm
Number of sensors required	Due to the relatively low resolution many sensors are required	Sensors can be placed at intervals along the track. When at least two sensors at a time can measure an edge of the wafer the velocity in both the x and y direction can be measured with high accuracy.	At least three edges have to be detected simultaneously to calculate the centre of the substrate. This means sensors will have to be placed on both sides of the track.
Complexity	Complex due to high amount of sensors required. All data will have to be processed and combined to create a pixel field of where the substrate is present.	Due to offset with increasing measurement distance the sensor will have to be reset frequently, which will decrease the bandwidth drastically	The complexity varies depending on sensor type, continuous sensors require less processing power than a high number of analog values.

In this paragraph it was concluded that for this particular system the preferred sensor type is optical displacement sensing. The optical fibre, position sensitive device and the linear sensor array are three possibilities within this field. Paragraph 4.3 to 4.3.3 give an in depth summary of the characteristics, performance and complexity of each sensor. Then once again a comparison between them is made to conclude this chapter in paragraph 4.4. For each sensor type a list of available products has been made, it can be found in appendix B.

4.3 Optical displacement sensing

4.3.1. Optical fiber

Figure 4.3 gives an overview of the working principle of an optical fibre. Optical fibres are flexible and transparent fibres made of plastic or silicium with a very thin diameter. Light is transmitted through the fibre at high speeds. Optical fibres are used in many applications including fibre-optic communications, where data are transported through the fibres instead of metal cables. The fibres can also be used as a sensing device by using two fibres, a light source and a receiver. The first fibre transports the light from a source to its other end where it shines on an object. This object reflects the light into the receiving end of the second fibre. This fibre transports the reflected light to a receiver which determines the intensity of the received light. The amount of reflected light determines the position of the object compared to the sensor. This sensor can be used for height measurement and edge detection.

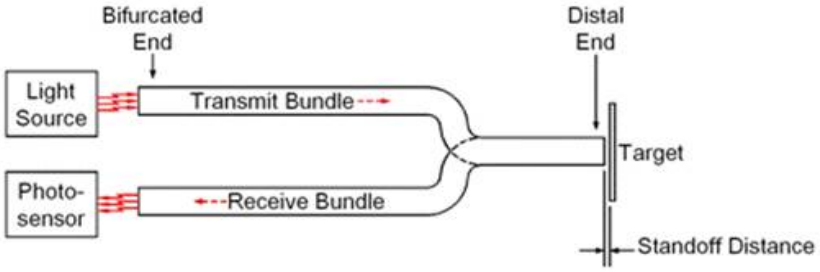

Figure 4.3: Optical fibre working principle

Characteristics The size of an optic fiber is ususally around 100 to 500 μm in diameter [25]. This is the size of the optic area, with a coating surrounding the area the sensor size increases easily to a few mm. The resolution for height or distance measurement can be as small as 1 μm. The range at which the sensor operates varies widely. The range depends on the sensitivity of the receiving fibre, the fibre width, light intensity, reflectivity of the object, etc. Due to the simple design a very high bandwidth can be reached. Bandwidths of 20 to 100 kHz are not uncommon. The best suitable optic fibre for this system would have a high bandwidth and sensitivity (high change in the output voltage due to small variation in measurement distance), a small diameter and a high resolution.

4.3.2. Position sensitive device

Position sensitive devices/detectors (PSDs) use the photoelectric effect to determine position. PSDs can supply either continuous or discrete position data. Discrete position sensors consist of a pixel field where each pixel generates a separate value depending on the brightness it is exposed to. A continues PSD consists of a uniform, isotropic resistive layer on top of a semiconductor substrate. Continuous PSDs have a much higher resolution because they are not limited to a certain number of pixels. When a light spot shines on the sensor, it creates an electric charge at this position which is proportional to the intensity of the incident light. The charge travels through the resistive layer and creates a current on each side of the sensor (electrode X_1 and X_2 in figure 4.4). The position can now be determined with these currents, as they are inversely proportional to the position where the light hit the sensor [8].

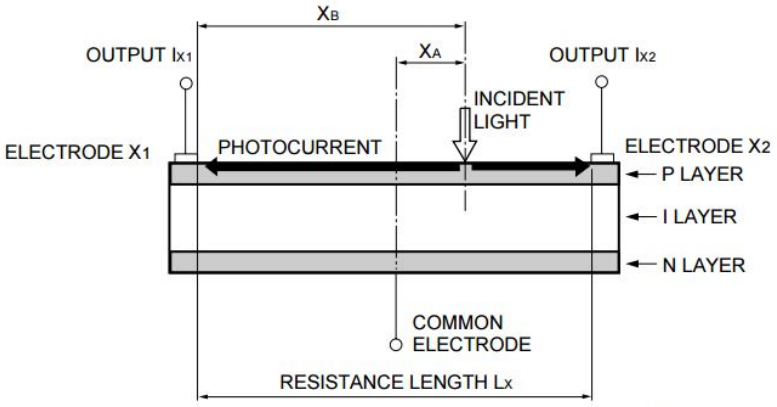

Figure 4.4: Cross sectional view of a one-dimensional PSD [8]

Characteristics A position sensitive device can be either one or two-dimensional. A duo-lateral (two-dimensional) PSD has the same working principle as the one-dimensional sensor, but instead of two there are four output electrodes, two for each direction. The sensor has two separate resistive layers. The x-location electrodes are connected to one layer, the y-direction measurement is done with the other. A tetra-lateral PSD has four electrodes connected to one layer. It has a faster response than the duo-lateral PSD, but there is more position distortion between the electrodes. The most important characteristic features are listed below:

- The saturation of the photo current: The saturation photo current is equal to the photocurrent measured when the entire active part of the sensor is illuminated. When the PSD is not saturated it has a good output linearity. This linearity is impaired when there is too much background light or when a large part of the active area is illuminated, resulting in a position output which is not accurate.
- Dark current: When the PSD is in a dark state and a reverse voltage is applied, a small current still flows, this is called the "dark current". The sensor gives the best performance when the (reverse) saturation current (the current measured when the whole sensor is illuminated) is lower than the dark current. This results in a high signal to noise ratio. The performance of the sensor decreases quickly when the saturation current is higher than the maximum allowable dark current [9].
- Signal to noise ratio: The reverse/forward voltage applied to the PSD can be increased to get a high signal to noise (S/N) ratio. Each sensor type has a different voltage characteristic. At a certain point the current will drastically increase, this point is known as the breakdown voltage. When higher voltages are applied the sensor performance decreases severely.
- Rise and response time: The rise or response time is a measure for the time it takes for the signal to be extracted (as a current) from the sensor by an external circuit. It is described as the time it takes the output current signal to rise from 10 to 90 percent of its maximum value.
- Spectral responsivity: The range of spectral responsivity of most sensors is for light with a wavelength between 300 to 700 and 1100 nm. The photo sensitivity is typically highest somewhere between 800 and 1000 nm. This means you will have to provide (infra) red illumination for the sensor to work in its most sensitive range. The maximum photo sensitivity is also called the peak spectral responsivity and is expressed in mA/W.
- Position detection error: PSDs always have a position detection error, which is the difference between the calculated and the actual location of the incident light. The error is around zero in the middle of the sensor, and increases towards the edge.

Electronic processing As mentioned before, the output of a PSD is given by two to four photo currents. We have to convert the current values to voltages in order to process them correctly. This can be done with a circuit as shown in figure 4.5. You have to be careful with the component selection because this influences the amount and type of noise which is measured in the sensor signal.

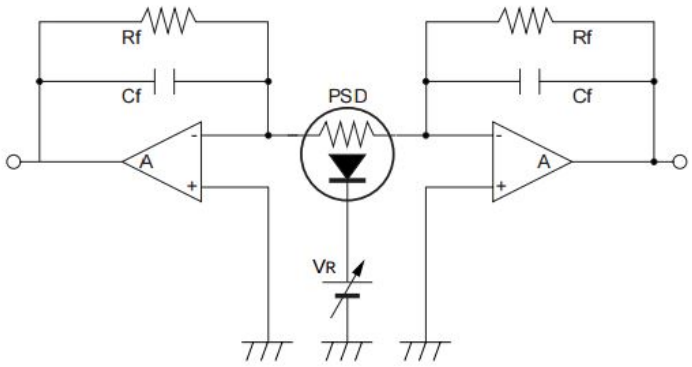

Figure 4.5: Simple current to voltage converter for a one-dimensional PSD with an operational amplifier [8]

PSD selection criteria The best suitable sensor for this system would be a continuous, one-dimensional PSD with a minimum length of 10 mm, and a maximum width of 5 mm. Continuous PSDs give a much higher resolution which is needed to fulfil the specifications for the measurement system. The minimum length is required to keep the number of sensors used within certain limits. The width restriction is due to the 10 mm width available for sensors next to the actuator cells, and infra red illumination will have to be integrated into this space as well. Most two-dimensional PSDs are wider than this space. The resolution and the position detection error should be as low as possible. The resolution (reduced by the position error)

should be in the order of micrometers to reach a high enough precision with the measurement system. A high saturation level would be beneficial as we are not measuring a light spot but the transition between reflected and non-reflected light.

4.3.3. Linear sensor array (LSA)

A Linear sensor array consists of an array of photosensitive diodes. The number of photo diodes defines the amount of 'pixels' of the sensor. Each pixel measures the incident light it receives and generates an equivalent output voltage. This voltage represents the amount of light to which the pixel is exposed. Due to the one sided sensing constraint, both the system and the illumination would have to be positioned underneath the substrate. The photo diodes then measure the amount of light reflected by the wafer when they are covered by the substrate.

Characteristics Linear sensor arrays have several selection criteria which are relevant to the system performance:

- Clock speed: The clock speed is the speed at which one pixel of the sensor can communicate its value to a data processing unit (like an ADC, see paragraph 5.3). The required clock speed depends on the pixel density of the sensor.
- Pixel density: The pixel density is the number of pixels per unit area. It is preferably as high as possible.
- Dynamic range: The dynamic range of the linear sensor array defines the number of voltage output values that can be defined by the sensor over the relevant output voltage range.
- Integration time: The integration time of a sensor gives information about how long it takes for the next sensor output cycle to start.
- Output voltage: In a typical LSA the output voltage value for each pixel is sent out in a string. When the last value has been given, the cycle starts over again.
- Illumination: A linear sensor array typically needs additional illumination to increase the resolution. The sensor is usually sensitive to light of a certain wavelength.
- Size: In the measurement setup, there is not much space for the measurement device. The sensors are not allowed to move too far to the side because then a deviating wafer could not be detected anymore. Furthermore, the sensor has to be illuminated on both sides. This means the sensors should have a small width.

4.4 Sensor type comparison

The optical fibre is a very cheap solution, but only gives a one-pixel measurement output. Many sensors would be needed to provide sufficient measurement resolution in the x-y-plane. The solution for this is to place many of them in a row to create a linear sensing array. This sensor type is not very expensive and can give the position of the edge of a substrate with a high accuracy. The other option would be a position sensitive device. Continuous PSDs give a high resolution. However, there might be a problem with using the PSD: they are not made to measure the size of an illuminated area, but to track the exact position of a laser or light spot which is usually not bigger than a few hundred micrometers. When for example three quarters of the sensor will be covered with high intensity light, the saturation level of the sensor is usually already reached. From the saturation point on, the measurement will not be accurate any more. Therefore we will be using the LSA sensor.

4.5 Selection of Linear Sensor Array

An overview of linear sensor arrays that can be ordered within a limited time span can be found in appendix B. When the sensors are compared on the characteristics of dynamic range, bandwidth, pixel density, clock speed, costs and size, there are two LSAs that seem the most suitable. The TSL1412S sensor has 1536 pixels

in a row, and a stroke of 94 mm. The TSL1401CL sensor consists of 1 row of 128 pixels and has a stroke of 8.1 mm. Both sensors have a dynamic range of 4000 (72 dB) and can operate at a speed of up to 8 MHz. The number of pixels of the sensors determines how often data from each separate pixel can be sent through to the ADC per second. Equation 4.5.1 shows the minimum integration time for each sensor.

$$t_{int(min)} = (n_{pixels} - 18) * clockperiod + 20\mu s \tag{4.5.1}$$

When we drive the sensor at its maximum frequency, one clock period is 1/8000000 seconds. This results in an integration time for the 1536 pixel sensor of 0.209 ms, corresponding to a bandwidth of 4.7 kHz. For the 128 pixel sensor the integration time is equal to 0.03375 ms, or a bandwidth of 29 kHz.

In- and output To ensure all sensors process their data simultaneously, there has to be a central clock which drives all sensors simultaneously. Besides the clock, each LSA needs a serial input or SI signal. When the sensor receives the SI pulse, a new cycle of pixel outputs is started (see figure 4.6).

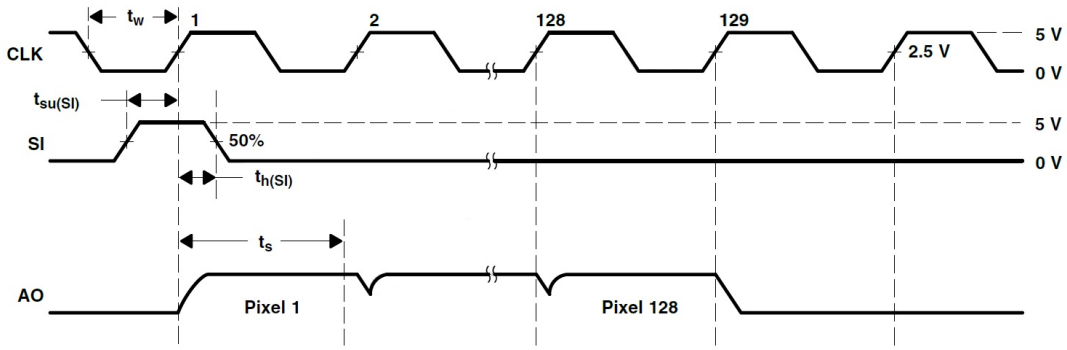

Figure 4.6: Operational waveforms for the 128 x 1 pixel linear sensor array [4]

A list of several types of optical displacement sensors can be found in Appendix B. The main requirement for the sensor is a small width because illumination has to be added to both sides of the sensor. The sensor with the smallest width is the TSL1401CL. This sensor is available for 6.5 Euro's and has a high pixel density of 128 pixels spread out over a length of 8.12 mm. The sensor has to be surface mounted to a printed circuit board. Surface mounted components on a pcb work best with a specially designed pcb with attachment spaces at exactly the right places. A component which is mounted through hole has legs that can be easily soldered to a pcb with holes in it and does not have to be designed and produced for the specific component. A sensor that is comparable to the TSL1401CL is the TSL1402R which has a through hole (DIP) mounting package. The length of the sensor is exactly twice as long, but so is the number of pixels. The sensor can be read out in a parallel way (there are two output channels that each read out 128 pixels) and the other characteristics like the illumination sensitivity and dynamic range are exactly the same. Therefore this sensor will be used in the experimental setup that is explained into more detail in chapter 6. The only negative side of this sensor is the increased width. The width of the active sensor area (the location where the sensor is measuring, depending on the pixel size) is equal, but the TSL1402R a much larger dead area on each side. This could cause problems with the illumination close to the sensor.

5

Implementation of the measurement system

Now that we have chosen a sensor, the details for the other measurement system components can be chosen so that they match the TSL1402R. This chapter describes the other required components and how they were selected. A new concept to process the data is introduced in paragraph 5.4.

5.1 Measurement system components

The measurement system does not only contain the sensors themselves, but all components which are needed to combine and evaluate the sensor output signals. Figure 5.1 gives an overview of how the different components will be connected to each other. Due to the small size of the sensors there is a high number of output signals which has to be evaluated. When the sensors are divided in groups and the location of a wafer is known, you will only have to evaluate the data of the relevant groups. The selection of components for the chosen sensor is described in chapter 5.

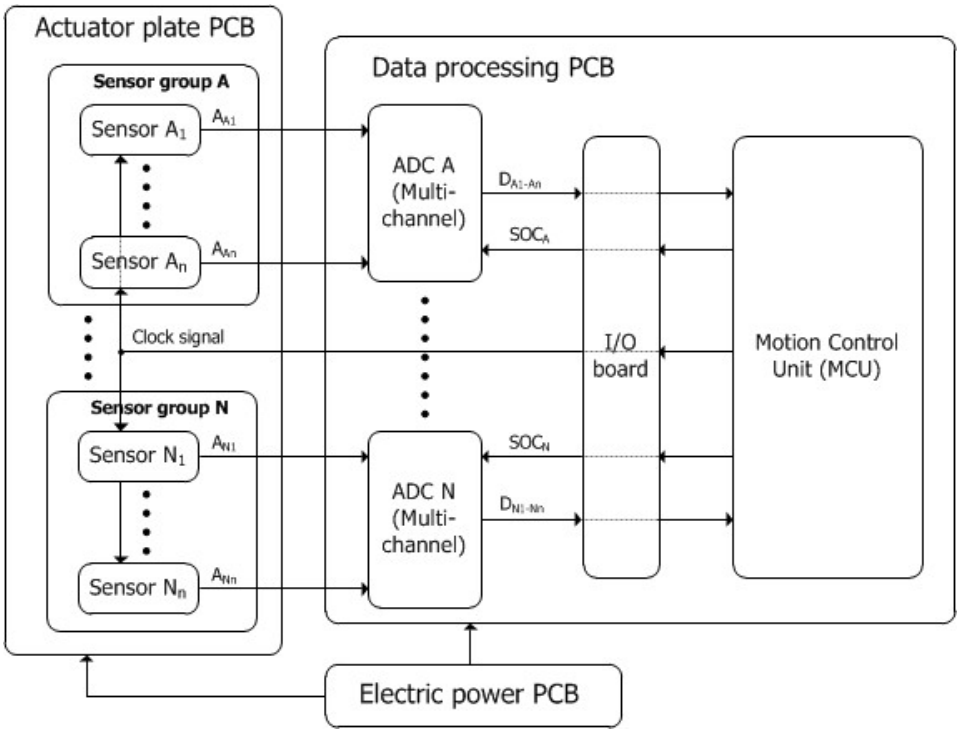

Figure 5.1: Schematic overview of the measurement system

Sensors One sensor usually covers a small area at a high accuracy. To cover the whole wafer track with a measurement system we need multiple sensors. When the wafer is not present in a certain area, the sensors in this area can be turned off, or the processor can only evaluate the data of sensors which are located in a relevant area. The sensors will be located on a printed circuit board (PCB) located directly underneath the wafer. All other components can be located farther away from the substrate at a second PCB, at a location where there is more space.

Analog to digital converter The sensor output of an LSA is an analog voltage. For data processing a digital signal is required. The conversion can be done with an analog to digital converter (ADC). When a multi channel ADC is used several sensor outputs can be connected to one converter. In chapter 5 the working principle and selection criteria for ADCs are explained .

I/O board The input/output board controls the communication between the in- and output signals of the devices in the system. It provides the input data for the sensors to work at the right synchronization and it delivers the (converted) digital output signal of the sensors to the controller.

Motion control unit The motion control unit combines all the data to determine the location of the centre of the wafer. With this information the actuation system can be controlled.

5.2 Illumination

The spectral responsivity of a linear sensor array type TSL1401CL is shown in figure 5.2. The sensor responsivity is highest for wavelengths of just below 800 nm or red light. The red illumination can be provided in numerous ways, like LEDs, a small fluorescent light tube, laser light or even by using plexiglass (with edge lighting). We want illumination on both sides of the sensor, with a maximum diameter of 3 mm.

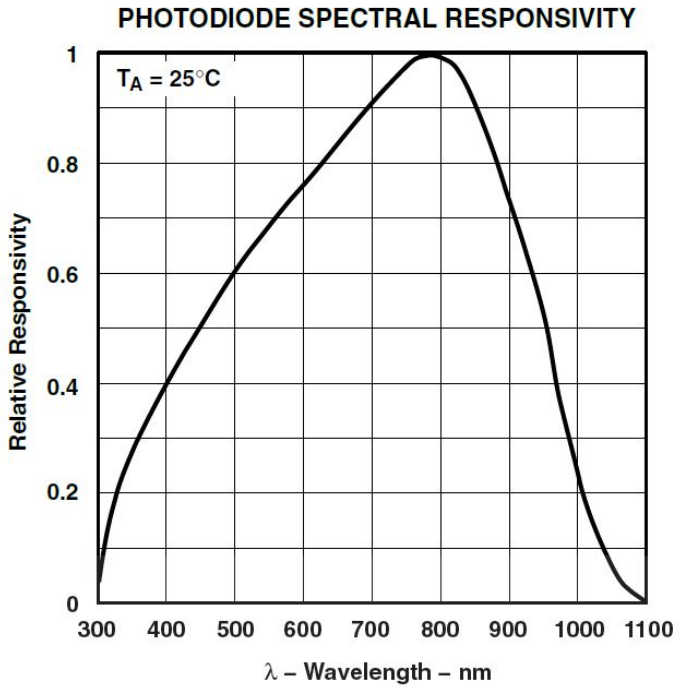

Figure 5.2: Responsivity of the photodiodes of the linear sensor array for light with varying wavelengths [4]

Linear sensor arrays are sensitive to changes in ambient light. Besides providing illumination at the right wavelength to create a high responsivity, we can modulate the light source to decrease the sensitivity. With on/off modulation you decrease the perceived luminance by the sensor, the degree of decrease can be controlled by varying the duty cycle. The duty cycle describes the fraction of each cycle that the light is turned on. When on/off modulation is used with a duty cycle of for example 50 percent, the sensor does not receive data for the same percentage of time.

LEDs LEDs are an easy and cheap way of illumination. Small red LEDs are easy to find and implement in the system. This solution is especially suitable when a small number of sensors is used. LEDs with a width of 3 mm are in general also 3 mm long, so you will need about 3 LEDs per centimetre. When sensors are used for a large area, the number of LEDs required increases rapidly. LEDs can produce noise on the frequencies used by the sensor, this has to be taken into consideration when they are chosen as the light source. The luminance of LEDs can be controlled by altering the currents which passes through them.

Fluorescent light A small fluorescent light bulb reduces the number of illumination devices drastically when compared to the LEDs. However, there is a minimum size in which fluorescent lights are produced. This solution is more suited for illuminating a large (row of) sensors than for separate small sensors.

Laser light When sensors are placed in a long row, a laser can be a good and economic solution for the illumination. Lasers can have a range of several meters. However, it can only work when enough light is emitted upwards, in the direction of the wafer. Otherwise there will not be enough reflected light to give the sensor a high responsivity.

Plexiglass Plexiglass can be used for illumination by using edge lighting (light enters and exits the glass only through the sides). When light enters the plexiglass boundary at an angle which is larger than the 'critical' angle of incidence above which total internal reflection occurs, the light will propagate through the material. The light is then only transmitted through the opposite edge of the glass. In this way a thin, light-emitting line can be created.

5.3 Analog to digital converter

An analog to digital converter (ADC) converts the physical analog signal, in this case a voltage, to a digital number. The ADC performs multiple conversions of the analogue signal, with a certain time interval between them. This results in a series of digital values, which can be used for data processing. Due to the quantization of the physical signal a small error is introduced. There are multiple working principles for an ADC. A common way is to convert the signal is with the help of a capacitor. The analog voltage is used to charge a capacitor, then the time it takes the capacitor to discharge is measured in a number of clock cycles. This number is then the resulting output signal of the ADC.

5.3.1. Characteristics

When selecting an ADC there are multiple criteria that influence the choice:

- Bandwidth: The bandwidth is basically the range of frequencies that the ADC can measure.
- Signal to noise ratio: The signal to noise ratio tells you the relation between the accuracy of the measured signal and the noise that is introduced by the conversion.
- Dynamic range: The dynamic range is the ratio between the highest and lowest value that can be measured.
- Resolution: The resolution is the smallest change the sensor can detect in the quantity that it is measuring. The resolution determines the initial dynamic range. This range is never reached due to non-linearity, accuracy of the quantization levels and other small errors in for example the timing. The resolution of an ADC depends on the number of bits (the number of discrete analog levels that can be distinguished by the converter).
- Effective number of bits: The effective number of bits (ENOB) is a value for the dynamic range which is the average number of bits in each measurement which give an output signal which is not influenced by noise.
- Full power bandwidth: The full power bandwidth is defined as the input signal frequency at which the amplitude of the digitized conversion signal has decreased by 3 dB (for a full-scale input). The FPBW gives you information about up to which input signal frequency the ADC can handle. It does not tell you anything about the performance of the ADC at this frequency.
- Samples per second: The last selection criterium for an ADC is the number of samples per second (SPS), or the sampling frequency. It is the amount of times per second that an ADC can sample the analog input signal to create a digital signal. Many ADC types have an SPS value which is equal to the clock frequency. In other types the sampling frequency is one or several factor(s) lower than the clock frequency.
- Serial or parallel: The difference between a serial and parallel ADC is found in the number of pins that are used to bring out the binary data. In a serial ADC this is only one pin, while in parallel ADCs this number is higher. The digital data output pins provide the link between the ADC and the CPU of the microprocessor or computer. For a serial output ADC the data is clocked out bit by bit. In a parallel ADC this can be done simultaneously for several bits, which reduces the time required for the signal conversion. Both serial and parallel output ADC are pretty common.

5.3.2. Requirements

To be sure that a signal which is coming in at 8 MHz can be accurately converted, there are several minimum requirements for the ADC:

- To ensure that the sensor can be operated at the highest accuracy, we have to make sure that the dynamic range of the ADC exceeds the range of the sensors. The sensors both have a dynamic range of 4000 (72 dB), therefore we are looking for an ADC with at least 12 bits, or $2^{12} = 4096$ discrete levels.
- The full power bandwidth indicates the maximum frequency of the input signal that the ADC can handle. This means that the minimum full power bandwidth should be equal or higher than the sensor frequency of 8 MHz.

- The bandwidth for the sensor is 29 kHz. The sensors are driven at a clock speed of 8 MHz. This means that the clock speed of the ADC converter should be at least 16 MHz when we want to drive the sensor at its maximum speed and prevent aliasing.

5.3.3. ADC selection

For the measurement setup described in chapter 6 all components will be soldered to a printed circuit board or placed on a breadboard, therefore the ADC should be mounted with through-hole package (DIP, CERDIP, PDIP, etc.). Such a dual in-line package includes a rectangular housing with two rows of pins connected to it that can be easily soldered by hand.

Multi-channel ADCs with a resolution of at least 12 bits that include a DIP package all have a limited sampling frequency of about 250 kHz. This means the LSA could be driven at maximum 125 kHz, or 2 sensors with 62.5 kHz and so on. For only one sensor this results in a high integration time for the LSA of 0.88 ms, or a bandwidth of 1134 Hz. For two sensors the bandwidth would go down to 567 Hz. The best suitable ADC seems to be the 14-bit AD7856 produced by Analog Devices, with a throughput rate of 285 kSPS and 4 input channels.

5.4 Analog integrator

If we want to drive the linear sensor array at its maximum clock-speed of 8 Mhz, the requirements and therefore also the costs of the ADC are high. The ADC clock speed can be greatly reduced when the signal would be analysed by one series of sensor pixels at once. This can be done by using an analog integrator. The integrator adds the value of each pixel for the length of the output series. Afterwards the integrator has to be reset before the new output signal series of the LSA starts. This is at the same moment that the LSA receives the SI signal (see paragraph 4.5).

The maximum voltage that can be collected by the integrator, V_{max}, is shown by the green line in figure 5.3. The maximum value is reached when the whole photosensitive area of the LSA is covered by the substrate. This value is equal to the sensor length L_{LSA} multiplied by the LSA voltage output for the covered sensor (V_h). When the substrate is not flying above the sensor, there will still be a small voltage output, V_l, due to the ambient light which is always present. When a part of the sensor is covered, the accumulated voltage by the integrator at the end of an output series (V_{end}) of the sensor can be calculated using equation 5.4.1.

$$V_{end} = L_c * V_h + \int^{L_t} V_t \, dx + L_u * V_l \tag{5.4.1}$$

$$L_{LSA} = L_c + L_t + L_u \tag{5.4.2}$$

There is a small transition area between the high and the low voltage. The length of this area, together with the high voltage (covered sensor) and the low voltage (uncovered sensor) will have to be verified experimentally. It is the assumption that the length of this transition area is a function of the fly height of the wafer, and perhaps also the light colour. The total LSA length is known, as is the fact that this is equal to the covered, transition and uncovered length together (equation 5.4.2). By measuring the voltage output for a totally covered and completely uncovered sensor, V_h and V_l can be determined. The length of the transition zone, L_t, can be experimentally determined. It is defined as the number of pixels it takes to go from V_h to V_l. There are now two equations which can together be used to calculate the two unknown variables of the covered and uncovered sensor length.

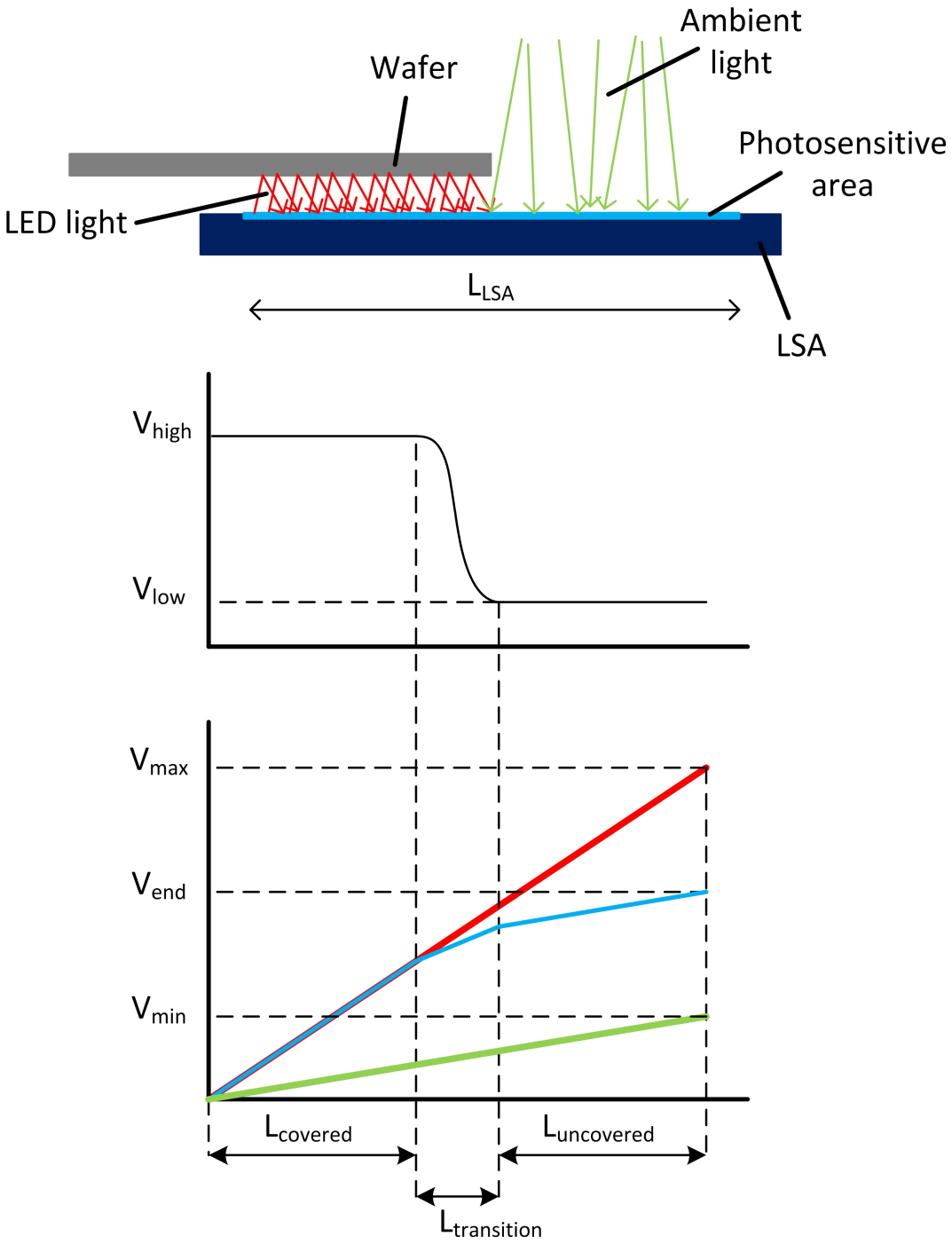

Figure 5.3: Selection of suitable ADC types

An analog integrator circuit which can be used is shown in figure 5.4. It can be reset with the switch that is located above the amplifier. The integrator can be reset with the SI signal which also starts the new sensor output sequence.

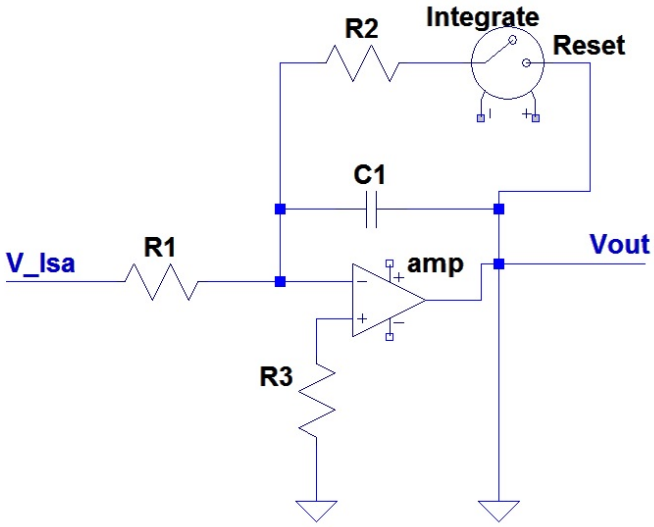

Figure 5.4: Integrator circuit

5.4.1. Components of the analog integrator

The capacitor must be able to contain the maximum charge which can be created in one sensor cycle. The maximum output voltage of the LSA at full saturation is 4.8 Volt. This is for ideal conditions, with maximum incident irradiance at the maximum sensor resistivity. The minimum cycle time is equal to 0.03375 ms (see paragraph 4.5), this includes a 20 μs pixel charge transfer time, the minimum time between two cycles. The maximum output voltage can be calculated with equation 5.4.3, by setting V_{lsa} to 4.8 Volt and the time to 0.03375 ms. This results in an output voltage of $1.62 * 10^{-4}/(R_1 * C_1)$ for when the sensor is operated at its maximum speed.

$$V_{out} = \frac{1}{R_1 C_1} \int_{t_1}^{t_2} V_{lsa}\, dt \tag{5.4.3}$$

The requirement for the sampling rate of the ADC is now decreased from 16 MHz to about 300 kHz, as there is a maximum of 29 kHz for the sensor (see paragraph 4.5). At this sampling frequency there are at least 10 samples available to detect the output voltage. An additional requirement is that a sample and hold should be placed behind the capacitor to make sure the final voltage value is not missed by the ADC. Another additional requirement for the ADC is an increased resolution because in this situation the system has to be able to distinguish more output values than before. The resolution requirement for an ADC that reads out the pixels in series is 12 bits. The required resolution for an ADC that measures the output of the analog integrator is higher, the minimum height has to be determined experimentally.
An integrator works as a low pass filter, meaning the bandwidth of the system becomes limited to the crossover frequency of the analog integrator circuit. The 3 dB cutoff frequency is calculated with equation 5.4.4. This frequency has to be at least 5 kHz to fulfill the bandwidth requirement of the measurement system.

$$f_a = \frac{1}{2\pi R_1 C_1} \tag{5.4.4}$$

5.4.2. Selecting components

LSA For the test setup described in chapter 6 the TSL1402R sensor will be used because it can be mounted on a PCB due to the through hole mounting package. The other components of the integrator circuit (opamp, capacitors, resistors and switch) are also selected with a through hole mounting style. In this way all components can be soldered to a PCB or placed on a breadboard.

Capacitors and resistors For each LSA we need a 0.1 μF ceramic capacitor that has to be connected between the supply voltage and the ground, as close to the sensor as possible. For the integrator circuit the minimum

capacitor value depends on the amount of charge that it should be able to collect. The LSA voltage output is maximum 5 Volt, so a voltage rating of at least 10 V is required.
The cut-off frequency cannot be lower than 5 kHz. This means that, according to equation 5.4.4, $2\pi R_1 C_1$ has to be smaller than $2 * 10^{-4}$, and $R_1 C_1$ should be smaller than $3.18 * 10^{-5}$. The smaller we make $R_1 C_1$, the higher the cut-off frequency becomes. However, by decreasing this value, we increase the output voltage and the ADC is limited to a maximum voltage input.

5.5 Summary

Now all measurement system components have been selected, they can be combined into a system that runs at a constant voltage of 5V. The whole measurement system has now been designed based on the specific information and requirements that were determined at the beginning of this thesis. The next step is to verify the working principle of the linear sensor array with these components. When we want to validate the complete measurement system, a moving substrate will have to be introduced that is levitated and transported by actuator cells. This degree of verification goes beyond the scope of this thesis. In the context of this preliminary investigation, I will focus on designing a measurement setup that will determine if the chosen sensor type is feasible. The resolution of the sensor will be determined and fine tuned by varying the light colour and the measurement height of the substrate. Chapter 6 focusses on the design of an experimental setup with which the sensor performance and the resolution of the analog integrator can be validated.

6 Experimental setup

In this chapter the design and implementation of the tsl1402R sensor into a test setup is described. The goal is to design a setup with which the predicted working principle of the sensor, the ADC, the illumination and the integrator circuit can be verified.

6.1 Test setup

The first step in designing the measurement setup is to define which components have to be included to perform an accurate measurement. The components that were selected in chapter 3 and 5 have been chosen for a system that transports a substrate with air actuation. The actuation principle is solely based on air flow and does therefore not affect the resolution of the measurement system. Hence the preliminary testing can be done with just the measurement system and the wafer. The components that are needed to thoroughly research this sensor are:

- Linear sensor array
- PCB to mount the sensor and the LEDs
- Illuminating LEDs in different colours
- A wafer with a diameter of 100 mm
- A stage with which the vertical position of the wafer in reference to the sensors (the 'fly height') can be varied
- A stage with which the horizontal position of the wafer with respect to the sensor can be varied
- A reference measurement in the horizontal direction
- A reference measurement in the vertical direction
- The components required to evaluate the sensor output, mounted on a breadboard

For a complete setup a movement in both the horizontal and vertical direction is required. I decided to mount the wafer on a stage that can be moved vertically, in order to change the distance between the wafer and the sensor. The sensor and illumination are mounted on a pcb. This is attached to an electronic stage that can move in the horizontal direction, to vary the part of the sensor that is covered by the wafer. Figure 6.1 shows a schematic overview that includes all components listed above. The breadboard with the additional measurement system components is not shown because it is located further away. The horizontal reference measurement is not shown because the movement of the horizontal stage is used as a reference. The horizontal and vertical reference measurements are explained into more detail in paragraph 7.1.

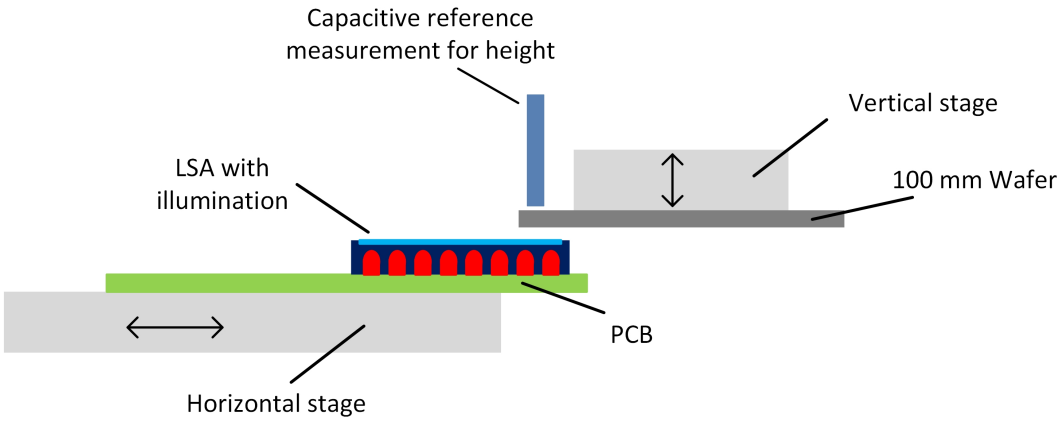

Figure 6.1: Schematic overview of experimental setup

For the horizontal movement a stage from Thorlabs [21] is used. This is an electric stage that can be controlled either manually or by a program like Labview. The stroke of the stage is 25 mm and the length of the photosensitive area of the LSA is 16.3 mm. Therefore the stage can move the sensor from a fully uncovered position to a point where the wafer is covering the whole sensor. Figure 6.2 shows an overview of the test setup.

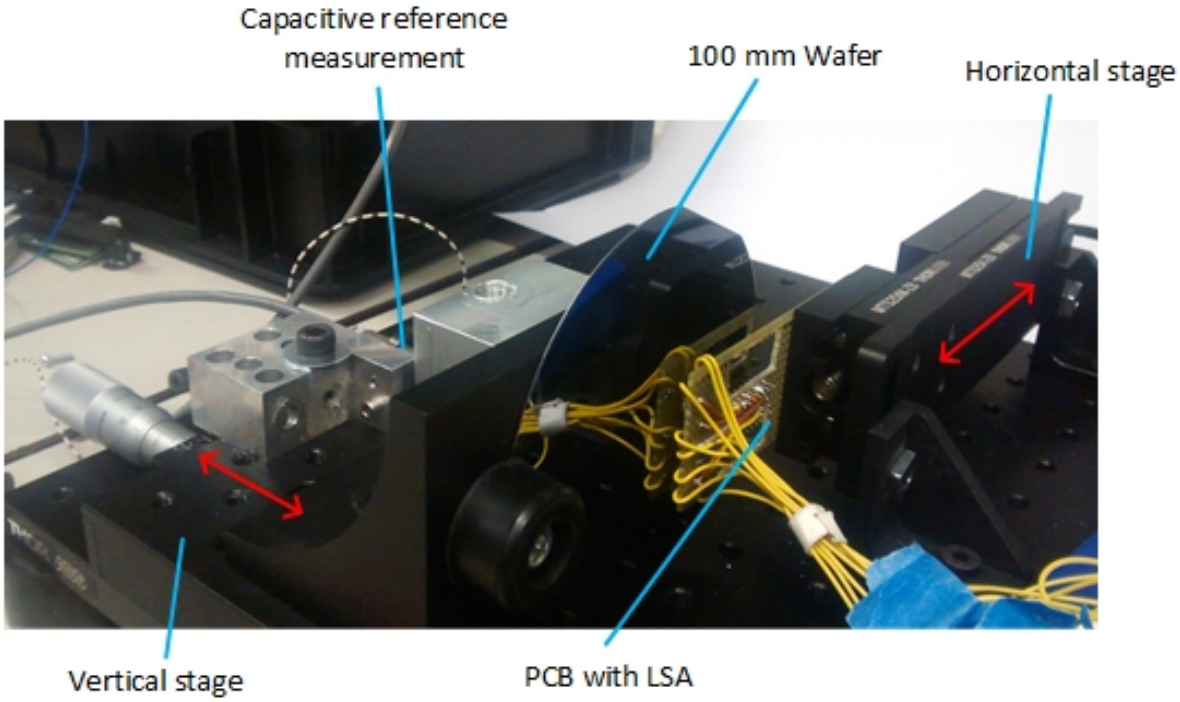

Figure 6.2: Experimental setup

The horizontal stage has an accuracy of 34304 counts per millimetre which corresponds with a resolution of 0.029 micro metres. This means that once the stage is calibrated for the position where the sensor starts to measure the presence of the wafer, the position feedback of the stage itself can be used as a reference measurement in horizontal direction. These data can be used to verify the resolution of the sensor with which it detects the position of the wafer's edge.

The distance between the wafer and the sensor can be varied by using the vertical stage on which it is mounted. This manual stage does not have a micrometer precision like the electric horizontal stage, therefore a capacitive

sensor has been added (see figure 6.3) as a reference measurement to ensure accurate fly height data. The capacitive sensor gives an output voltage that increases if it is moved closer to a metal object. The capacitive sensor is mounted to the same stage as the wafer. A metal block is mounted separately to the base plate of the setup. When the vertical stage is moved, the distance between the capacitive sensor and the metal block changes, which results in a change in the voltage output. When the sensor is calibrated correctly this voltage can be used as a reference height measurement for the distance between the wafer and the sensor.

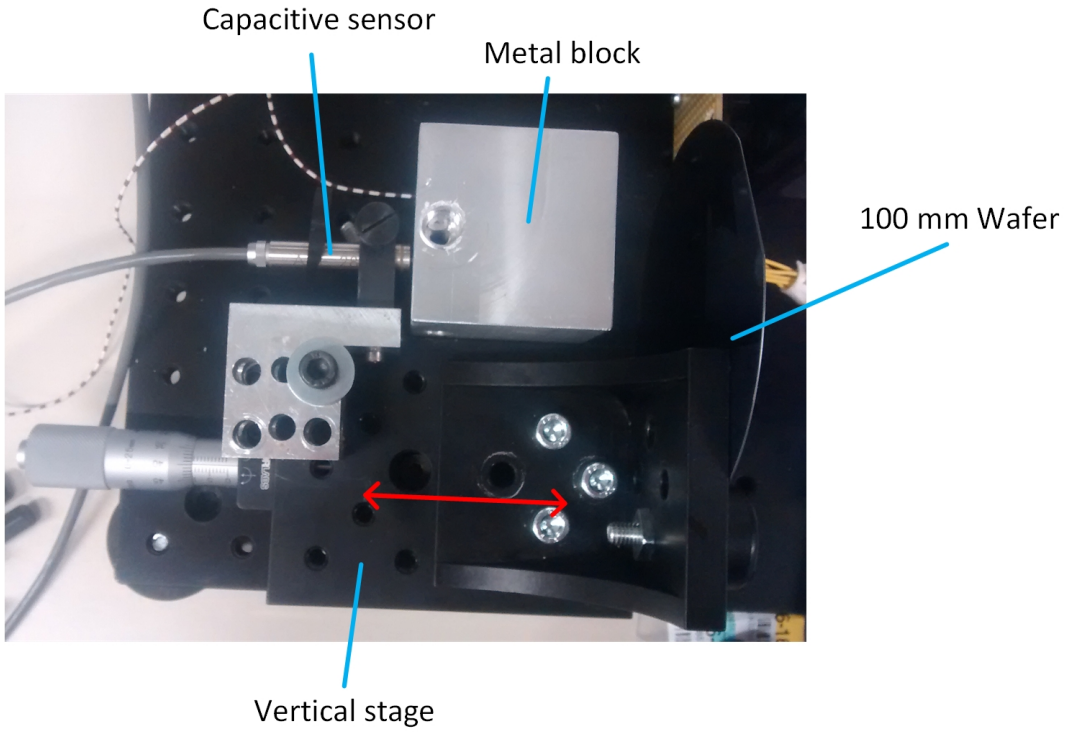

Figure 6.3: The capacitive reference sensor

6.2 Sensor connection scheme

The sensor has 14 connection pins. Eight pins are in- and output channels that have to be connected for the sensor to function properly, an overview of the pins and their function can be found in figure 6.4, a functional description of the abbreviations can be found in Appendix C.

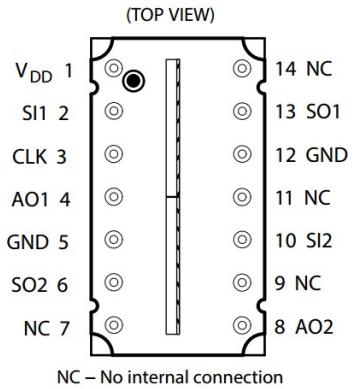

Figure 6.4: Pin layout of TSL4102R [5]

An Arduino Zero [22] is used to drive and read out the sensor. The sensor has 256 pixels and can be read out in two ways: A parallel connection, where the data from pixel 1-128 are read out simultaneously with the data from pixel 129-256. Or a serial connection, where the data of pixel 1-256 are read out in one go, this will take twice as long and reduce the maximum sensor frequency. For the analog integrator circuit, the serial connection will be used, the analog pixel output can be connected to the op-amp. For the direct sensor processing the parallel connection will be used.

A schematic overview of the parallel sensor connection is shown in figure 6.5. The sensor has two analog output channels (pin 4 and 8) which are connected to the analog inputs of the Arduino. Both the clock (pin 3) and the serial input channels (pin 2 and 10) are connected to the digital output channels. Pins 5 and 12 should be grounded and are connected to the ground of the breadboard [23]. The supply voltage is connected to pin 1 of the sensor, an additional capacitor (1 μF) is connected from pin 1 to the ground, as specified in the data sheet.
The only difference for the serial sensor connection is that the serial output 1 (pin 13) is connected to serial input 2 (pin 10). Serial output channel one will give a pulse when the data output transfer of the first 128 pixels is finished. The output pulse is now used as the (serial) input pulse for channel two, to start the output of pixels 129 to 256.

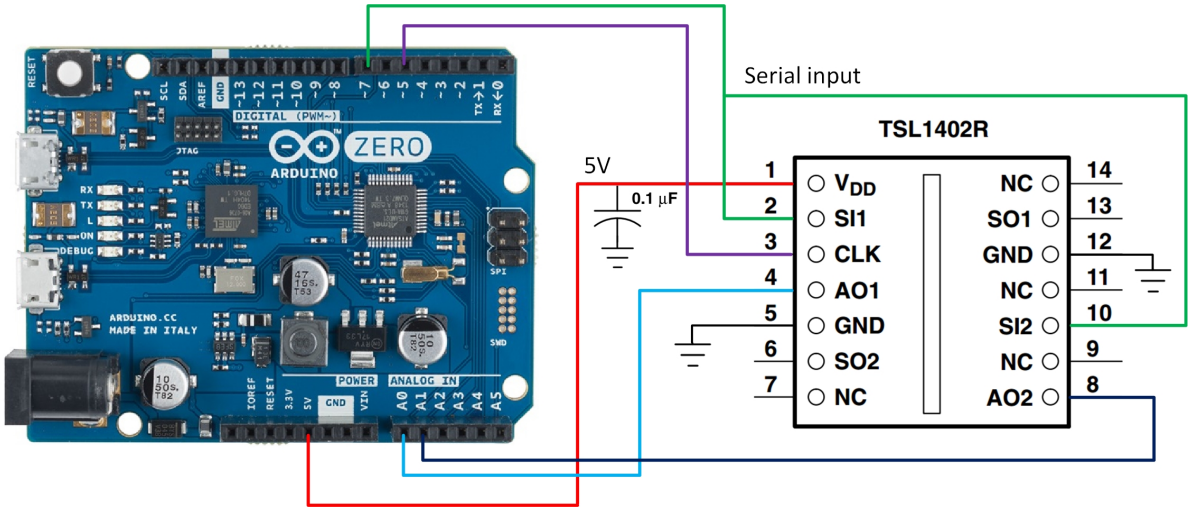

Figure 6.5: The schematic parallel connection of the TSL1402R

6.3 Illumination

The LSA will be illuminated on both sides by a bar of LEDs of different colours. The sensor height is about three millimetres but the height of the led bars is 5 mm. Therefore the LEDs have been soldered to a second pcb and can be mounted underneath the first pcb to which the lsa is soldered (as shown in figure 6.6). In this way the wafer can be positioned very close to the sensor without touching the leds.

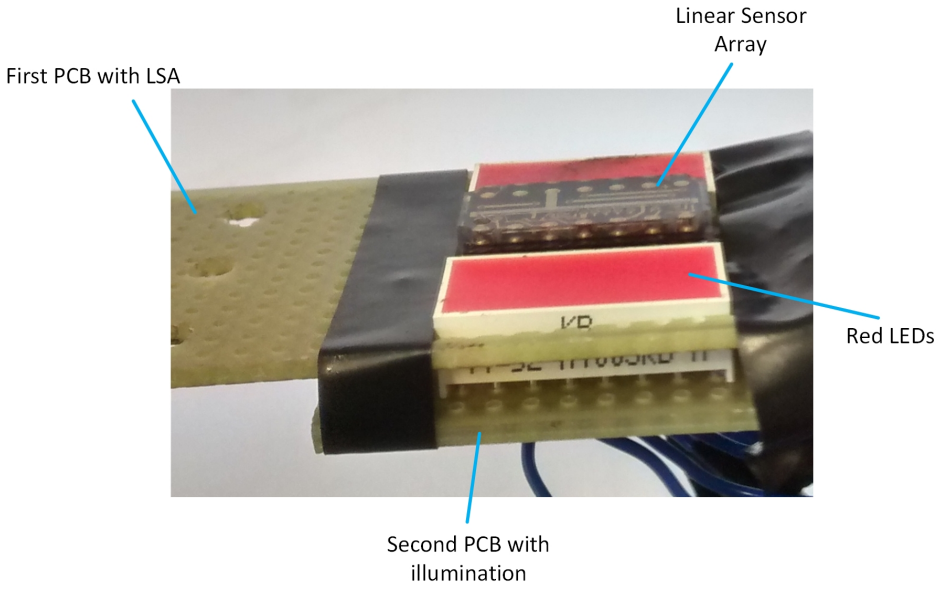

Figure 6.6: Side view of the double PCB

The wafer has a highly reflective surface. The leds have been placed close to the sensor with the idea that the surface of the wafer will reflect the light of the leds onto the sensitive area of the sensor. Due to the reflected light, the measured light intensity for a covered sensor is expected to be higher than that of an uncovered one. Figure 6.7 shows a schematic overview of the expected sensor output values.

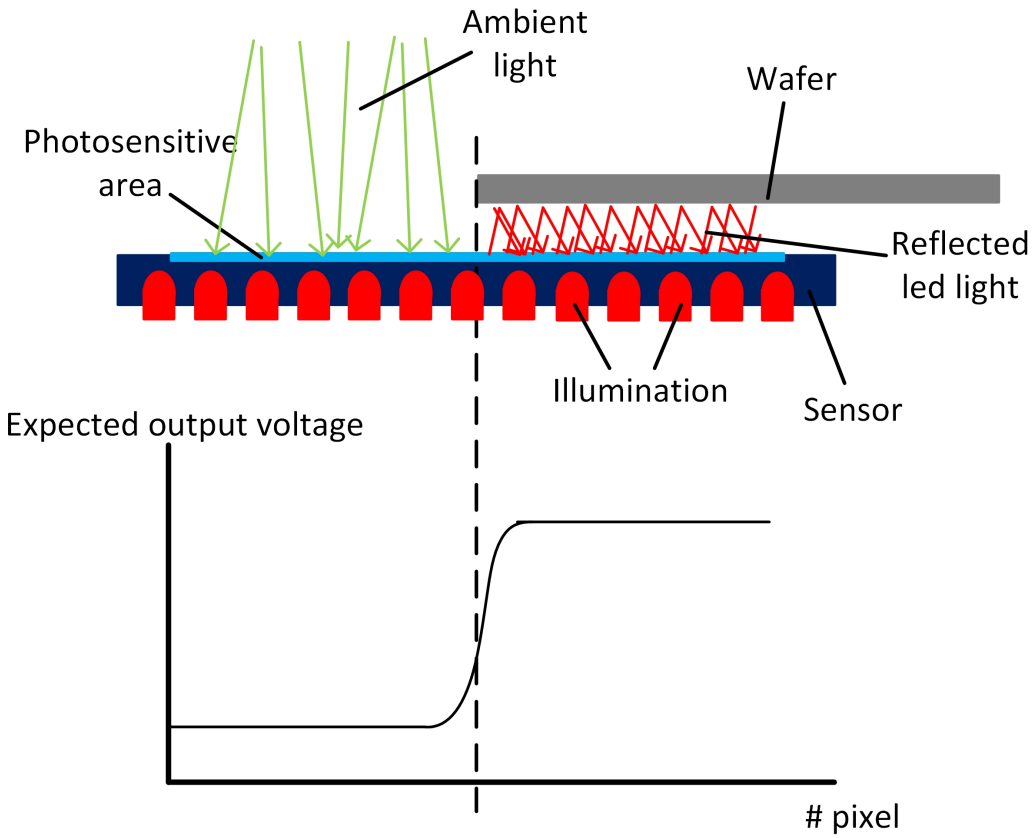

Figure 6.7: Schematic overview of expected sensor output voltage

Ideally, the high voltage is as close to the maximum voltage output of the sensor as possible. This happens when the sensor is fully saturated. The low voltage output is ideally as low as possible. In between the high and the low voltage output, at the edge of the wafer, is a transition area. This area is several pixels in width. The accuracy of the sensor will be highest when there is a large difference in the high and low voltage outputs. The transition area will always have the same length for a certain fly height, but for a steeper slope there is a higher variation in the voltage difference between two pixels. This variation can be used to determine if the whole pixel is covered or only a part of it.

The sensor and illumination were mounted to the stage and the sensor was moved to a position where half the sensor is covered by the wafer. The resulting output voltage of the ADC is shown in figure 6.8. The y-axis shows the full range of the 12-bit ADC that has been used. You can see that the output voltage for the covered part of the sensor (the left half of the graph) is higher than that of the uncovered part, but the difference is small compared to the full range of the adc.

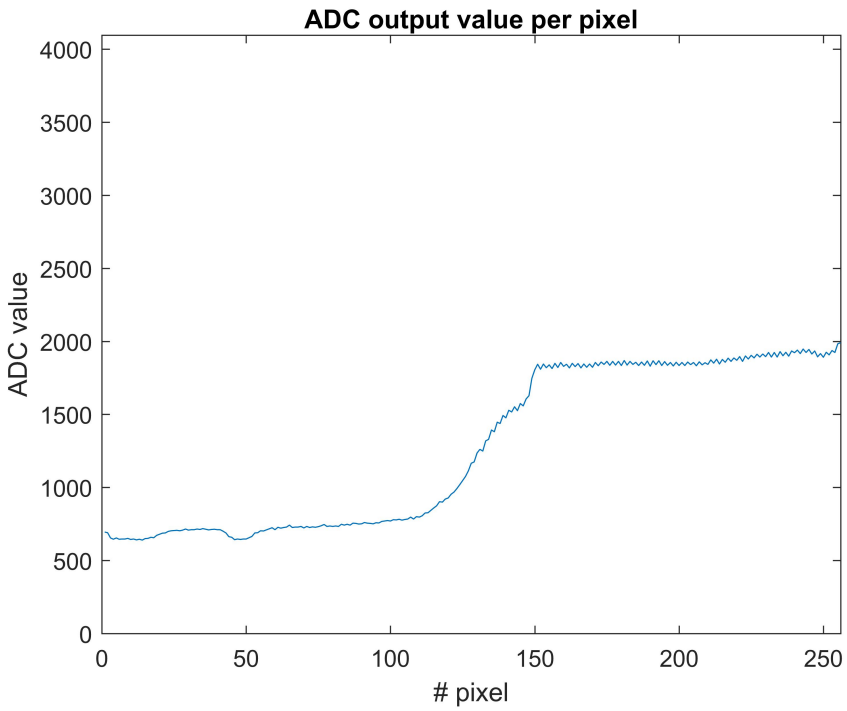

Figure 6.8: Output voltage of a 12-bit ADC for a partly covered sensor

The reflected light is lower than anticipated. As mentioned before, the sensor used in this setup is three times as wide as the small linear sensor array that was originally selected. The extra width of the sensor decreases the amount of reflected light that is received by the photosensitive area of the LSA.

The light can still be used to improve the resolution of the sensor by increasing the difference between the maximum and minimum voltage value that is measured, by placing the leds at the opposite side of the wafer. This is in violation with one of the system requirement that all sensing must be done one sided, but for this test setup it is a temporary solution to still increase the sensor resolution with illumination. Instead of a high sensor output underneath the wafer, the output for the uncovered sensor will now be higher due to the light provided by the leds. The led array is slightly longer and much wider than the sensing part of the sensor. When the lights are placed close to the wafer it can therefore be ensured that the illumination value will be equal along the uncovered sensor. A schematic overview of the new setting can be found in figure 6.9.

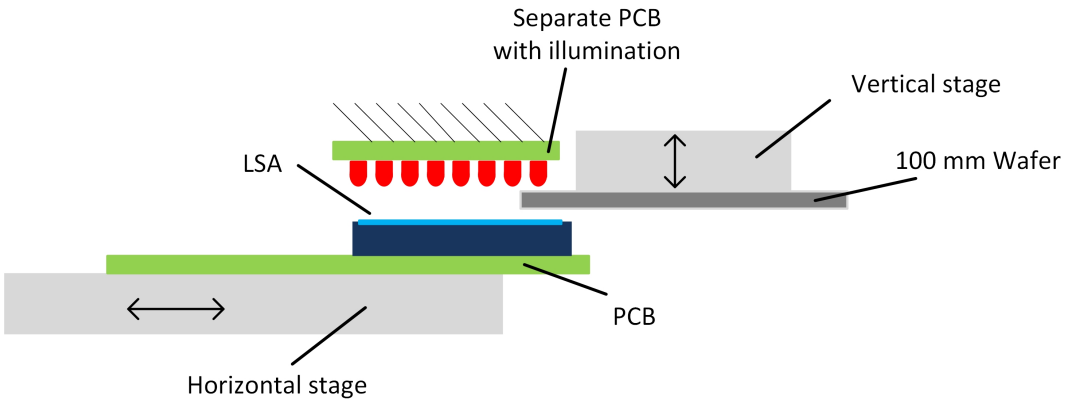

Figure 6.9: Schematic overview of setup with the illumination moved to the opposite side of the wafer

7

Experimental results

Now that the tesagt setup has been designed and the illumination has been moved to the opposite side of the wafer, the experiments can begin. In this chapter the measurement results are presented. Several measurements have been done to see the influence of the light colour (paragraph 7.4), fly height (paragraph 7.5) and the analog integrator (paragraph 7.6).

7.1 Initial conditions

First of all the capacitive sensor has to be calibrated to ensure that the distance between the wafer and sensor is correct. The capacitive voltage output varies with two Volts per 10 μm. The sensor has been calibrated at a zero height difference (when the wafer touches the LSA). The capacitive sensor can be used up until a height difference of 90 μm, but the measurements will be done in between heights of 5 to 30 μm, which lie close to the originally designed substrate fly height of 10 micrometers.

Next a measurement has to be done to determine the absolute horizontal position of the wafer relative to the photosensitive part of the sensor. As mentioned before, the electric stage that is used for the horizontal movement has a very high resolution of 0.03 μm. This measurement is started by moving the stage to a position where the whole sensor is not covered by the wafer. The voltage output of the sensor is monitored and stays constant as long as the edge of the wafer is not detected yet. One sensor pixel has a diameter of 55.5 μm. The amount of light that is received by the pixel is translated in a certain output voltage level. When a pixel is partly covered, the output voltage will be higher than if the pixel is completely covered, but lower than if it would be completely uncovered. As soon as the voltage output of the first pixel of the sensor starts to decrease, the increment value of the stage at this position is saved. This is the position where the edge of the wafer is located at the edge of the photosensitive area of the first pixel of the lsa.

Figure 7.1 shows what the analog sensor output voltage looks like when a completely covered sensor is sampled at a high frequency. You can see that each output pixel has the shape of a small hill. You can see that the amplitude of the deviation within one pixel output is roughly equal. Figure 7.2 shows what the ADC output of the same signal looks like. A twelve bit ADC is used, which means that the output values lie between 0 and 4095.

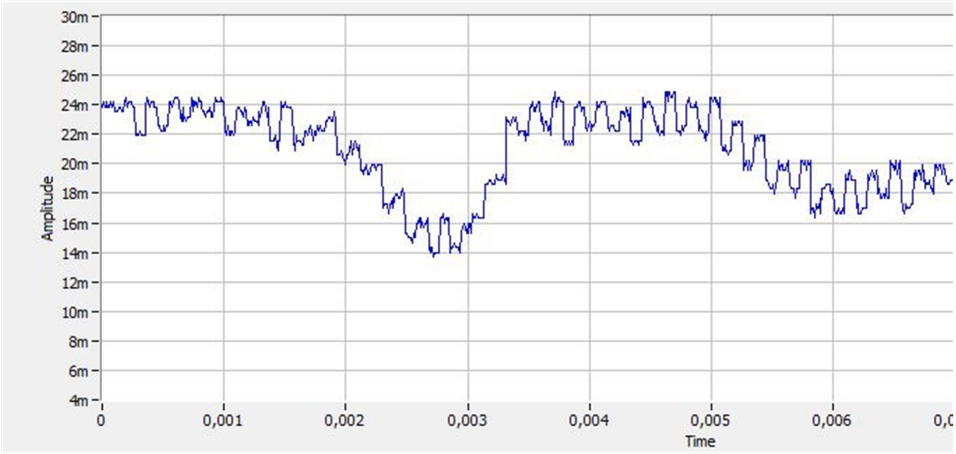

Figure 7.1: Analog output of the last 50 pixels of an LSA for a fully covered sensor

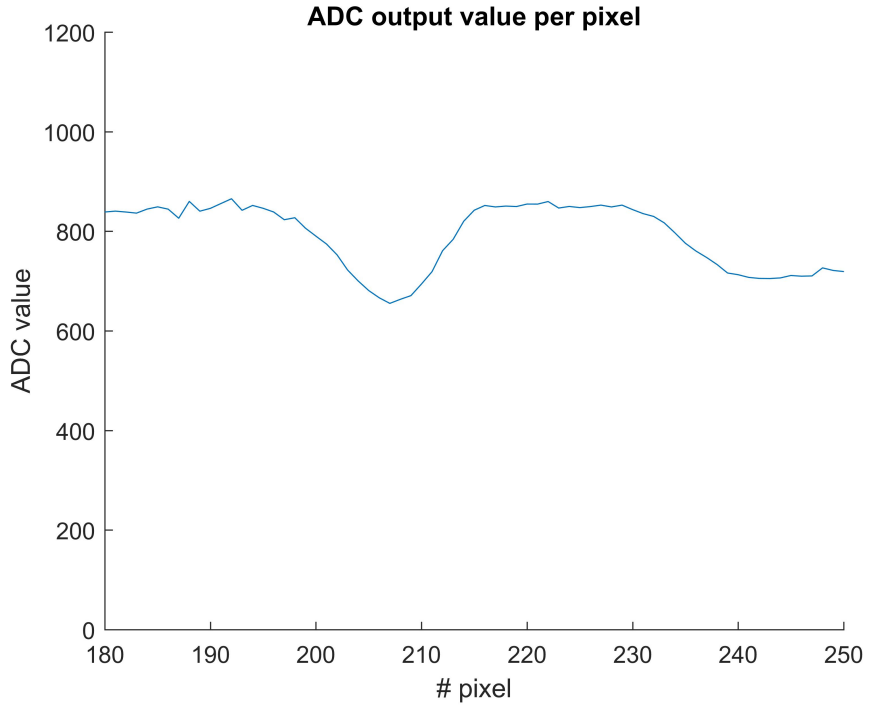

Figure 7.2: Digital output of the analog signal shown in figure 7.1

Figures 7.1 and 7.2 show that the output values of the LSA are not a smooth straight line as would be expected. The differences in pixel output are quiet big considering that there is supposed to be an equal lack of illumination along the whole sensor when it is covered by the wafer. For repeated measurements there is always the same pattern of deviation.
Noise on the output signal can be caused by several factors. It cannot be caused by the frequency of the light source (due to the DC current) because the disturbance is not periodic noise with a frequency of 50-60 Hz. If the wafer was not positioned exactly perpendicular to the sensor, the output would be a slowly increasing or decreasing line, but this is not the case. If the wafer surface was damaged, the deviation pattern should be equal for a different sensor. This cause has been eliminated by doing the same measurement with a different sensor. This resulted in a different deviation pattern. Dust particles on the sensor surface could also disrupt the measurement results. The sensor was cleaned, but this had no significant effect on the output values.

Luckily, the deviation repeats itself in each measurement, which means it can be corrected with a baseline measurement.

7.2 Baseline measurement

For a baseline measurement we measure the sensor output when the wafer covers the whole LSA, at a height of 10 μm with red illumination. Figure 7.3 gives the result of a baseline measurement, and the average output value for a covered sensor. The difference between the average value and the output for each pixel can now be added (or subtracted) from a measured sensor output to create a more even signal for the covered part of the sensor.

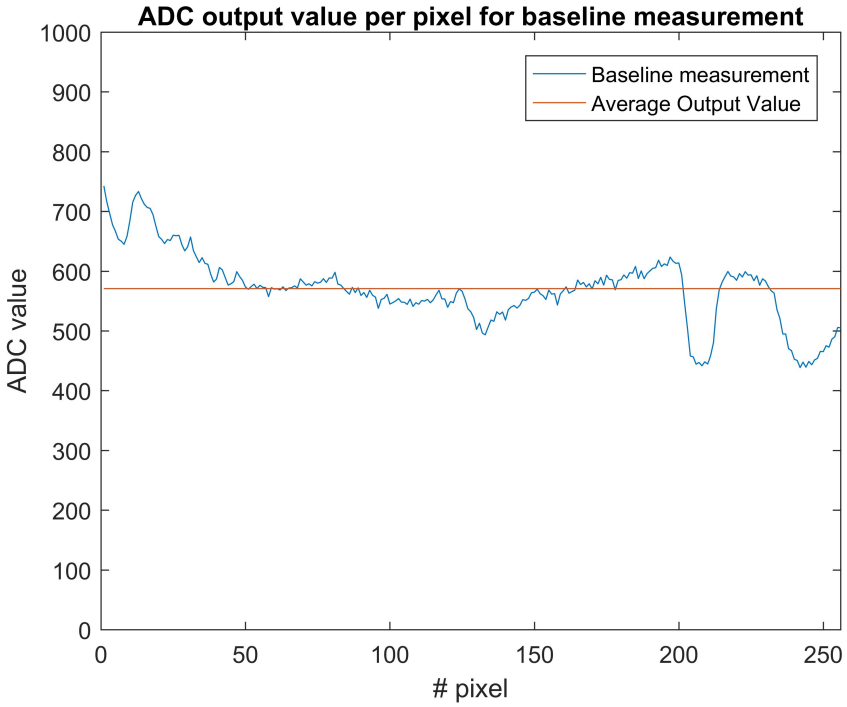

Figure 7.3: Baseline measurement and average value

7.3 Resolution

Before the influence of factors like light colour and fly hight can be tested, the sensor resolution should be determined. In the sampled sensor output it can be seen that the transition from the covered to the uncovered part of the sensor has a width of several pixels. In the first pixel that is covered by the wafer, a sharp drop in output voltage is seen. The size of the drop is dependant on how much of the pixel is covered. The maximum size of the drop is determined by placing the wafer between two pixels (there is a 'dead zone' between each pixel that is not light sensitive). This is repeated for 10 different pixels, and afterwards the value is averaged.

The ADC that is used has a resolution of 12 bits. The leds give light with such an intensity that the pixels for the uncovered part on the sensor are saturated. The maximum voltage drop along the first pixel goes from an ADC value of 4092 (saturated value) to an average of 3883. This is equivalent to a drop of 5,21 percent of the saturated value. Each pixel has a width of 55 μm. For a movement of 1 μm, the output value will drop about 0.1 percent of the saturated output value. This is equal to a different ADC output value of 4.

Figure 7.4 shows the zoomed in sensor output on the voltage drop, between pixel number 13 and 14. You

see the output values for different measurements, where the sensor has been moved for 1 micrometer each time. You can see that the voltage drop increases when the sensor is covered for a larger part, as would be expected. In figure 7.5 a close-up of the endpoint of the voltage drop can be found. You can see that the difference in voltage drop is averaged around 4 (for repeated measurements with two different sensors the value always stayed between 3 and 5).

The absolute position of the wafer (mounted on the electronic stage) in reference to the sensor has been determined in paragraph 7.1. The sensor output data were used to establish the absolute position. The resolution of the stage is 0.03 μm, the resolution of the LSA is 1 μm. When comparing the measured data to the absolute position, a deviation of max. 4 μm is found. This results in a sensor accuracy of 6 μm.

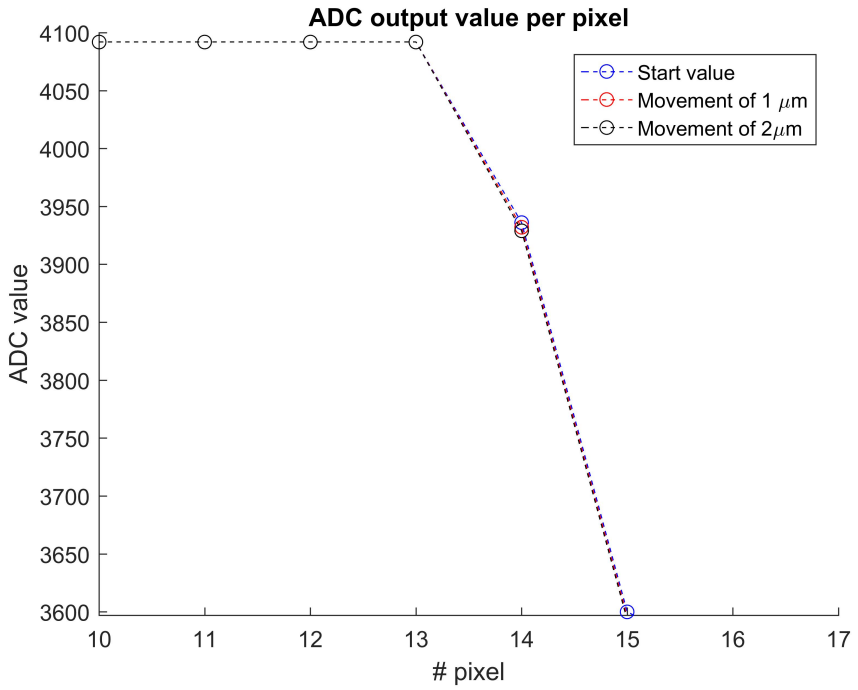

Figure 7.4: Difference in sensor output for a moved step size of 1 μm

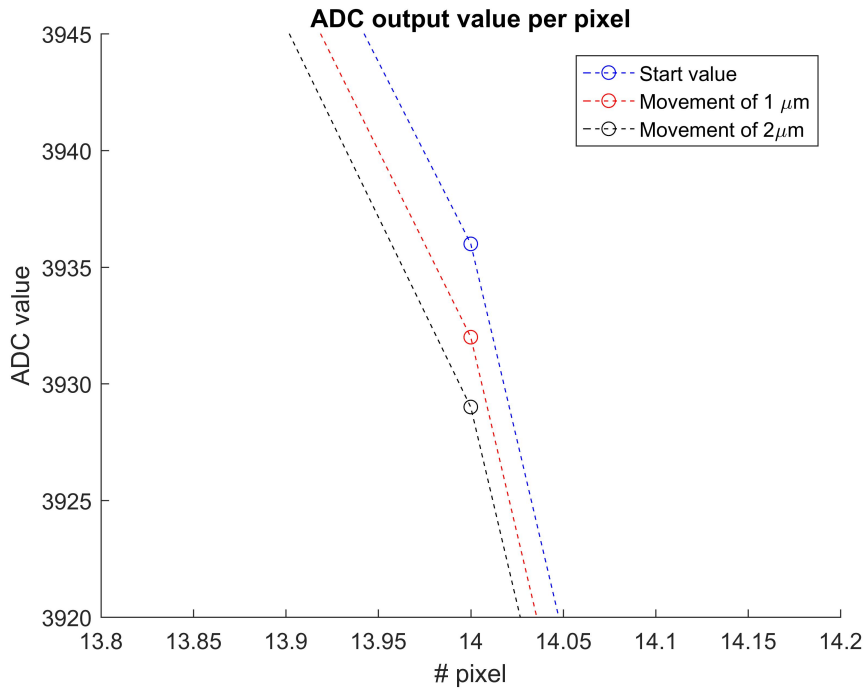

Figure 7.5: Zoomed in on the difference in sensor output for a moved step size of 1 μm

7.4 Changing light colour

As explained in chapter 6, the leds have been moved to the opposite side of the wafer. To maximise the difference between the high and low output voltage, I increased the brightness of the leds until the uncovered part of the sensor was saturated. This results in a graph that starts with a straight line for the uncovered sensor part, as shown in the figures with measurement results below. As soon as the pixel value starts to decrease, the correction for the output voltage determined by the base measurement is applied.

There are three led colours available, red ones with a dominant wavelength at 640 nm, green ones with the peak wavelength at 548 nm and yellow ones with a dominant wavelength of 588 nm. Figure 7.6 shows that the spectral responsivity of the sensor will vary from 0.84 to 0.67 between the red and green lights.
Due to the decision to satirize the uncovered sensor pixels, the difference in light colour will be harder to detect. However, the ambient light of the environment (mainly created by the light source) has some influence on the amount of light that the sensor receives when it is covered by the wafer.

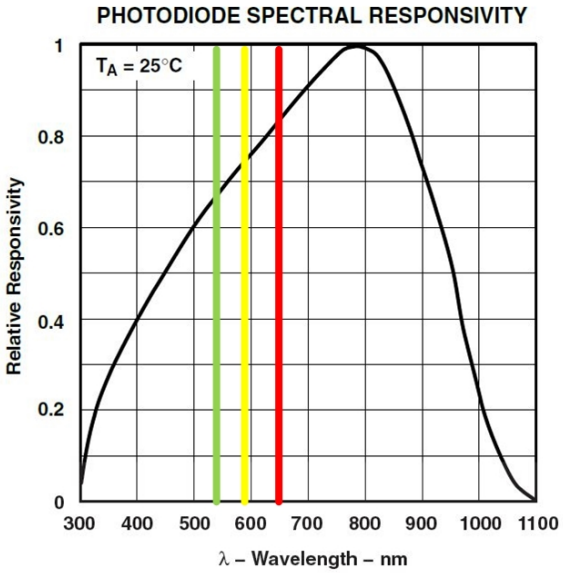

Figure 7.6: Spectral responsivity of lsa at different colours

In the graph in figure 7.7 the sensor output values for a wafer at a constant location and fly height, but for the different light colours are shown. You can see that there is no difference in output value for the covered part of the sensor (as expected) or during the voltage drop. There seems to be a small difference in the output data for the covered part of the sensor. However, this difference is sometimes positive and sometimes negative, so no conclusions can be drawn from these results.

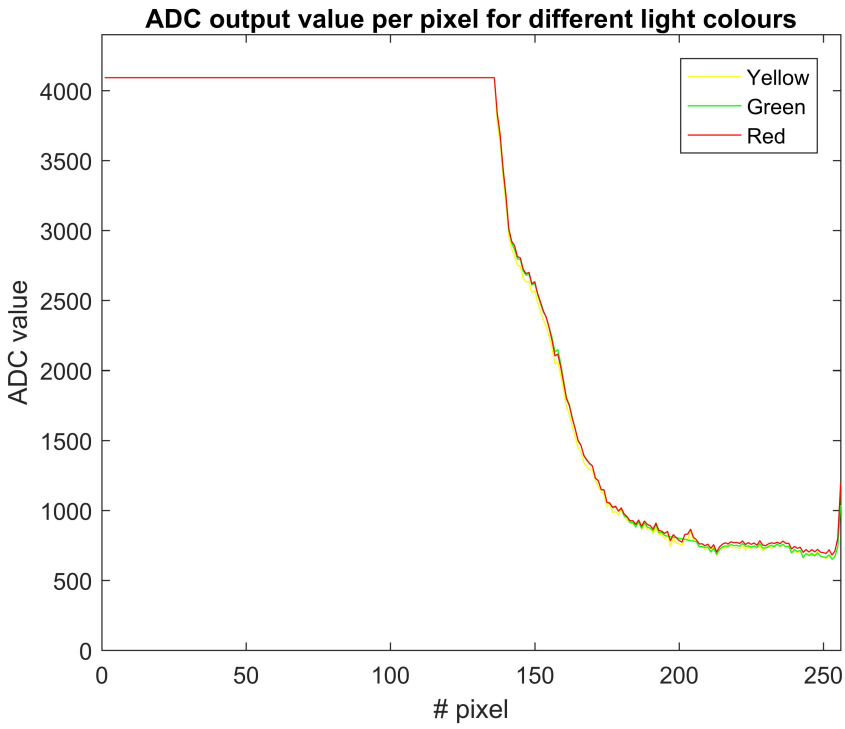

Figure 7.7: ADC output value per pixel for different light colours

7.5 Influence of the fly height

The height measurements are all done with the red illumination. I measured the transition from high to low light intensity at fly heights between 5 and 30 micrometer, the gap has been increased with an additional 5 micrometers for every next measurement. The transition was measured at ten fixed positions along the stage to ensure that the data at different fly heights can be compared at exactly the same positions. When all the results are obtained, the sensor output at the same position for a varying fly height can be compared, or at an equal fly height at multiple positions.

When the gap between the substrate and the sensors is increased, it is expected that more ambient light can be captured by the covered photo diodes. This will result in a higher sensor output for the covered part of the waver and therefore a smaller transition zone.

The location at which the sensor outputs have been measured along the stage are chosen at regular intervals of two millimetre. Figure 7.8 gives an overview of the results at the same position for a fly height of 10, 20 and 30 μm. There is no notable difference along the uncovered part of the sensor and the voltage drop. When we get to the transition zone, it can be seen that the output value is slightly higher for an increasing fly height. This differences diminishes to almost zero after the transition zone.

It should be noted that all height measurements have been corrected with the same baseline measurement, which was done at a fly height of 10 μm.

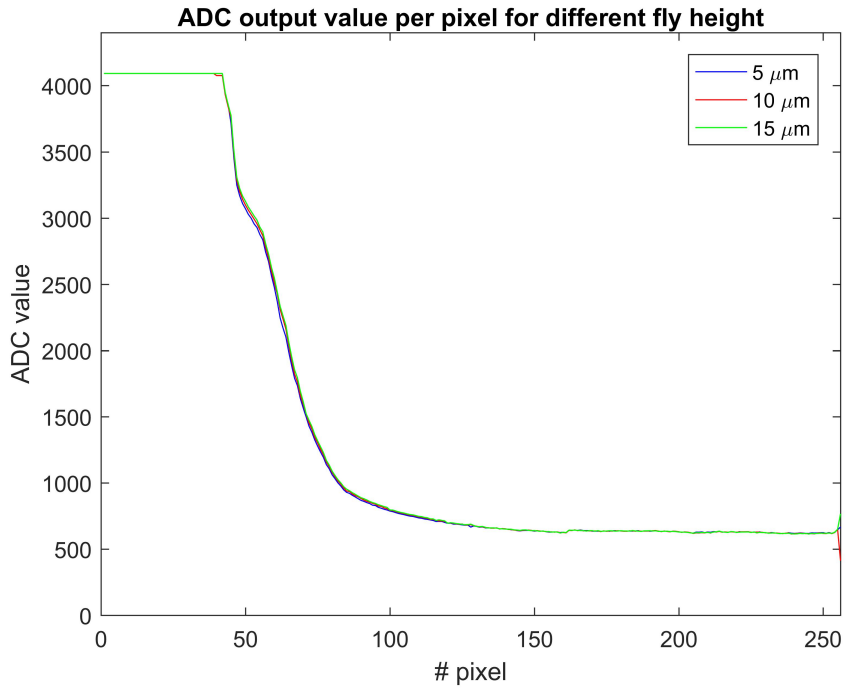

Figure 7.8: Results of the fly height measurement

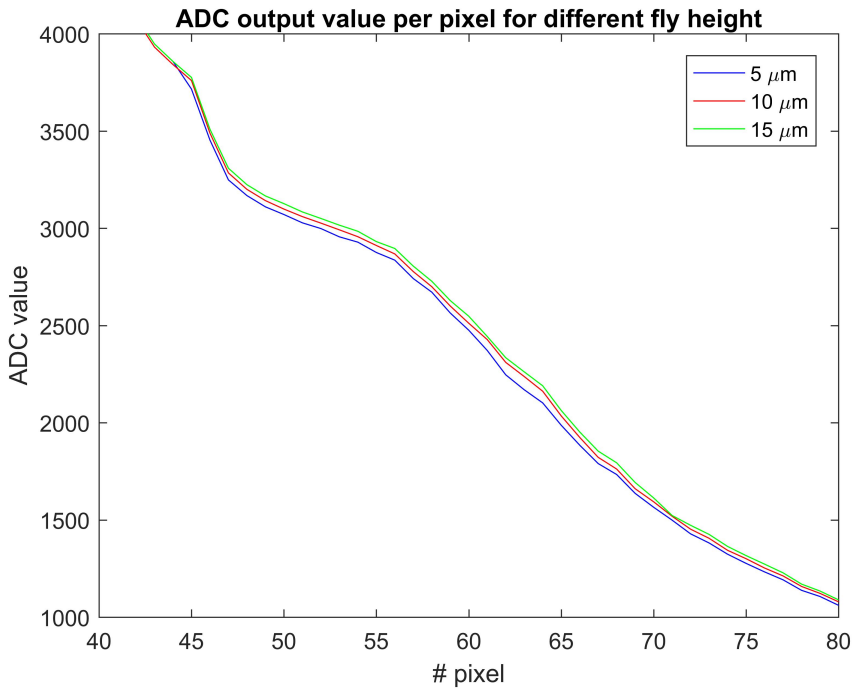

Figure 7.9: Zoomed in result of the fly height measurement

7.6 Analog integrator

The correction (baseline) measurement done in the paragraph 7.1 is typical for this sensor. It can easily be applied to a direct sensor read out, but for the analog integrator this is not possible, because all sensor values are added up by the integrator circuit.
The sensor is now connected in the serial connection as explained in paragraph 6.2. Pin 6 of the TSL4102R (serial output 2) will be connected to the switch of the integrator circuit. When the last pixel output value has been send, pin 6 of the sensor will give a signal. At this point all 256 voltage signals from the pixels will have been accumulated in the capacitor. Now the switch is closed and the capacitor is depleted. The output voltage that can now be measured by an ADC.

As explained in paragraph 5.4 the integrator circuit includes a resistor, which is chosen at 1.5 kΩ and a capacitor, which is chosen at 0.2 μF. With these values, the conditions presented in paragraph 5.4.2 are satisfied. Another possible combination would be to choose the resistor at 500 Ω and the capacitor at 0.56 μF. The resistor and capacitor value, together with the time it will take to complete one sensor read out and the voltage at which this happens determine the accumulated voltage value that will be received from the capacitor when the reset switch is closed. Equation 7.6.1 explains how the accumulated voltage can be predicted:

$$V_{capacitor} = -\frac{t_{cycle} * V_{sensor}}{1.5k\Omega * 0,2\mu F} \tag{7.6.1}$$

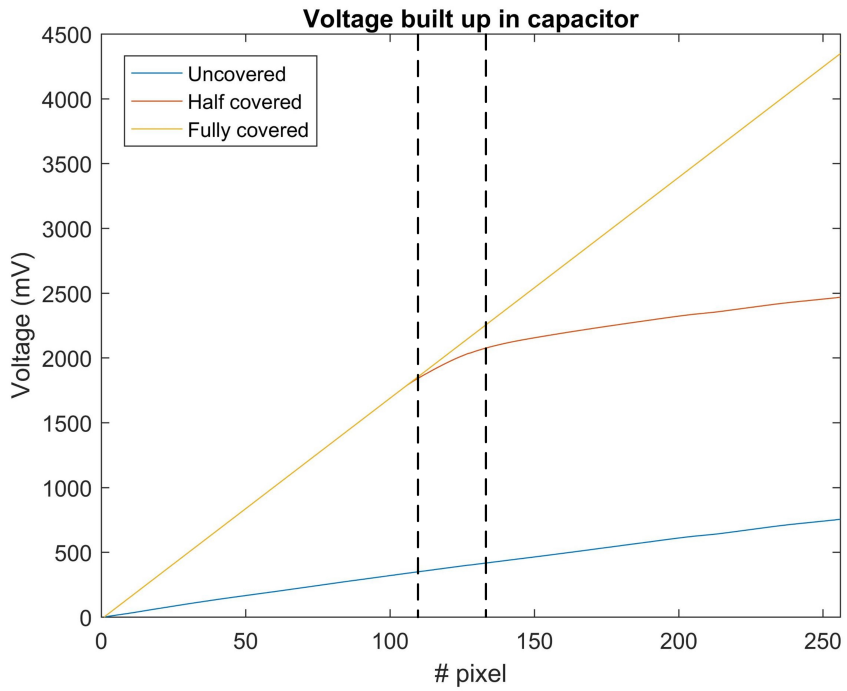

Figure 7.10: Output values of the analog integrator

Several measurements have been done to ensure that the output data from the analog integrator can be interpreted correctly. First of all, the sensor has been measured in a totally covered and uncovered state. The average voltage output values were 20 mV and 128 mV respectively. When using equation 7.6.1, this results in a total predicted capacitor output voltage of 0.73V for the covered sensor. For a totally uncovered sensor the calculated output voltage is equal to 4,69 Volt. Afterwards the length of the transition zone was measured. The transition zone starts at the pixel where the first voltage drop occurs, and ends when the output value of the pixel falls within 10% of the sensor output value of a covered sensor. The length of the transition zone is defined as 29 pixels.

When the sensor is driven at 20 kHz, the time of one cycle is equal to 12 ms. This is calculated using equation 4.5.1. With equation 5.4.1 and 5.4.2 we can now predict the output voltage of the capacitor at each wafer location. Figure 7.10 gives an overview of the voltage built up in the capacitor for a fully covered, half covered and uncovered wafer. The dotted lines define the beginning and the end of the transition zone. The values lie in the predicted range. The length of the transition zone is much larger than the expected transition area length of several pixels. The accuracy of the analog integrator is lower than that of a normal sensor read out. It is possible to determine the wafer position with the accuracy of 60 μm. This is almost equal to the centre to centre distance between two pixels (63.5 μm).

8

Conclusion and recommendations

In this thesis I have been looking for a cheap, simple sensor that can locate the position of a substrate that is transported by an air bearing. I found a sensor that is cheap and has a simple working principle that can be used for a distributed sensing system.

8.1 Conclusions

Four main measurements have been done in this research. Each measurement was meant to research a specific system property.

The resolution for the sensor was found to be 1 μm. By moving the substrate a distance of 1 μm within the same pixel, a difference in absolute voltage output of 0.1 percent is measured. This fulfils the set requirement. From this we can conclude that with the linear sensor array an affordable, reliable sensor has been found for determining the position of the substrate. When the wafer is located in the 'dead zone' of 8 μm between to pixels, no measurement output is generated.
Afterwards a measurement where different light colours were used was performed. It is clear that the differences in sensor output are minimal for the applied change in light colour. However, the illumination was moved to the opposite side of the sensor. With additional research it could be explored if a change in wavelength makes a difference when the illumination is placed next to the sensor.
For the height measurement, a difference could be seen when the fly height was varied with steps of 5 μm. The difference is visible in the transition area, but disappears when the sensor is fully covered.
Applying an analog integrator circuit to reduce the requirements for data processing turned out to be a good solution. The position of the substrate can be predicted. However, the accuracy was in the range of 60 μm (almost equal to the centre to centre distance between 2 pixel): this does not fulfil the measurement system requirements, it has to be improved before it can be used as a reliable measurement system.

The requirement that the measurement should be one sided (all components should be located on one side of the substrate) has not yet been fulfilled in the conducted experiments. However, literature has shown that the 'light reflection' theory, where the illumination is placed on the same side, right next to the sensor is plausible. So this is not a limitation for the intended use of this sensing method [1].

8.2 Recommendations

There are several recommendation for future research that would increase the knowledge about the linear sensor array. The first recommendation is to produce a test setup in which the smaller sensor (the TSL1401CL) is used, so that the illumination can be placed next to the sensor on the same side of the wafer. Due to the high reflectivity of the wafer, the light will be reflected onto the sensor if it is covered by a substrate. If the sensor is tested in an environment with little ambiant light, the size of the transition area will decrease. This in turn will

increase the voltage drop, and thereby the accuracy of the sensor. In a setup where the illumination is located on the same side as the sensor, it will also be interesting to test the influence of different light colours. For the type of illumination there is a promising method beside the LEDs that would be valuable to investigate: the use of a plexiglass lens, or multiple plexiglass lenses. With this the light from a light source can be conducted to the surface, and from the surface back again to the sensor pixels. That may provide a method to eliminate the dead zone between the individual LEDs, and reduce the width of the sensor assembly.

The next logical step would be to test the possibility of the sensor to detect a faster moving substrate. This measurement could be done by connecting a wafer to a stepper motor, that is positioned at a distance of 10 μm to the sensor. The wafer should not be positioned in the centre, but slightly more to the side to create a leading and a trailing edge that could be measured by the LSA. By rotating the motor, the wafer moves at a high speed past the sensor. An advantage of this setup is that the sensor can be tested at higher speed, without the need to build an air based actuation system. When the sensor is driven at its highest speed it should still be able to detect the substrate with a high accuracy.

When both of the above tests give a positive result, it would be interesting to see how a test setup that includes the actuator and bearing cells would interact with the sensor system.

To conclude, with this research I have found a reliable sensor with which I can measure the position of a substrate with an accuracy of 6 μm at a bandwidth of 2 kHz, well within the required positioning accuracy for the measurement system of 15 μm. The analog integrator is a promising concept to reduce the system costs and complexity, although the concept should be fine tuned before it can be used to estimate the wafer position with the required accuracy.

Appendix

.1 List of displacement sensors from Jansen electronics [10]

PRECISION POINT

Actuators &Sensors	DISPLACEMENT SENSORS - CONCEPT OVERVIEW	1 / 1

Physical principle	concept	Contactless	friction, wear	size	Vacuum	Cryo	€	Environmental robustness	Linearity /	Tranverse directional	Complexity	Surface requirements	resolution	range	bandwidth
Resistive	**Linear/rotary Potentiometer** Resistance proportional to displacement along resistor.	⊗	⊗	☺	☺	☺	☺	⊗	😐	☺	☺	⊗	10 [µm]	1000 [mm]	
	Strain gauge Resistance changes when under strain. Secondary position sensor.	⊗	☺	☺	☺	☺	☺	☺	😐	😐	☺	☺	Depends on primary sensor to convert displacement to strain.		
Capacitive	**Variable seperation, area or dielectric** Change in capacitance due to change in plate area, seperation or intermidiate dielectric	😐	☺	☺	☺	☺	☺	⊗	⊗	⊗	⊗	⊗	1 [nm]	0.01 – 2 [mm]	100 [kHz]
Inductive	**LVDT** Linear Variable Differential Transformer displacement sensor	⊗	☺	⊗	☺	☺	☺	☺	⊗	☺	⊗	☺	0.0001% of Full Scale	0.25-250 [mm]	50 [kHz]
	Eddy Current Interaction of the magnatic field of two conducting surfaces.	😐	☺	☺	☺	😐	😐	☺	⊗	⊗	☺	⊗	[µm]	[mm]-[cm]	100 [kHz]
	Variable reluctance sensor Displacement causes change in total reluctance and hence inductance.	😐	☺	☺	☺	☺	☺	☺	⊗	☺	☺	⊗		10 [mm]	Not good for static/low speed
Piezo	**Piezo electric accelerometer** Accelerometer/force sensor	⊗	☺	☺	☺	☺	😐	☺	☺	☺	😐	☺	Depends on primary sensor to convert displacement to force.		
	Piezo strain gauge Piezo resistive	⊗	☺	☺	☺	☺	😐	☺	☺	☺	😐	☺	Depends on primary sensor to convert displacement to strain.		
Electro magnetic	**Hall effect** Lorentz force based	😐	☺	☺	☺	😐	☺	☺	⊗	⊗	☺	☺	100 [µm]	10 [mm]	100 [kHz]
	Variable reluctance sensor (VRS) Measuring thooted wheel speed	😐	☺	☺	☺	☺	☺	☺	⊗	⊗	☺	⊗	Less good than hall effect sensors.		[Hz]- 100 [kHz]
Optical	**Laser interferometer** Measuring surface shape and transmitted wavefronts	☺	☺	⊗	☺	☺	⊗	⊗	😐	😐	⊗	⊗	λ/8000	0-10[m]	Depends on signal conditioning
	Encoder Incremental linear or rotary optical encoders.	😐	☺	😐	☺	⊗	☺	⊗	☺	☺	☺	⊗	[nm]	[nm]-[m]	[MHz]
	Optical proximity detector Reflection of (usually) IR light	☺	☺	☺	☺	☺	☺	☺	☺	☺	☺	☺	[mm]	[mm]	500 [kHz]
	Confocal Chromatic measurement	☺	☺	😐	☺	☺	😐	⊗	☺	☺	☺	☺	10 [nm]	[mm]	100 [kHz]
	PSD Position sensitive detector.. Ex triangulation based distance sensor, quad cell,	☺	☺	⊗	☺	⊗	😐	☺	☺	☺	☺	☺	[µm]	[mm] to [m]	[MHz]
	Optical fiber Ex.fibre bragg grating strain or pressure sensor	⊗	☺	☺	☺	☺	☺	☺	☺	☺	☺	☺	[µm]	[m]	[Hz]

Parameter	☺	😐	⊗
Contactless	No contact: long working distance	No contact: short working distance	Contact
Friction, wear	No wear	/	Significant wear
Size	Relatively small ..... relatively large		
Vacuum	Vacuum compatible version	/	No vacuum compatible versions
Cryo	< 10 [K]	>200 [K]	Ambient
€	Reletively low cost ..... Relatively high cost		
Environmental robuustness	Operatable in every environment	/	Requires relatively clean environment
Linearity	Low linearity error ..... Large linearity error		
Transverse directional sensitivity	No influence ..... high influence from displacement in a transverse direction than measured		
Complexity	Relatively simple ..... relatively complex System including signal conditioning and processing		
Surface requirements	No measuring surface requirements	/	Special measuring surface required

.2 Sensor selection

Linear sensor array

Sensor	Brand	Pixel array	Sensor pitch [DPI]	Dynamic Range	Resolution [µm]	Clock [kHz]	Integration time [ms]	Integration time [kHz]	Number of outputs	Active length [mm]	Length [mm]	Width [mm]	Unit price	Mounting	Remarks
TSL1401CS-LF	AMS/TAOS	128x1	400	4000:1 (72 dB)		8000	0.03375 - 100	26.62 – 0.010	1	8.12	8.87	1.0	?	SMD/SMT	Obsolete
TSL1401CL	AMS/TAOS	128x1	400	4000:1 (72 dB)		8000	0.03375 - 100	C c – 0.010	1	8.12	9.4	3.0	~ €6.27 ~ €6.46	SMD/SMT	
TSL1402R	AMS/TAOS	256x1	400	4000:1 (72 dB)		8000	0.04975 – 100 (S) 0.03375 – 100 (P)	20.1 – 0.010 (S) 26.62 – 0.010 (P)	2	16.23	19.30	10.67	~ €14.52	Through Hole	Too broad for a light source in the same plane?
TSL1406R	AMS/TAOS	768x1	400	4000:1 (72 dB)		8000	0.11375 – 100 (S) 0.06575 – 100 (P)	8.79 – 0.010 (S) 15.2 – 0.0010 (P)	2	48.69	61.33	12.95	~ €24.62	SMD/SMT	Too broad for a light source in the same plane?
TSL1410R	AMS/TAOS	1280x1	400	4000:1 (72 dB)		8000	0.17775 – 100 (S) 0.097775 – 100 (P)	5.62 – 0.010 (S) 10.23 – 0.0010 (P)	2	81.15	93.85	12.95	~ €36.27	SMD/SMT	Too broad for a light source in the same plane?
TSL1412S	AMS/TAOS	1536x1	400	4000:1 (72 dB)		8000	0.20975 - 100 (S) 0.11375 – 100 (P)	4.76 – 0.010 (S) 8.79 – 0.010 (P)	2	97.38	103.60	12.95	~ €42.88	SMD/SMT	Too broad for a light source in the same plane?
TSL201	AMS/TAOS	64x1	200	2000:1 (66 dB)		5000	0.013 - 100	76.92 – 0.010	1	8.26	9.4	3.0	~ €3.12[1]	SMD/SMT	
TSL202R	AMS/TAOS	128x1	200	2000:1 (66 dB)		5000	0.026 – 100 (S) 0.013 – 100 (S)	38.46 – 0.010 (S) 76.92 – 0.010 (P)	2	16.52	19.30	10.67	~ €14.23	Through Hole	Too broad for a light source in the same plane?
TSL208R	AMS/TAOS	512x1	200	2000:1 (66 dB)		5000	0.1026 - 100	9.746 – 0.010	1	66.06	76.33	12.83	~ €34.10	SMD/SMT	Too broad for a light source in the same plane?
TLS210	AMS/TAOS	640x1	200	2000:1 (66 dB)		5000	0.128 – 100 (S) 0.026 – 100 (P)	7.812 – 0.010 (S) 38.46 – 0.0010 (P)	5	82.58	93.875	12.95	~ €36.01	SMD/SMT	Too broad for a light source in the same plane?
TSL2014	AMS/TAOS	896x1	200	2000:1 (66 dB)		5000	0.1792 – 100 (S) 0.090 – 100 (P)	5.85 – 0.010 (S) 11.11 – 0.010 (P)	2	115.61	120.24	16.942	~ €45.40	SMD/SMT	Too broad for a light source in the same plane?
S11107-10	Hamamatsu	64x1		5700:1 (75 dB)		10000	0.0065	153.84 111111 frames/s	1	8.06	9.1	2.4		SMD/SMT	
S11106-10	Hamamatsu	128x1		6600:1 (76 dB)		10000	0.0129	77.5 64935 frames/s	1	8.06	9.1	2.4		SMD/SMT	
S10227-10	Hamamatsu	512x1		9555:1 (79 dB)		5000	0.1057	9.46 9434 frames/s	1	6.4	9.1	4.4		SMD/SMT	
S10226-10	Hamamatsu	1024x1		4570:1 (73 dB)		800	5.1	0.196 194 frames/s	1	7.9872	9.1	2.4		SMD/SMT	
S12443	Hamamatsu	2496x1		1666:1 (64 dB)		10000	0.2518	3.971 3924 frames/s	1	17.472	22.9	2.7		SMD/SMT	
MLX90255BA	Melexis	128x1	385	1000:1 (60 dB)		500	0.125 - 100	8 – 0.0010	1	9.5	15.2	7.8	~$25	SMD/SMT	Replacement for TSL1401
MLX90255BC	Melexis	128x1	385	1000:1 (60 dB)		800	0.125 - 100	8 – 0.0010	1	9.5	15.2	7.8		SMD/ST	Replacement for TSL1401

1. Only sold in reels of 1000.

Position sensitive device

1-dimensional PSD Sensor	Brand	Photosensitive area (mm)	Spectral response range (nm)	Peak responsivity wavelength (nm)	Responsivity max. (A/W)	Dark current (nA) Typ. (max)	Rise time (µs)	Capacitance (pF) Typ. (max)	Breakdown voltage (V)	Interelectrode resistance (kΩ) (V_{bias} (V))	Position detection error (µm) typ. (max.)	Position resolution (µm)	Saturation photocurrent (µA)	Sensor length x width [mm]	Sensor Hight [mm]	Photo sensitive area/sensor length	Unit Price	Mounting package	Remarks
501278	First sensor	6 x 1	400-1100	850	0.59	10 (20)	0.2		30	65-105 (15)	0.2-1 %	0.05 (**Noise lim.**)		9.92 x 6	1.39	0.605	€ 30,43	SO-16 SMD/SMT	
501115	First sensor	6 x 1	700-1100	850	0.59	10 (20)	0.2	12	30	65-105 (15)	0.2-1 %	0.05 (**Noise lim.**)		7,2 x 4	1,2	0.833	?		
SL5-1	Osio opto electronics	5 x 1	400-1100	920	0.4	10 (100)	0.1	5 (9)		20-100 (-15)	5	5		13,97 Ø	5,08	0.358	€ 74,92	42 / TO-8	Minimum order size of 10 for each PSD type
SL5-2	Osio opto electronics	5 x 1	400-1100	920	0.4	10 (100)	0.1	5 (9)		20-100 (-15)	5	5		13,21 x 7.62	3,175	0.379	€ 94,08	48 / 8-pin DIP	
SL15	Osio opto electronics	15 x 1	400-1100	920	0.4	150 (300)	0.1	15 (25)		60-300 (-15)	15	15		30,48 x 15.24	3,175	0.492	€ 342,43	49 / 24-pin DIP	
SL30	Osio opto electronics	30 x 4	400-1100	920	0.4	150 (1000)	0.6	125 (150)		40-80 (-15)	30	0		44,07 x 9,80	1,905	0.681	€ 400,51	51 / Ceramic	
SL76-1	Osio opto electronics	76 x 2.5	400-1100	920	0.4	100 (1000)	1.4	190 (250)		120-600 (-15)	76	76		127.76 x 12.7	6.35	0.594	€ 592,9	50 / Special	
LSC-5D	Osio opto electronics	5.3 x 2.2	400-1100	920	0.42	10 (100)	0.25	50		2-50 (-15)	40	40		35,56 x 12,7	4,318	0.146	€ 77,56	47 / plastic	
LSC-30D	Osio opto electronics	30 x 4.1	400-1100	920	0.42	25 (250)	3.0	300		4-100 (-15)	240	240		60,96 x 16,26	4,318	0.492	€ 258,34	46 / plastic	
S5629	Hamamatsu	1 x 6	760-1100	960	0.51	0.1 (2)	5	60		30-80 (0.1)	20 (60 max.)		80	9.7 x 8.0	1.7	0.619	€ 3,76	9 / Plastic	Minimum order size is 20 of the same PSDs, delivery time of 4-5 weeks on average for all Hamamatsu sensors
S5629-01	Hamamatsu	1 x 6	320-1100	960	0.55	0.1 (2)	5	60		30-80 (0.1)	20 (60)		80	9.7 x 8.0	1.7	0.619	€ 4,01	10 / Plastic	
S5629-02	Hamamatsu	1 x 6	760-1100	960	0.51	0.1 (2)	10	60		240-360 (0.1)	20 (60)		20	9.7 x 8.0	1.7	0.619	€ 4,01	9 / Plastic	
S3931	Hamamatsu	1 x 6	320-1100	920	0.55	0.15 (10)	1.5	40		30-80 (0.1)	30 (120)	0.2	100	9.2 x 4.8	1.5	0.652	€ 26,80	12 / Ceramic	Minimum order size is 3 PSDs
S3932	Hamamatsu	1 x 12	320-1100	920	0.55	0.2 (20)	3	80		30-80 (0.1)	60 (240)	0.3	100	15.2 x 4.8	1.5	0.789	€ 42,60	13 / Ceramic	Minimum order size is 2 PSDs
S1352	Hamamatsu	34 x 2.5	320-1100	920	0.6	2 (150)	0.7	150		10-30 (0.1)	125 (500)	2.1	250	57 x 9	5.0	0.596	-	14 / Ceramic	No longer available
S3270	Hamamatsu	37 x 1	700-1100	960	0.55	0.5 (20)	1	100		10-20 (0.1)	100 (400)	2.8	300	55 x 5	2.5	0.672	€ 39,90	15 / Ceramic	Minimum order size is 2 PSDs
S8543	Hamamatsu	24 x 0.7	320-1100	960	0.58	1 (15)	20	65 (130)		100-180	50 (250)	0.6	200	36.7 x 4	1.36	0.654	-	Ceramic	No longer available
IC-ODL	ICHaus	8.4 x 0.88	500-1050	830	0.5									9.5 x 4.7	1.75	0.884	$12.76	iC-ODL OBGA ODL2C	Voltage output
S-50VL	Osio optoelectronics																		
JQ 50P	Electro Optical Components, Inc.	12.5 x 4	400-1100	850	0.6	2 (10)	0.4	20						13.97 Ø	4.5				
JI 576	Electro Optical Components, Inc.	2.99 Ø	400-1100	850			3.5							9.1 Ø	6.5				
JL 577	Electro Optical Components, Inc.	2.99 Ø	400-1100	850			20							9.1 Ø	6.5				
JL 578	Electro Optical Components, Inc.	2.99 Ø	400-1100	850			50							9.1 Ø	6.5				

Optical fiber

Parameter	Philtec RC10-DC-20 kHz	Mti instruments (MTI-2020R)	Micro epsilon	Unit					
Size (tip diameter)	2	0.2	3.18	mm					
Costs				€ per sensor					
(environmental) robustness			IP 65						
Linearity									
Transverse directional sensitivity									
Complexity (signal conditioning and processing									
Substrate surface requirements	Higher sensitivity for reflective surfaces								
Resolution (smallest detectable increment)	0.5 for 100 Hz 1 for 20 kHz	1	5	μm					
Accuracy				% or μm					
Range	1.3			mm					
Linear range	0.25	4		mm					
Stand-off (distance between sensor and minimal detectable value)	0.5	2	4	mm					
Bandwidth	20 kHz	100 kHz							
Sensitivity	6.7 mV/μm	0.65 μm/mV							

.3 Datasheet linear sensor array TSL1402R [4]

TAOS Inc.

is now

ams AG

The technical content of this TAOS datasheet is still valid.

Contact information:

Headquarters:
ams AG
Tobelbaderstrasse 30
8141 Unterpremstaetten, Austria
Tel: +43 (0) 3136 500 0
e-Mail: ams_sales@ams.com

Please visit our website at **www.ams.com**

l

TAOS TEXAS ADVANCED OPTOELECTRONIC SOLUTIONS®

TSL1402R
256 × 1 LINEAR SENSOR ARRAY WITH HOLD

TAOS041G – NOVEMBER 2011

- **256 × 1 Sensor-Element Organization**
- **400 Dots-Per-Inch (DPI) Sensor Pitch**
- **High Linearity and Uniformity**
- **Wide Dynamic Range . . . 4000:1 (72 dB)**
- **Output Referenced to Ground**
- **Low Image Lag . . . 0.5% Typ**
- **Operation to 8 MHz**
- **Single 3-V to 5-V Supply**
- **Rail-to-Rail Output Swing (AO)**
- **No External Load Resistor Required**
- **Replacement for TSL1402**

(TOP VIEW)

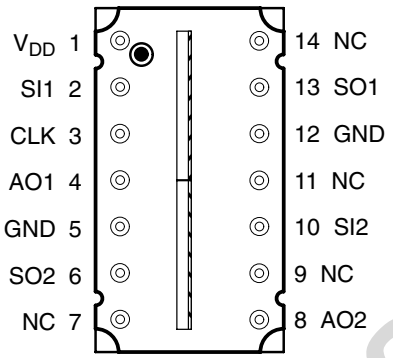

NC – No internal connection

Description

The TSL1402R linear sensor array consists of two sections of 128 photodiodes each and associated charge amplifier circuitry, aligned to form a contiguous 256 × 1 pixel array. The device incorporates a pixel data-hold function that provides simultaneous integration start and stop times for all pixels. The pixels measure 63.5 µm by 55.5 µm, with 63.5-µm center-to-center spacing and 8-µm spacing between pixels. Operation is simplified by internal logic requiring only a serial-input pulse (SI) and a clock.

The TSL1402R is intended for use in a wide variety of applications including mark and code reading, OCR and contact imaging, edge detection and positioning, and optical encoding.

Functional Block Diagram (each section – pin numbers apply to section 1)

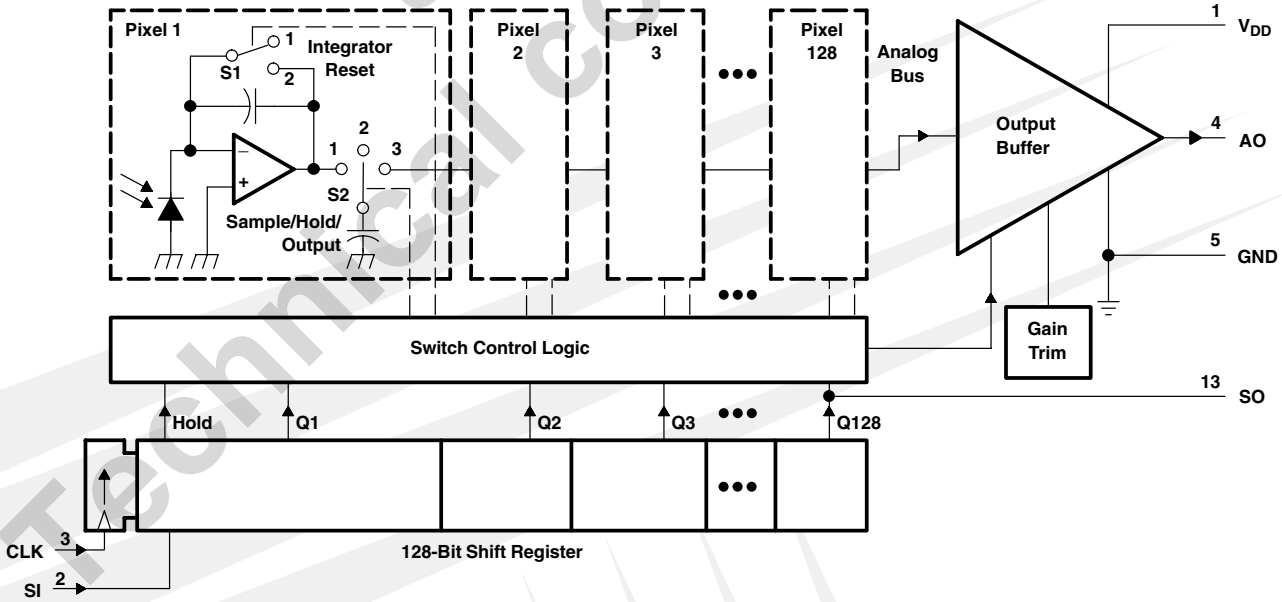

Texas Advanced Optoelectronic Solutions Inc.
1001 Klein Road • Suite 300 • Plano, TX 75074 • (972) 673-0759
www.taosinc.com

TSL1402R
256 × 1 LINEAR SENSOR ARRAY WITH HOLD

Terminal Functions

TERMINAL NAME	TERMINAL NO.	DESCRIPTION
AO1	4	Analog output of section 1.
AO2	8	Analog output of section 2.
CLK	3	Clock. Clk controls charge transfer, pixel output, and reset.
GND	5,12	Ground (substrate). All voltages are referenced to GND.
NC	7, 9, 11, 14	No internal connection.
SI1	2	Serial input (section 1). SI1 defines the start of the data-out sequence for section 1.
SI2	10	Serial input (section 2). SI2 defines the start of the data-out sequence for section 2.
SO1	13	Serial output (section 1). SO1 provides a signal to drive the SI2 input (in serial connection).
SO2	6	Serial output (section 2). SO2 provides a signal to drive the SI input of another device for cascading or as an end-of-data indication.
V_{DD}	1	Supply voltage. Supply voltage for both analog and digital circuitry.

Detailed Description

Device operation (assumes serial connection)

The sensor consists of 256 photodiodes, called pixels, arranged in a linear array. Light energy impinging on a pixel generates photocurrent, which is then integrated by the active integration circuitry associated with that pixel.

During the integration period, a sampling capacitor connects to the output of the integrator through an analog switch. The amount of charge accumulated at each pixel is directly proportional to the light intensity on that pixel and the integration time.

The output and reset of the integrators is controlled by a 256-bit shift register and reset logic. An output cycle is initiated by clocking in a logic 1 on SI1. An internal signal, called Hold, is generated from the rising edge of SI1 and simultaneously transmitted to sections 1 and 2. This causes all 256 sampling capacitors to be disconnected from their respective integrators and starts an integrator reset period. As the SI pulse is clocked through the shift register, the charge stored on the sampling capacitors is sequentially connected to a charge-coupled output amplifier that generates a voltage on analog output AO. Simultaneously, during the first 18 clock cycles, all pixel integrators are reset, and the next integration cycle begins on the 19th clock. On the 128th clock rising edge, the SI pulse is clocked out on the SO1 pin (section 1) and becomes the SI pulse for section 2 (SI2). The rising edge of the 129th clock cycle terminates the SO1 pulse, and returns the analog output AO1 of section 1 to high-impedance state. Analog output AO2 now becomes the active output. As in section 2, SO2 is clocked out on the 256th clock pulse. Note that a 257th clock pulse is needed to terminate the SO2 pulse and return AO2 to the high-impedance state. If a minimum integration time is desired, the next SI pulse may be presented after a minimum delay of t_{qt} (pixel charge transfer time) after the 257th clock pulse.

AO is an op amp-type output that does not require an external pull-down resistor. This design allows a rail-to-rail output voltage swing. With V_{DD} = 5 V, the output is nominally 0 V for no light input, 2 V for normal white level, and 4.8 V for saturation light level. When the device is not in the output phase, AO is in a high-impedance state.

The voltage developed at analog output (AO) is given by:

$$V_{out} = V_{drk} + (R_e)(E_e)(t_{int})$$

where:

V_{out}	is the analog output voltage for white condition
V_{drk}	is the analog output voltage for dark condition
R_e	is the device responsivity for a given wavelength of light given in V/(μJ/cm^2)
E_e	is the incident irradiance in μW/cm^2
t_{int}	is integration time in seconds

The TSL1402R can be connected in the serial mode, where it takes 256 clocks to read out all pixels, or in the parallel mode where it takes 128 clocks to read out all pixels (see *APPLICATION INFORMATION* and FIgures 9 and 10).

A 0.1 μF bypass capacitor should be connected between V_{DD} and ground as close as possible to the device.

TSL1402R
256 × 1 LINEAR SENSOR ARRAY WITH HOLD

Absolute Maximum Ratings†

Supply voltage range, V_{DD} . . . . . –0.3 V to 6 V
Input voltage range, V_I . . . . . –0.3 V to V_{DD} + 0.3V
Input clamp current, I_{IK} (V_I < 0) or (V_I > V_{DD}) . . . . . –20 mA to 20 mA
Output clamp current, I_{OK} (V_O < 0 or V_O > V_{DD}) . . . . . –25 mA to 25 mA
Voltage range applied to any output in the high impedance or power-off state, V_O . . . –0.3 V to V_{DD} + 0.3 V
Continuous output current, I_O (V_O = 0 to V_{DD}) . . . . . –25 mA to 25 mA
Continuous current through V_{DD} or GND . . . . . –40 mA to 40 mA
Analog output current range, I_O . . . . . –25 mA to 25 mA
Maximum light exposure at 638 nm . . . . . 5 mJ/cm^2
Operating free-air temperature range, T_A . . . . . –25°C to 85°C
Storage temperature range, T_{stg} . . . . . –25°C to 85°C
Lead temperature 1,6 mm (1/16 inch) from case for 10 seconds . . . . . 260°C

† Stresses beyond those listed under “Absolute Maximum Ratings” may cause permanent damage to the device. These are stress ratings only, and functional operation of the device at these or any other conditions beyond those indicated under “Recommended Operating Conditions” is not implied. Exposure to absolute-maximum-rated conditions for extended periods may affect device reliability.

Recommended Operating Conditions (see Figure 1 and Figure 2)

	MIN	NOM	MAX	UNIT
Supply voltage, V_{DD}	3	5	5.5	V
Input voltage, V_I	0		V_{DD}	V
High-level input voltage, V_{IH}	2		V_{DD}	V
Low-level input voltage, V_{IL}	0		0.8	V
Wavelength of light source, λ	400		1000	nm
Clock frequency, f_{clock}	5		8000	kHz
Sensor integration time, Parallel, t_{int} (see Note 1)	0.03375		100	ms
Sensor integration time, Serial, t_{int} (see Note 1)	0.04975		100	ms
Setup time, serial input, $t_{su(SI)}$	20			ns
Hold time, serial input, $t_{h(SI)}$ (see Note 2)	0			ns
Operating free-air temperature, T_A	0		70	°C

NOTES: 1. Integration time is calculated as follows:
$t_{int(min)}$ = (256 – 18) × clock period + 20 μs
where *256* is the number of pixels in series, *18* is the required logic setup clocks, and *20 μs* is the pixel charge transfer time (t_{qt})
2. SI must go low before the rising edge of the next clock pulse.

Electrical Characteristics at f_{clock} = 1 MHz, V_{DD} = 5 V, T_A = 25°C, λ_p = 640 nm, t_{int} = 5 ms, R_L = 330 Ω, E_e = 11 μW/cm² (unless otherwise noted) (see Note 3)

PARAMETER		TEST CONDITIONS	MIN	TYP	MAX	UNIT
V_{out}	Analog output voltage (white, average over 256 pixels)	See Note 4	1.6	2	2.4	V
V_{drk}	Analog output voltage (dark, average over 256 pixels)	E_e = 0	0	0.1	0.2	V
PRNU	Pixel response nonuniformity	See Note 5			±10%	
	Nonlinearity of analog output voltage	See Note 6		±0.4%		
	Output noise voltage	See Note 7		1		mVrms
R_e	Responsivity	See Note 8	25	35	45	V/(μJ/cm²)
V_{sat}	Analog output saturation voltage	V_{DD} = 5 V, R_L = 330 Ω	4.5	4.8		V
		V_{DD} = 3 V, R_L = 330 Ω	2.5	2.8		
SE	Saturation exposure	V_{DD} = 5 V, See Note 9		136		nJ/cm²
		V_{DD} = 3 V, See Note 9		78		
DSNU	Dark signal nonuniformity	All pixels, E_e = 0, See Note 10		0.04	0.12	V
IL	Image lag	See Note 11		0.5%		
I_{DD}	Supply current	V_{DD} = 5 V, E_e = 0		6	9	mA
		V_{DD} = 3 V, E_e = 0		5	8	
I_{IH}	High-level input current	$V_I = V_{DD}$			10	μA
I_{IL}	Low-level input current	V_I = 0			10	μA
C_i	Input capacitance, SI			5		pF
C_i	Input capacitance, CLK			10		pF

NOTES: 3. All measurements made with a 0.1 μF capacitor connected between V_{DD} and ground.
4. The array is uniformly illuminated with a diffused LED source having a peak wavelength of 640 nm.
5. PRNU is the maximum difference between the voltage from any single pixel and the average output voltage from all pixels of the device under test when the array is uniformly illuminated at the white irradiance level. PRNU includes DSNU.
6. Nonlinearity is defined as the maximum deviation from a best-fit straight line over the dark-to-white irradiance levels, as a percent of analog output voltage (white).
7. RMS noise is the standard deviation of a single-pixel output under constant illumination as observed over a 5-second period.
8. $R_{e(min)} = [V_{out(min)} - V_{drk(max)}] \div (E_e \times t_{int})$
9. $SE(min) = [V_{sat(min)} - V_{drk(min)}] \times \langle E_e \times t_{int}) \div [V_{out(max)} - V_{drk(min)}]$
10. DSNU is the difference between the maximum and minimum output voltage for all pixels in the absence of illumination.
11. Image lag is a residual signal left in a pixel from a previous exposure. It is defined as a percent of white-level signal remaining after a pixel is exposed to a white condition followed by a dark condition:

$$IL = \frac{V_{out\ (IL)} - V_{drk}}{V_{out\ (white)} - V_{drk}} \times 100$$

Timing Requirements (see Figure 1 and Figure 2)

		MIN	NOM	MAX	UNIT
$t_{su(SI)}$	Setup time, serial input (see Note 12)	20			ns
$t_{h(SI)}$	Hold time, serial input (see Note 12 and Note 13)	0			ns
t_w	Pulse duration, clock high or low	50			ns
t_r, t_f	Input transition (rise and fall) time	0		500	ns
t_{qt}	Pixel charge transfer time	20			μs

NOTES: 12. Input pulses have the following characteristics: t_r = 6 ns, t_f = 6 ns.
13. SI must go low before the rising edge of the next clock pulse.

TSL1402R
256 × 1 LINEAR SENSOR ARRAY WITH HOLD

Dynamic Characteristics over recommended ranges of supply voltage and operating free-air temperature (see Figures 7 and 8)

PARAMETER		TEST CONDITIONS	MIN	TYP	MAX	UNIT
t_s	Analog output settling time to ±1%	R_L = 330 Ω, C_L = 10 pF		120		ns
$t_{pd(SO)}$	Propagation delay time, SO1, SO2			50		ns

TYPICAL CHARACTERISTICS

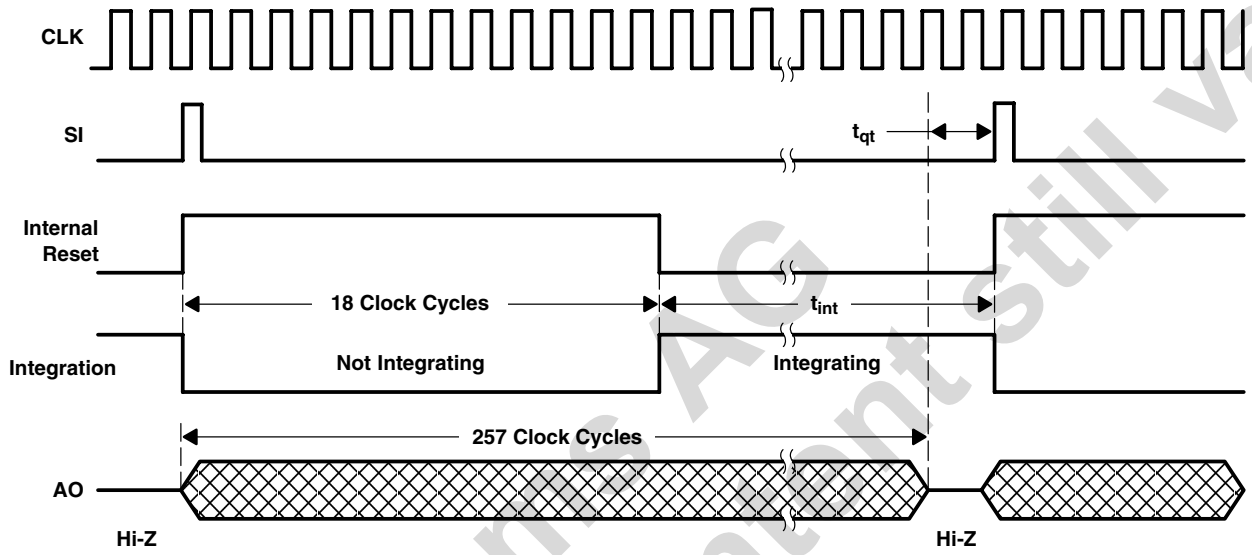

Figure 1. Timing Waveforms (Serial Connection)

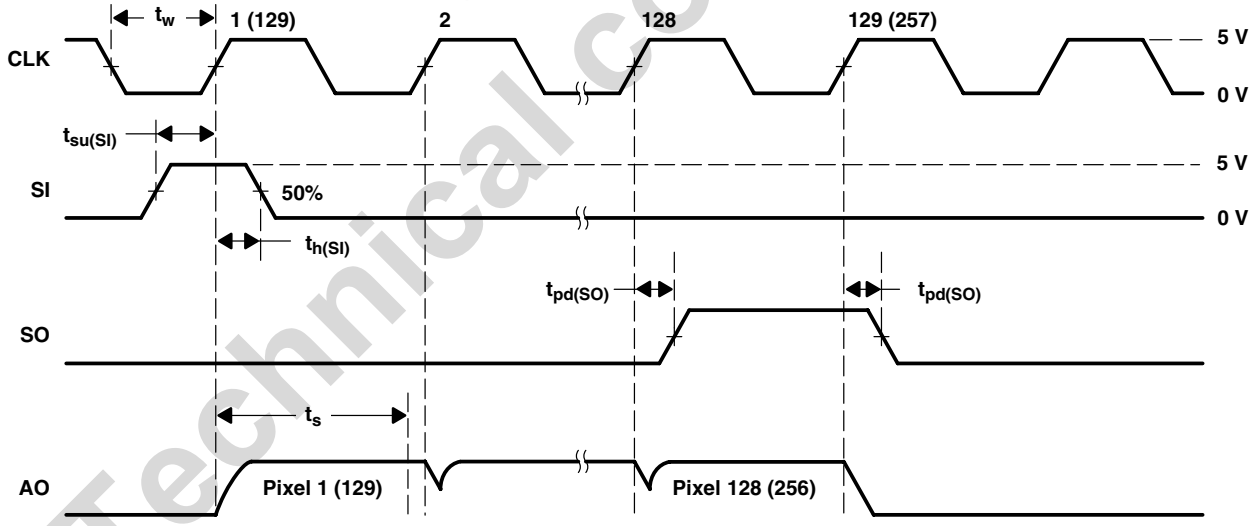

Figure 2. Operational Waveforms (each section)

TYPICAL CHARACTERISTICS

PHOTODIODE SPECTRAL RESPONSIVITY

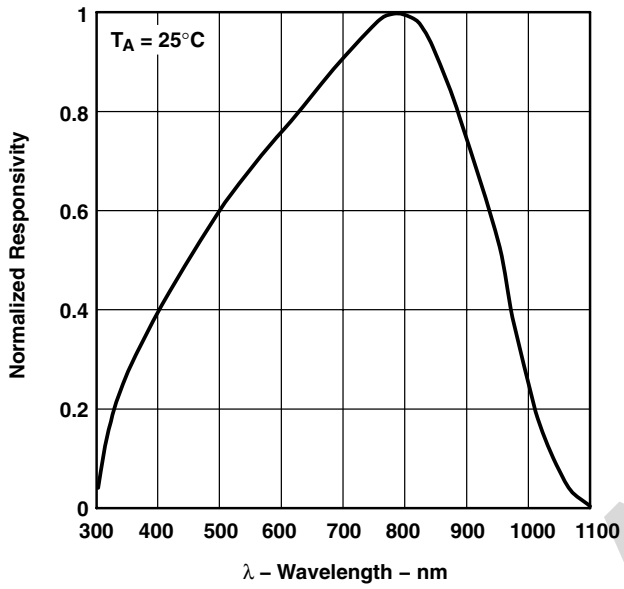

Figure 3

NORMALIZED IDLE SUPPLY CURRENT
vs
FREE-AIR TEMPERATURE

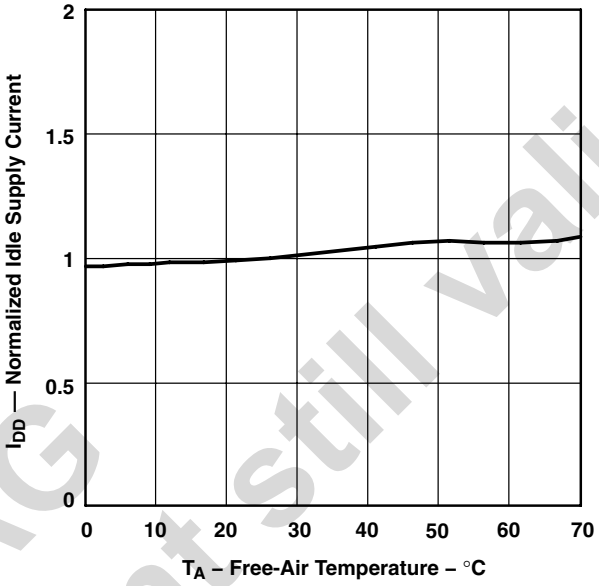

Figure 4

WHITE OUTPUT VOLTAGE
vs
FREE-AIR TEMPERATURE

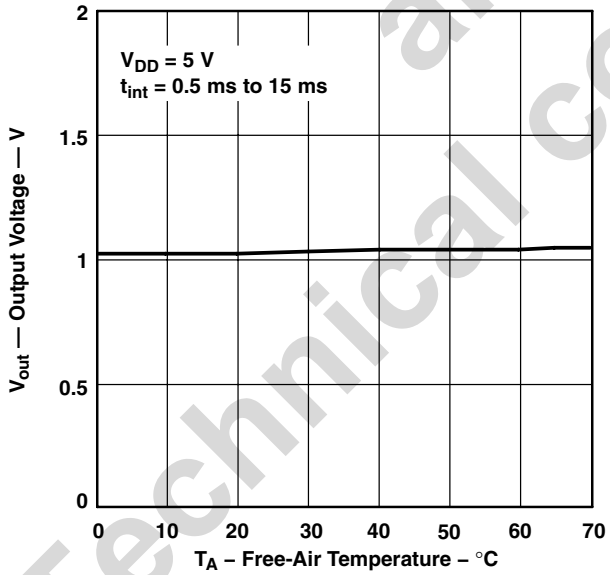

Figure 5

DARK OUTPUT VOLTAGE
vs
FREE-AIR TEMPERATURE

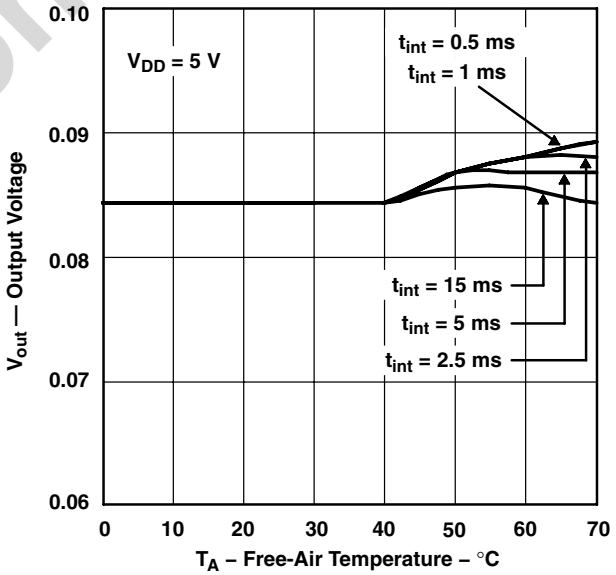

Figure 6

TYPICAL CHARACTERISTICS

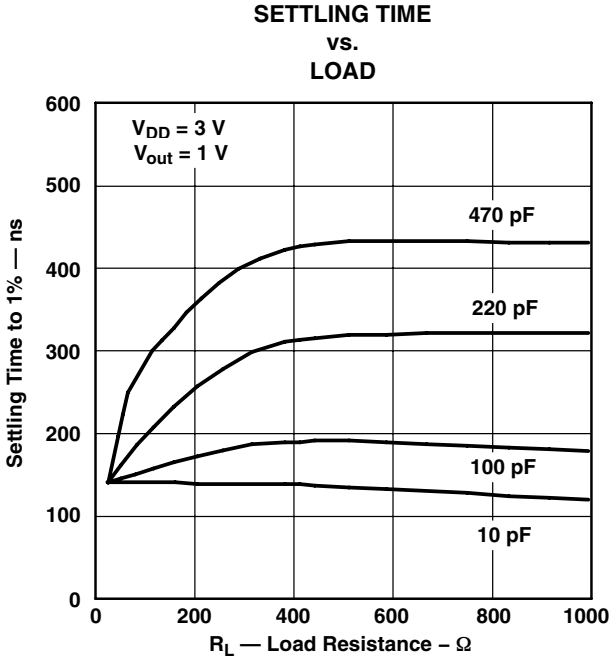

Figure 7

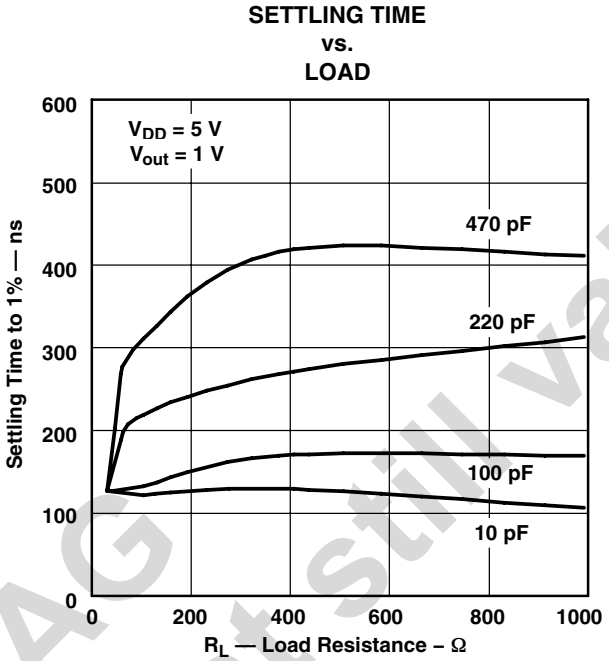

Figure 8

APPLICATION INFORMATION

Power Supply Considerations

For optimum device performance, power-supply lines should be decoupled by a 0.01-μF to 0.1-μF capacitor with short leads mounted close to the device package (see Figure 9 and Figure 10).

Connection Diagrams

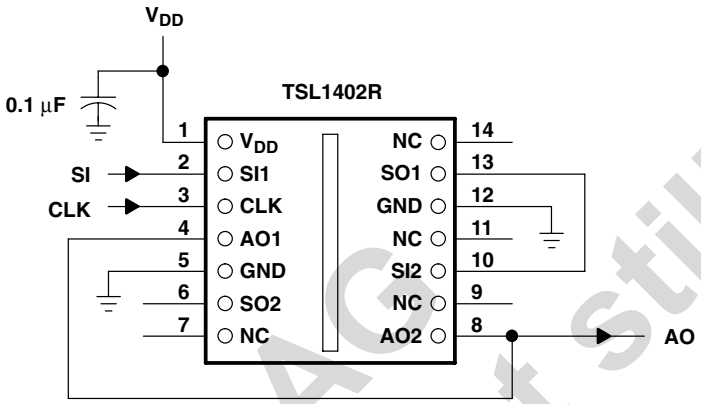

Figure 9. Serial Connection

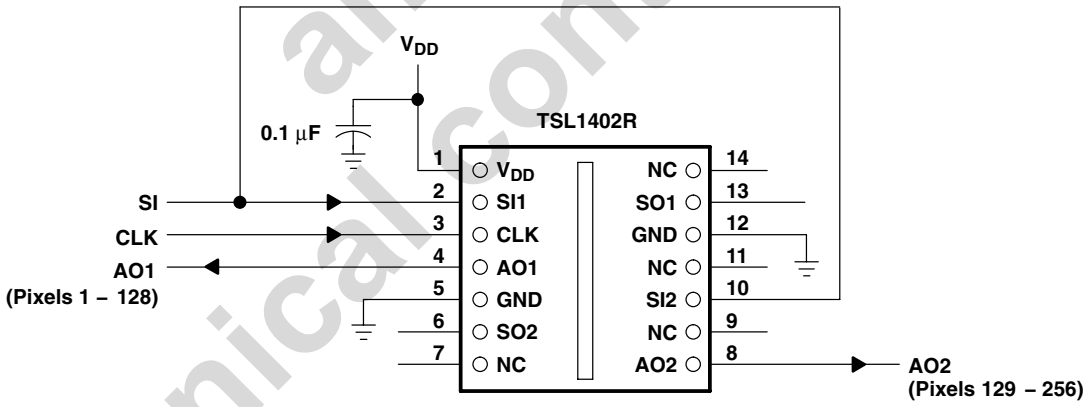

Figure 10. Parallel Connection

APPLICATION INFORMATION

Integration Time

The integration time of the linear array is the period during which light is sampled and charge accumulates on each pixel's integrating capacitor. The flexibility to adjust the integration period is a powerful and useful feature of the TAOS TSL14xx linear array family. By changing the integration time, a desired output voltage can be obtained on the output pin while avoiding saturation for a wide range of light levels.

The integration time is the time between the SI (Start Integration) positive pulse and the HOLD positive pulse minus the 18 setup clocks. The TSL14xx linear array is normally configured with the SI and HOLD pins tied together. This configuration will be assumed unless otherwise noted. Sending a high pulse to SI (observing timing rules for setup and hold to clock edge) starts a new cycle of pixel output and integration setup. However, a minimum of (*n*+1) clocks, where *n* is the number of pixels, must occur before the next high pulse is applied to SI. It is not necessary to send SI immediately on/after the (*n*+1) clocks. A wait time adding up to a maximum total of 100 ms between SI pulses can be added to increase the integration time creating a higher output voltage in low light applications.

Each pixel of the linear array consists of a light-sensitive photodiode. The photodiode converts light intensity to a voltage. The voltage is sampled on the Sampling Capacitor by closing switch S2 (position 1) (see the Functional Block Diagram on page 1). Logic controls the resetting of the Integrating Capacitor to zero by closing switch S1 (position 2).

At SI input, all of the pixel voltages are simultaneously scanned and held by moving S2 to position 2 for all pixels. During this event, S2 for pixel 1 is in position 3. This makes the voltage of pixel 1 available on the analog output. On the next clock, S2 for pixel 1 is put into position 2 and S2 for pixel 2 is put into position 3 so that the voltage of pixel 2 is available on the output.

Following the SI pulse and the next 17 clocks after the SI pulse is applied, the S1 switch for all pixels remains in position 2 to reset (zero out) the integrating capacitor so that it is ready to begin the next integration cycle. On the rising edge of the 19th clock, the S1 switch for all the pixels is put into position 1 and all of the pixels begin a new integration cycle.

The first 18 pixel voltages are output during the time the integrating capacitor is being reset. On the 19th clock following an SI pulse, pixels 1 through 18 have switch S2 in position 1 so that the sampling capacitor can begin storing charge. For the period from the 19th clock through the n^{th} clock, S2 is put into position 3 to read the output voltage during the n^{th} clock. On the next clock the previous pixel S2 switch is put into position 1 to start sampling the integrating capacitor voltage. For example, S2 for pixel 19 moves to position 1 on the 20th clock. On the *n*+1 clock, the S2 switch for the last (n^{th}) pixel is put into position 1 and the output goes to a high-impedance state.

If a SI was initiated on the *n*+1 clock, there would be no time for the sampling capacitor of pixel *n* to charge to the voltage level of the integrating capacitor. The minimum time needed to guarantee the sampling capacitor for pixel *n* will charge to the voltage level of the integrating capacitor is the charge transfer time of 20 µs. Therefore, after *n*+1 clocks, an extra 20 µs wait must occur before the next SI pulse to start a new integration and output cycle.

The minimum integration time for any given array is determined by time required to clock out all the pixels in the array and the time to discharge the pixels. The time required to discharge the pixels is a constant. Therefore, the minimum integration period is simply a function of the clock frequency and the number of pixels in the array. A slower clock speed increases the minimum integration time and reduces the maximum light level for saturation on the output. The minimum integration time shown in this data sheet is based on the maximum clock frequency of 8 MHz.

APPLICATION INFORMATION

The minimum integration time can be calculated from the equation:

$$T_{int(min)} = \left(\frac{1}{maximum\ clock\ frequency}\right) \times (n - 18)\ pixels + 20\mu s$$

where:

n is the number of pixels

In the case of the TSL1402R with the maximum clock frequency of 8 MHz, the minimum integration time would be:

$$T_{int(min)} = 0.125\mu s \times (128 - 18) + 20\mu s = 33.75\mu s$$

It is good practice on initial power up to run the clock (*n*+1) times after the first SI pulse to clock out indeterminate data from power up. After that, the SI pulse is valid from the time following (*n*+1) clocks. The output will go into a high-impedance state after the *n*+1 high clock edge. It is good practice to leave the clock in a low state when inactive because the SI pulse required to start a new cycle is a low-to-high transition.

The integration time chosen is valid as long as it falls in the range between the minimum and maximum limits for integration time. If the amount of light incident on the array during a given integration period produces a saturated output (Max Voltage output), then the data is not accurate. If this occurs, the integration period should be reduced until the analog output voltage for each pixel falls below the saturation level. The goal of reducing the period of time the light sampling window is active is to lower the output voltage level to prevent saturation. However, the integration time must still be greater than or equal to the minimum integration period.

If the light intensity produces an output below desired signal levels, the output voltage level can be increased by increasing the integration period provided that the maximum integration time is not exceeded. The maximum integration time is limited by the length of time the integrating capacitors on the pixels can hold their accumulated charge. The maximum integration time should not exceed 100 ms for accurate measurements.

It should be noted that the data from the light sampled during one integration period is made available on the analog output during the next integration period and is clocked out sequentially at a rate of one pixel per clock period. In other words, at any given time, two groups of data are being handled by the linear array: the previous measured light data is clocked out as the next light sample is being integrated.

Although the linear array is capable of running over a wide range of operating frequencies up to a maximum of 8 MHz, the speed of the A/D converter used in the application is likely to be the limiter for the maximum clock frequency. The voltage output is available for the whole period of the clock, so the setup and hold times required for the analog-to-digital conversion must be less than the clock period.

TSL1402R
256 × 1 LINEAR SENSOR ARRAY WITH HOLD

MECHANICAL INFORMATION

This assembly consists of 2 sensor chips mounted on a printed-circuit board in a clear molded plastic package.

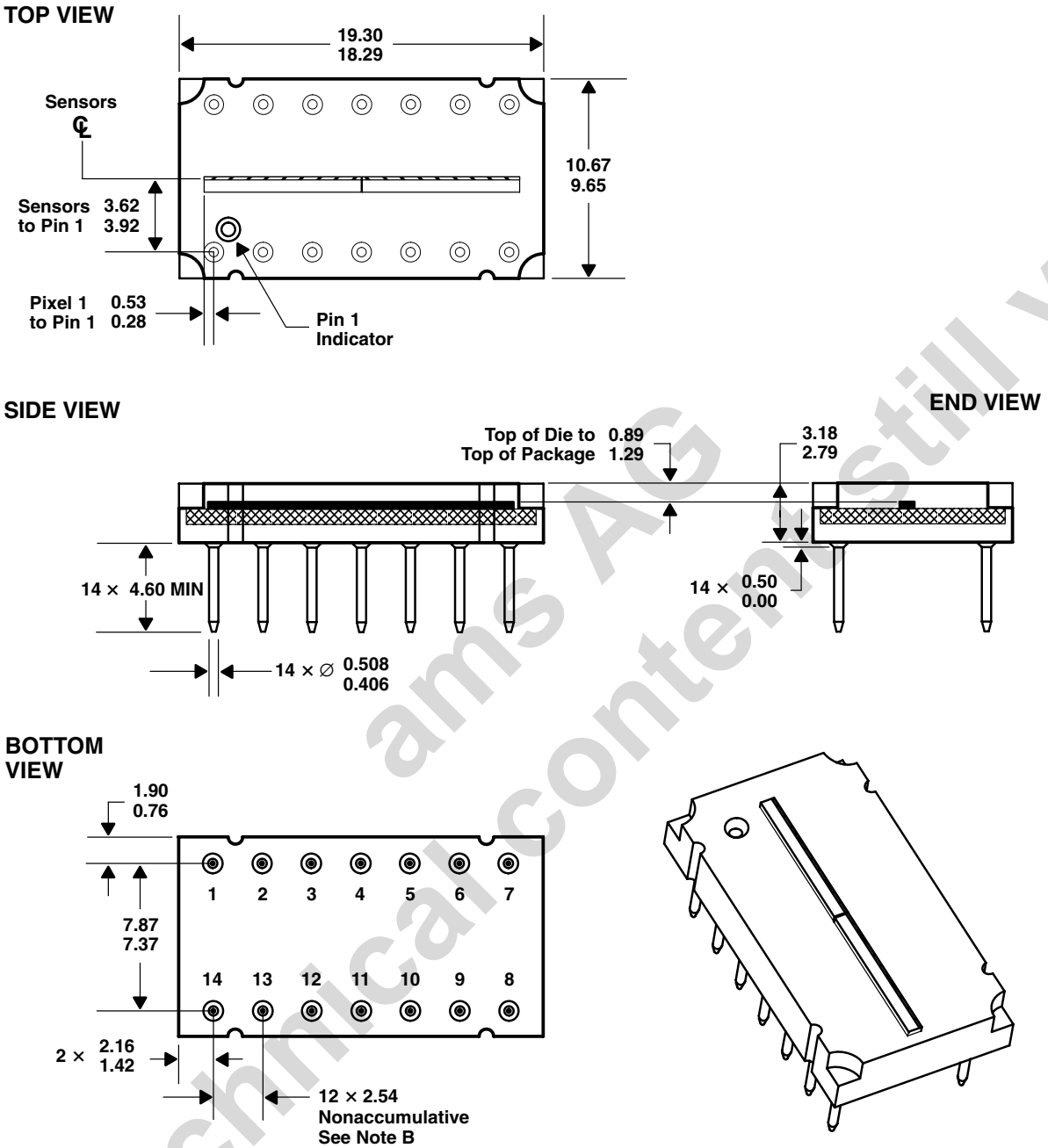

NOTES: A. All linear dimensions are in millimeters.
B. The true-position spacing is 2.54 mm between lead centerlines. Each pin centerline is located within 0.25 mm of its true longitudinal positions.
C. Index of refraction of clear plastic is 1.52.
D. The gap between the individual sensor dies in the array is 57 µm typical (51 µm minimum and 75 µm maximum).
E. This drawing is subject to change without notice.

Figure 11. Packaging Configuration

MECHANICAL INFORMATION

THEORETICAL PIXEL LAYOUT FOR IDEAL CONTINUOUS DIE

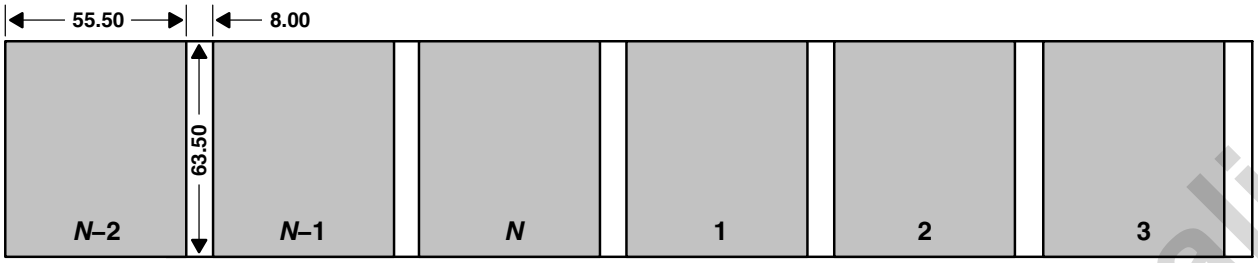

ACTUAL MULTI-DIE PIXEL LAYOUT FOR DIE-TO-DIE EDGE JOINING

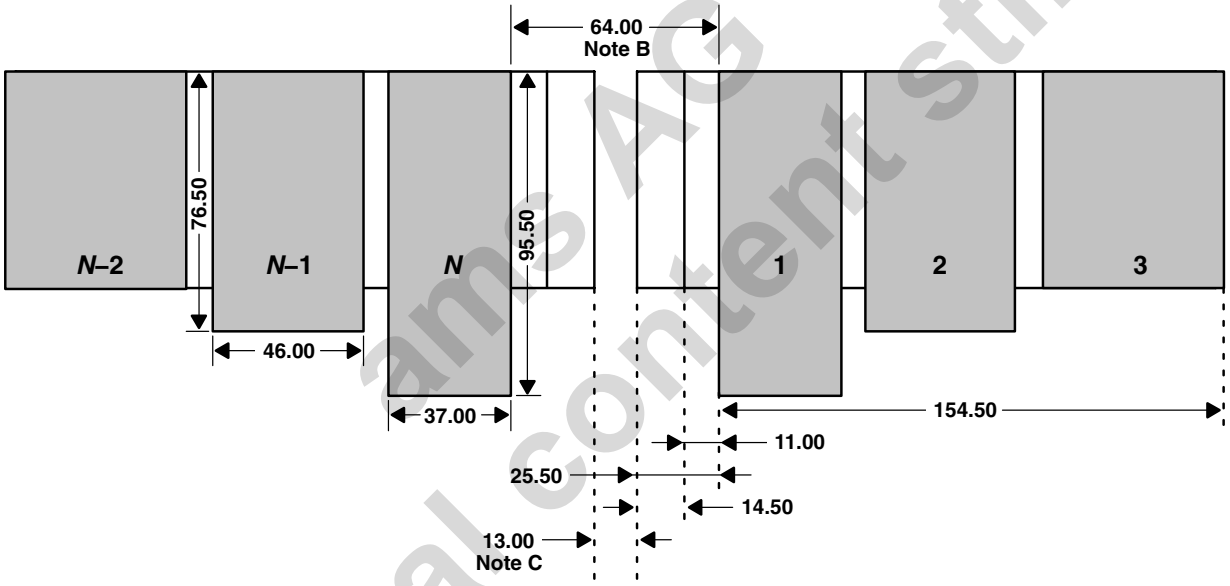

NOTES: A. All linear dimensions are in micrometers.
B. Spacing between outside pixels of adjacent die is typical.
C. Die-to-die spacing.
D. This drawing is subject to change without notice.

Figure 12. Edge Pixel Layout Dimensions

SOLDERING INFORMATION

TSL1402 256 × 1 linear array 14-lead gold pin package soldering instructions:

- The TSL1402R has been designed to withstand a lead temperature during soldering of 260°C for 10 seconds at a distance of 1.6 mm from the package body.
- In most applications, these *through-hole* parts will be sufficiently protected by the combination of the PCB or flex plus the standoff provided by the package.
- If lead clipping is required, this should be performed after solder attach to prevent the pulling of the lead from the package body.
- As in all board manufacturing, care should be taken to prevent part bending during board singulation or final assembly.
- If the process includes both surface-mount parts and the TSL1402R, the surface mount operations should be completed first with the through-hole parts afterward.

These parts can be washed as a part of the flux cleanup operation. A final top-surface cleanup may be required with water or alcohol to remove any remaining particles.

PRODUCTION DATA — information in this document is current at publication date. Products conform to specifications in accordance with the terms of Texas Advanced Optoelectronic Solutions, Inc. standard warranty. Production processing does not necessarily include testing of all parameters.

NOTICE

Texas Advanced Optoelectronic Solutions, Inc. (TAOS) reserves the right to make changes to the products contained in this document to improve performance or for any other purpose, or to discontinue them without notice. Customers are advised to contact TAOS to obtain the latest product information before placing orders or designing TAOS products into systems.

TAOS assumes no responsibility for the use of any products or circuits described in this document or customer product design, conveys no license, either expressed or implied, under any patent or other right, and makes no representation that the circuits are free of patent infringement. TAOS further makes no claim as to the suitability of its products for any particular purpose, nor does TAOS assume any liability arising out of the use of any product or circuit, and specifically disclaims any and all liability, including without limitation consequential or incidental damages.

TEXAS ADVANCED OPTOELECTRONIC SOLUTIONS, INC. PRODUCTS ARE NOT DESIGNED OR INTENDED FOR USE IN CRITICAL APPLICATIONS IN WHICH THE FAILURE OR MALFUNCTION OF THE TAOS PRODUCT MAY RESULT IN PERSONAL INJURY OR DEATH. USE OF TAOS PRODUCTS IN LIFE SUPPORT SYSTEMS IS EXPRESSLY UNAUTHORIZED AND ANY SUCH USE BY A CUSTOMER IS COMPLETELY AT THE CUSTOMER'S RISK.

TSL1402R
256 × 1 LINEAR SENSOR ARRAY WITH HOLD

Bibliography

[1] J. Wesselingh, Contactless positioning using an active air film, Delft university of technology http://repository.tudelft.nl/view/ir/uuid:4f90d3b0-1698-4885-b4b4-bdec9d886893/

[2] H.P.Vuong, Air-based contactless actuation system for thin substrates: The concept of using a controlled deformable surface https://repository.tudelft.nl/islandora/object/uuid:2d375f1b-3857-4c03-87e8-cb0fc45f3f13?$collection = research$

[3] Digikey product index, picture of AMS TSL1402R https://www.digikey.com/product-detail/en/ams/TSL1402R/TSL1402-R-ND/3095085

[4] AMS TSL1401CL, 128x1 Linear Sensor Array with hold 400 DPI https://ams.com/eng/Products/Light-Sensors/Linear-Array/TSL1401CL

[5] AMS TSL1402R, 256x1 Linear Array sensor with hold 400 DPI https://ams.com/eng/Products/Light-Sensors/Linear-Array/TSL1402R

[6] S. Matasci, What is the average solar panel size and weight?, 1 June 2017 http://news.energysage.com/average-solar-panel-size-weight/

[7] Analog devices, All A/D converters http://www.analog.com/en/parametricsearch/10169?mtuid=ab234d6063bd4684b9 6465f2d82fc40

[8] PSD techinfo, characteristics and use http ://www.hamamatsu.com/ resources/pdf/ssd/

[9] Optical engineering, Spie digital library http://opticalengineering.spiedigitallibrary.org/article.aspx?articleid=1076468

[10] Janssen Precision Engineering http://www.jpe.nl/downloads/Displacement-sensors-Concept-overview.pdf

[11] JEL corporation, *Wafer size: SEMI standards* $http://www.jel-robot.com/term/wsize1.html$.

[12] *Periodic table: Silicon* $http://www.chemicalelements.com/elements/si.html$.

[13] $http://www.kissolar.com/solarcells.html$

[14] Sumco corporation, *The next generation wafer* $http://www.sumcosi.com/english/products/next_generation/problem_bending.html$

[15] James E. Terry, Corning Announces Investment in Gen 10 LCD Glass Substrates, $http://www.businesswire.com/news/home/20071205006090/en/Corning-Announces-Investment-Gen-10-LCD-Glass$.

[16] Guillaume J. Laurent, Anne Delettre, Rabah Zeggari, Reda Yahiaoui, Jean-Franc¸ois Manceau and Nadine Le Fort-Piat, Micropositioning and Fast Transport Using a Contactless Micro-Conveyor, FEMTO-ST Institute, 12 February 2014

[17] K.H. Park, Contactless magnetically levitated silicon wafer transport system, Department of Mechanical Engineering, Korea Advanced Institute of Science and Technology, august 1996

[18] H. Moon and J. Luntz, Distributed manipulation of flat objects with two airflow sinks, IEEE Transactions on robotics, vol. 22, no. 6, pp. 1189–1201, 2006

[19] $http://www.mathopenref.com/sagitta.html$

[20] A. Berlin, D. Biegelsen, P. Cheung, M. Fromherz, D. Goldberg, W. Jackson, B. Preas, J. Reich, and L.-E. Swartz, Motion control of planar objects using large-area arrays of mems-like distributed manipulators, Micromechatronics, 2000.

[21] $https://www.thorlabs.com/newgrouppage9.cfm?objectgroup_id = 3423$

[22] Arduino Zero, overview and specifications
https://www.arduino.cc/en/Main/ArduinoBoardZero

[23] Reading a photodiode array
https://playground.arduino.cc/Main/TSL1402R

[24] G. Mok, The design of a planar precision stage using cost effective optical mouse sensors, Delt University of Technology, January 2015

[25] L. Boyd, Diameter of an optical fibre, viewed on 19-4-2016
http://hypertextbook.com/facts/1997/LaurenBoyd.shtml

[26] $http://www.sydor.com/wp-content/uploads/SEMI-Wafer-Flat-M1-0302-Specifications.pdf$